IN THE UNITED STATES PATENT AND TRADEMARK OFFICE

In re Patent Application of
THOMAS RAUSCH
Serial No.: 10/785,367
Filed: February 23, 2004

Confirmation No.: 8977
Group Art Unit: 1638
Examiner: Russell Kallis

For: TRANSGENIC PLANTS AND PLANT CELLS WITH REDUCED EXPRESSION OF INVERTASE INHIBITOR

VIA EFS-WEB
Commissioner for Patents
P.O. Box 1450
Alexandria, VA 22313-1450

DECLARATAION OF THOMAS RAUSCH

I, Thomas Rausch, declare under penalty of perjury as follows:

1. I am fully knowledgeable concerning the facts as set forth below.

2. I am the named inventor on United States Patent Application Serial No. 10/785,367 filed February 23, 2004, which is the subject of this declaration.

3. My *curriculum vitae* is attached hereto as Exhibit 1.

4. I studied biology and chemistry for 5 years at Frankfurt University. Thereafter, I obtained my PhD degree in the field of physiological plant pathology, working on biochemical aspects of hormonal regulation of sink development (clubroot disease). This was followed by a first post-doctoral period, during which I focused on the regulation of sugar transport in sink tissues. During this time (1982-1987), my experimental approaches extended to molecular biology. A second post-doctoral period (1988-1989) at the University of California, Santa Cruz, switched my topic to cloning and molecular analysis of vacuolar ATPase genes in Eukaryotes, including higher plants. During this period, I became familiar with the entire spectrum and potential of PCR-based techniques to isolate novel genes related to known genes, using so-called consensus primers. From 1989 onwards, my research extended to several aspects of molecular plant biology. However, regulatory aspects of sugar metabolism related to the development of sink tissues (seeds, but also vegetative sink tissues) have remained a major focus ever since.

5. In 1995, I moved to Heidelberg University, where I took over the chair of Molecular Ecophysiology of Plants. Since 1996, my research group has extensively studied molecular

aspects of carbohydrate metabolism in sink tissues of crop plants (potato, tomato, oil seed rape, maize, sugar beet, chicory). While the generation of transgenic plants affected in the expression of invertase inhibitors has been routinely carried out by industrial partners, the comprehensive analysis of transformants was done in my group, using advanced technologies of molecular and cellular plant biology.

6. I have authored over 90 papers, and was awarded 5 patents, mostly dealing with transgenic approaches to optimize sink development (seeds, vegetative storage organs), but also dealing with reducing post harvest sucrose losses. Among the papers dealing with transgenic plants are the following:

(i) Greiner et al. (1999), in which we demonstrated a reduced cold sweetening in potato in response to ectopic expression of a vacuolar invertase inhibitor (Exhibit 8);

(ii) Greiner (1999; PhD thesis), in which the effect of antisense expression of a tobacco invertase inhibitor on the process of seed filling is described;

(iii) Link et al. (2004), in which we demonstrated the *in vivo* effect of an invertase inhibitor knock out in *Arabidopsis thaliana* (T-DNA insertion) (Exhibit 9);

(iv) Eufinger (2006; PhD thesis), in which the effect of ectopic expression of a tobacoo invertase inhibitor on post harvest sucrose metabolism of sugar beet taproot is described, and

(v) Ergen (2006; PhD thesis), in which the effect of overeexpression of vacuolar and cytosolic pyrophosphatases on the development of sugar beet taproot is analyzed.

7. I am also the inventor of the invention claimed in United States Patent No. 6,784,339 B1 entitled, "TRANSGENIC PLANTS AND PLANT CELLS COMPRISING A REDUCED EXPRESSION OF INVERTASE INHIBITORS", which is incorporated by reference in the instant application.

8. A list of my papers is set forth in my *curriculum vitae* (Exhibit 1).

9. My current research work encompasses the following topics:

(a) post-translational regulation of carbohydrate-active enzymes in the cell wall and in the vacuole, with emphasis on inhibitor-mediated regulation of invertases, fructan-metabolizing enzymes and pectin methylesterases. This work extends from functional genomics (including transgenic work: *Arabidopsis thaliana*, but also crop plants) over cell biology to structural biology and is

performed in close collaboration with my colleague (and former PhD student) Dr. Steffen Greiner.

(b) regulation of glutathione (GSH) biosynthesis, relevant to plant stress biology. This work has a strong focus on the molecular aspects of γ-glutamylcysteine ligase regulation (GCL, first enzyme of GSH synthesis). We have determined the first plant GCL structure and unravelled its redox-regulation via intramolecular disulfide bridges. However this work also extends to several other aspects of plant redox homeostasis, including the role of the ascorbate-GSH-cycle and the regulation of phytochelatin synthesis in response to heavy metal exposure.

(c) regulatory aspects of secondary metabolism in plants, adaptation of primary metabolism (yielding the building blocks for secondary plant products) and pathway control via R2R3-myb-type transcription factors. Currently, the focus is on glucosinolate biosynthesis and monoterpene indolealkaloid biosynthesis.

10. In all of the above-described research fields, a major focus is on the model plant *Arabidopsis thaliana*. However, our work always extends to relevant crop plants, including sugar beet, chicory, oil seed rape and broccoli.

11. I have studied claims 1, 3-5 and 8-15 as amended in response to the U.S.P.T.O. Office Action dated July 5, 2007 in the instant application. I have also studied the Examiner's statements and rejection of the claims in the July 5, 2007 Office Action, as well as the previous Office Action dated October 2, 2006. The October 2, 2006 Office Action forms the basis for the Examiner's rejections in the July 5, 2007 Office Action (see July 5 Action at page 2). I have also reviewed the specification of the instant application.

12. In particular, I have reviewed the statements in the October 2, 2006 Office Action and in the July 5, 2007 Office Action in connection with the rejection of Claims 1, 3-5 and 8-15 on written description grounds, including the following passage from the October 2, 2006 Office Action:

> Applicant does not describe any sequence expressed during seed development in flowers with young ovules other than the apoplastic invertase inhibitor gene from tobacco and rapeseed. . . A description of a genus of cDNAs may be achieved by means of a recitation of a representative number of cDNAs, defined by nucleotide sequence, falling within the scope of the genus or of a recitation of structural features common to members of the genus, which features constitute a substantial portion of the genus. *University of California*

> *v. Eli Lilly and Co.*, 119 F.3d 1559 (Fed. Cir. 1997). . . . Since the genus of nucleotide sequences expressed during seed development in flowers with young ovules has not been described by specific structural features, the specification fails to provide an adequate written description to support the breadth of the claims.

(October 2, 2006 Office Action at pages 3-5). As stated, the Office Action dated July 5, 2007 incorporates the reasoning in the October 2, 2006 Action. In addition, the July 5, 2007 Action states that the alleged failure to provide a sufficient written description is not cured by the previous amendment which recites an apoplastic invertase inhibitor and that the nucleotide sequence has 80% sequence identity to a cDNA from a cDNA library from flowers with young ovules. I note here that main claim 1 has been amended to exclude the reference to a cDNA library and amends the claim to refer to the "endogenous" apoplastic invertase inhibitor.

13. For the following reasons, I respectfully disagree with the current rejection of Claims 1, 3-5 and 8-15 on written description grounds.

14. I have searched and consulted the literature relevant to the topic of this declaration, including the several PhD thesis generated in my own research group over the period 1999-2007. While the molecular biology of invertase inhibitors is a research field largely dominated by my group's studies, several papers have independently confirmed the importance of a tight invertase regulation during the process of seed filling for different plant families, as demonstrated by my and my colleagues' work in oil seed rape, the work in maize done by Bate and others (Exhibit 2), the work by Weschke and others in barley (Exhibit 3) and the work by Weber and Wobus in *Vicia faba* (Exhibit 4).

15. Plant invertase inhibitors are a small, distinct and well-defined subgroup of the larger protein family of pectin methylesterase inhibitor-like genes. They are characterized by 4 cysteine residues in highly conserved positions. While several amino acid residues are conserved across plant families (see "multiple sequence alignment" set forth below), no extended stretches of conserved amino acids exist which would allow one to amplify partial invertase inhibitor cDNAs across plant families (here the degree of conservation is up to 40% at the amino acid level). However, cloning additional members within a plant family using PCR with consensus primers may be successful (see tomato, tobacco, potato; *Arabidopsis thaliana, Brassica napus;* etc.). Some examples of structural commonalities across plant family invertase inhibitors are set forth (see below):

```
CLUSTAL W (1.83) multiple sequence alignment

NtVIF                   ------NNIINTTCRATTNYPLCLTTLHSDPRTSEAEGADLTTLGLVMVDAVKLKSIEIM 54
CiC/VIF                 -----DRKLIESTCKATPSYNLCLSTLLSNPKSSSGD---VSDLGLIMVGATRVKATQAI 52
NtCIF                   ------NNLVETTCKNTPNYQLCLKTLLSDKRSATGD---ITTLALIMVDAIKAKANQAA 51
AT1G47960_AtC/VIF1      -------SIIEPTCKETPDFNLCVSLLNSDPRGSSAD---TSGLALILIDKIKGLATKTL 50
BvC/VIF                 YSRKTTNDLVTTTCKQTPDPILCEASLRSDSRSSKAAD--SEGLILIMIDVVKTRFSDSF 58
AT5G64620_AtC/VIF2      --KSNTTTIIESTCKTTNYYKFCVSALKSDPRSPTAD---TKGLASIMVGVGMTNATSTA 55
                               :: .**: *    :*   * *: : . .       *  :::.       .

NtVIF                   KSIKK-LEKSNP--ELRLPLSQCYIVYYAVLHADVTVAVEALKRGVPKFAENGMVDVAVE 111
CiC/VIF                 QHIKS-LYRSHP--ELRRSLNQCAQMYMAVVKADVPSAIEALDGGQPKFAEDGMADTAVE 109
NtCIF                   VTISK-LRHSNPPAAWKGPLKNCAFSYKVILTASLPEAIEALTKGDPKFAEDGMVGSSGD 110
AT1G47960_AtC/VIF1      NEING-LYKKRP--ELKRALDECSRRYKTILNADVPEAIEAISKGVPKFGEDGVIDAGVE 107
BvC/VIF                 RYVED-LTRKTHDPDVIRALQECKQLYRVVLDVSVGLAVRAVKQGDPKFGEQAMVDAGNE 117
AT5G64620_AtC/VIF2      NYIAGNLSATVKDTVLKKVLQDCSEKYALAADS-LRLTIQDLDDEAYDYASMHVLAAQDY 114
                          :   *  .          *.:*   *       :  ::. :     .:..  :

NtVIF                   AETCEFSFKYNG---LVSPVSDMNKEIIELSSVAKSIIRMLL- 150
CiC/VIF                 AQACERSFSDGG---HKSPVTEMNKGVENIANVARAIIRMLL- 148
NtCIF                   AQECEEYFK--G---SKSPFSALNIAVHELSDVGRAIVRNLL- 147
AT1G47960_AtC/VIF1      ASVCQGGFN------GSSPLTSLTKSMQKISNVTRAIVRMLL- 143
BvC/VIF                 AEGCRMAFPEGK---VPGRIVGRTRMLHGVSNVAASMIKSLE- 156
AT5G64620_AtC/VIF2      PNVCRNIFRRVKGLAYPVEIRRREASLRRICGVVSGILDRLVE 157
                        .. *.  *          .      :  :..*  .::  *
```

Alignment of plant invertase inhibitor protein sequences from different plant families

NtCIF and NtVIF, cell wall and vacuolar inhibitor of tobacco (*Solanaceae*); CIC/VIF, invertase inhibitor from chicory (Asteraceae); AT1G47960_AtC/VIF1 and AT5G64620_AtC/VIF2, invertase inhibitor from *Arabidopsis thaliana* (Brassicaceae); BvC/VIF, invertase inhibitor from sugar beet (Chenopodiaceae). The four conserved cysteine and several other highly conserved residues are highlighted

16. Thus, all functionally confirmed invertase inhibitors (at least within dicot plants) cloned over the last few years (chicory, sugar beet, *Arabidopsis,* oil seed rape, tobacco, soybean etc.) group with the invertase inhibitor sub-group of *Arabidopsis thaliana*, and are therefore clearly separated from pectin methylesterase inhibitors. Thus, plant invertase inhibitors form a clearly defined genus of proteins. In summary, once a putative invertase inhibitor from a given plant species has been cloned, it is possible to identify it as a member of the "invertase inhibitor genus" by sequence comparison with other functionally confirmed invertase inhibitors, and via its position in the evolutionary tree of pectin methylesterase inhibitors from *Arabidopsis thaliana.*

17. Moreover, the analysis of structure-functional relationships in the relevant genus of invertase inhibitors has confirmed the role of two intramolecular disulfide bridges and a unique N-terminal hairpin structure, which is structurally aligned with the four-helix-bundle motif. (See Exhibits 5 and 6). In particular, certain amino acids may be replaced by others, as long as important structural features, e.g., conserved cysteines residues involved in attaching the hairpin to the core structure, are not compromised. When using related/mutated nucleotide sequences to a given invertase inhibitor in a crop plant species of interest,

antisense or RNAi-constructs of such related/mutated sequences will be effective as long as perfectly conserved stretches of 21-25 nucleotides are included. This is common knowledge now. Therefore, the claim for down-regulation of a particular invertase inhibitor via antisense or RNAi always has to include derived nucleotide sequences known to perform the same function as the original, endogenous sequence.

18. I have also reviewed the statements in the October 2, 2006 Office Action and in the July 5, 2007 Office Action in connection with the rejection of Claims 1, 3-5 and 8-15 on non-enablement grounds. For the reasons which follow, I also disagree with those statements.

19. The experimental approach to the isolation of the particular invertase inhibitor protein impacting on the seed filling process in a given plant species is straight forward and exclusively uses standard methods in molecular biology. In particular, the purification of the inhibitor protein is simplified by its co-purification with the target enzyme (glycosylated invertase; see Krausgrill et al. 1998 Plant J 13: 275-280). Thus, after salt-eluting the cell wall-bound protein fraction from the appropriate tissue (flowers after fertilization, early seed development; however, there is strong evidence for members of several plant families that the same invertase inhibitor is also expressed in heterotrophic suspension-cultured cells), simple ConA-chromatography is used to concentrate the glycoprotein fraction which includes invertase and inhibitor protein bound to it. Subsequently, this enriched fraction is subject to standard gel permeation chromatography. The complex of invertase with inhibitor shows a mobility corresponding to a 1:1 complex, usually in the range of approx. 80-90 kDa. The corresponding fractions are then subject to SDS-PAGE (denaturing conditions). Here, the inhibitor (approx. 17-20 kDa) is separated from invertase (approx. 65-70 kDa). The gel is stained with colloidal Coomassie Blue, and the inhibitor protein is subject to standard mass-spectrometric analysis (nano ESI qTOF [**E**lectrospray **Q**uadrupole - **T**ime **o**f **F**light]; MALDI-TOF [**M**atrix **A**ssisted **L**aser **D**esorption/**I**onisation/**T**ime **o**f **F**light]). Based on the obtained peptide sequence, consensus primers (in different orientations, as the position of peptide sequences in the complete protein sequence can not always be predicted) are designed to amplify a core sequence with 1.strand cDNA as template (isolated from the same tissue). Missing N- and C-terminal sequences may subsequently be amplified by standard 3'- and 5'-RACE procedures.

20. In summary, the entire streamlined procedure described in the preceding paragraph does indeed not involve any non-standard protocol. The initial purification of inhibitor

protein can be performed in 2-4 days in any protein biochemistry lab equipped for standard operations. Having obtained the results from mass-spectrometric analysis, the subsequent cloning of a full-length inhibitor cDNA can be accomplished in 2-3 days. Again, standard PCR reactions and RACE protocols do not require any undue or excessive experimentation. In my laboratory, this approach has been successfully implemented for tobacco and for sugar beet.

21. Indeed, for most of the plant species included in claim 12 of the instant patent application, transformation protocols based on gene delivery via *Agrobacterium tumefaciens* exist and are published. Therefore, stable plant transformation with a construct including any part of invertase inhibitor cDNA sequence in sense or antisense orientation (or as RNAi construct) and an appropriate promoter sequence can be regarded as established technology (with some specific variations depending on the species of interest; the respective procedures can be executed by any trained technician). Meanwhile, the approach described for tobacco has been extended to oil seed rape and basically gave similar results as concluded from a first preliminary analysis of transformants. (see declaration of Thomas Rausch under C.F.R.§1.132, as filed in Application Serial No. 09/762,782, Exhibit 7).

22. The isolation of a novel invertase inhibitor from a given plant species exactly follows the procedures described above for tobacco, since the characteristics of invertase inhibitors, on which the isolation and cloning procedures are based, extend to the entire genus of plant invertase inhibitors (see above). In summary, the present state of knowledge predicts that:

a. during the initial phase of seed development the required high hexose/sucrose ratio is provided via the activity of invertase;

b. the high hexose/sucrose ratio is essential for the meristematic activity of this developmental phase and, consequently, affects the total final seed cell number (which in turn determines, among other factors, the potential for subsequent accumulation of reserve compounds);

c. for the transition from the early meristematic to the later storage phase, the sugar balance shifts to a high sucrose/hexose ratio, and this shift is the result of a down-regulation of invertase activity;

d. an invertase inhibitor is involved in post-translational silencing of invertase, mediating either exclusively (or jointly with additional yet unknown factors) the inactivation of invertase;

e. while the spatial and temporal patterns of invertase down-regulation via invertase inhibitor may show some variation between different plant species and families, a simple time course of invertase activity measurements will identify the time point of beginning inhibitor action, hereby defining the developmental stage from which the inhibitor purification should proceed;

f. the protocols for invertase inhibitor purification, mass-spectrometric analysis and subsequent cloning have been described in detail above. Here, it has to be emphasized that based on the structural features of the protein genus "invertase inhibitor", the protocol given for tobacco and outlined again in detail in this declaration has a universal character. The procedures are straight foward, are entirely based on standard protocols for protein purification and cDNA cloning, and therefore do not require any undue or excessive experimentation.

I declare under penalty of perjury under the laws of the United States that all statements made herein are made of my own knowledge and are true except for those statements made on information and belief and statements made on information and belief are believed to be true; and further that these statements were made with the knowledge that willful false statements and the like so made are punishable by fine or imprisonment, or both, under Section 1001 of Title 18 of the United States Code, and that such willful false statements may jeopardize the validity of this statement, this application and any patent that may be issued thereon.

Date: 24/11/07

Thomas Rausch

The Plant Journal (1998) **13**(2), 275–280

SHORT COMMUNICATION

In transformed tobacco cells the apoplasmic invertase inhibitor operates as a regulatory switch of cell wall invertase

Silke Krausgrill, Steffen Greiner, Ulrike Köster, Rolf Vogel and Thomas Rausch*
Botanisches Institut, Im Neuenheimer Feld 360, D-69120-Heidelberg, Germany

Summary

***Agrobacterium tumefaciens*-transformed tobacco suspension-cultured cells (TSCC) exhibit no significant quantitative changes of cell wall invertase protein (CWI) during a culture period of 40 days, whereas CWI activity decreases strongly between 10 and 30 days after cell transfer to fresh medium. Western blot analysis revealed that the apoplasmic invertase inhibitor (INH) is equally expressed throughout the entire culture period. When apoplasmic protein fractions from 4 and 28 days old cell cultures are chromatographed on Concanavalin A(ConA)-Sepharose, the non-glycosylated INH always coelutes with the ConA-bound fraction, suggesting that (i) INH and the glycosylated CWI form a complex in the apoplasmic space, and (ii) INH binding is not sufficient for CWI inhibition. The high specificity of INH binding to CWI was confirmed by native cathodic polyacrylamide gel electrophoresis. Expression analysis of CWI and INH indicates that, at least during certain stages of plant development (seedlings, roots of adult plants), CWI activity may be modulated by INH, the latter operating as a regulatory switch.**

Introduction

In higher plants sucrose metabolism is catalysed by sucrose synthases and/or invertases (Delmer and Amor, 1995; Frommer and Sonnewald, 1995; Koch, 1996; Stitt and Sonnewald, 1995). Both enzyme classes occur as a set of isoenzymes expressed at particular stages of plant development (Cheng *et al.*, 1996; Koch, 1996; Miller and Chourey, 1992; Sturm *et al.*, 1995; Weber *et al.*, 1995; Zrenner *et al.*, 1995). Cloning of several cell wall (CWI) and vacuolar (VI) invertases has revealed that for both several isoforms exist which are distinct not only in their expression pattern during plant development, but also show significant structural differences (Sturm *et al.*, 1995; Weber *et al.*, 1995). In particular the nutrient status of the cells may decide which CWI isoform is expressed ('feast' and 'famine' isoforms; Koch, 1996, and references cited therein). CWI has been analysed in different sink tissues, and it has been proposed that CWI activity may stimulate phloem unloading by steepening the sucrose gradient (Eschrich, 1989; Miller and Chourrey, 1992; Roitsch *et al.*, 1995; Ruan and Patrick, 1995; Weil and Rausch, 1990). However, high CWI activity has also been found in *Ricinus communis* crown gall tumors, for which symplastic unloading has been demonstrated (Pradel *et al.*, 1996).

The existence of putative invertase inhibitor proteins (INH) has been shown for a number of sink tissues (Bracho and Whitaker, 1990; Ovalle *et al.*, 1995; Pressey, 1968, 1994; Sander *et al.*, 1996; Schwimmer *et al.*, 1961; Weil *et al.*, 1994). Recently, INHs from potato, tomato and tobacco have been purified to homogeneity (Bracho and Whitaker, 1990; Pressey, 1994; Weil *et al.*, 1994). In a previous study we have shown that in suspension-cultured *Agrobacterium tumefaciens*-transformed tobacco cells (TSCC) CWI expression may not only be regulated at the transcript level (Greiner *et al.*, 1995; Krausgrill *et al.*, 1996), but that enzyme activity may be further modulated by the presence of an apoplasmic inhibitor protein (Krausgrill *et al.*, 1996). The putative INH has been purified to homogeneity and partially characterized (Krausgrill *et al.*, 1996; Weil *et al.*, 1994). The protein has an M_r of about 17 kDa, is located in the apoplasmic space, and inhibits CWI *in vitro*. CWI may be protected against INH by its substrate, 1.2 mM sucrose providing half-maximum protection. Inhibition occurs in the pH-range of 4.5–6.5, indicating that CWI activity and inhibition by INH have a similar pH-dependence. When partially purified INH was added to TSCC an *in vivo*-inhibition could be demonstrated (Sander *et al.*, 1996). It is noteworthy, that INH from TSCC, and a structurally related invertase inhibitor from tomato fruit (Pressey, 1994), both inhibit CWI from tobacco cells and VI from tomato fruits (Sander *et al.*, 1996), however, only CWI, but not VI, was protected by its substrate.

In TSCC the extractable CWI activity shows a cycloheximide-sensitive four-fold increase after transfer of cells to fresh medium but declines later during the culture period (Krausgrill *et al.*, 1996; Weil and Rausch, 1990). In view of

Received 6 June 1997; revised 29 September 1997; accepted 15 October 1997.
*For correspondence (fax +06221 546621; e-mail TRausch@botanik1.bot.uni-heidelberg.de).

the reported substrate protection of CWI against INH (Weil *et al.*, 1994) we asked the question whether the pronounced changes in apparent CWI activity were due to changes in CWI amount, or, alternatively, the result of an *in vivo* downregulation of CWI by INH. We have extracted CWI and INH from the apoplasmic space at different times of the culture period and determined their amounts by Western blot analysis. Since only CWI, but not INH, is a glycosylated protein, complex formation between INH and CWI could be monitored by chromatography on ConA-Sepharose (Weil *et al.*, 1994), the specificity of INH binding to CWI being demonstrated by native gel electrophoresis. The results strongly suggest that (i) CWI and INH form complexes throughout the entire culture period, and (ii) sucrose depletion may be one of the factors inducing the transition of the complex from the non-inhibited to the inhibited state.

Results

For the quantitative analysis of CWI and INH protein, the cell wall proteins were salt-eluted at different culture stages from TSCC (Figure 1a). This procedure allows selective extraction of apoplasmic proteins with no detectable contamination by cytosolic proteins (Weil and Rausch, 1994). The presence of CWI (M_r 69 kDa) and INH (M_r 17 kDa) was detected by Western blot with polyclonal antisera (Krausgrill *et al.*, 1996; Sander *et al.*, 1996). Figure 1b shows that CWI and INH were both expressed throughout the culture period, the observed quantitative changes being not significant when replicate samples were compared (data not shown). No evidence was obtained for proteolytic degradation of either protein, except for a minor CWI splitting product of 28 kDa (not shown), the formation of which has been shown to be the result of intrinsic CWI lability (Weil and Rausch, 1994).

Apparent CWI activity was determined under conditions that do not lead to removal of CWI-bound INH. A pronounced increase was observed shortly after transfer of TSCC to fresh medium (Figure 2a), followed by a constant decrease between 3 and 30 days after transfer. Since sucrose may protect CWI from inhibition by INH, the concentrations of sucrose, fructose and glucose in the growth medium were monitored during culture development. Sucrose concentration decreased from about 65 mM to 1.3 mM within the first 11 days (Figure 2b), remaining between 1.3 and 1.6 mM up to the 30th day after transfer and further declining to 10 µM at 40 days after transfer.

As both CWI activity and the sensitivity towards INH are pH-dependent (Weil *et al.*, 1994), we have also monitored the medium pH during culture development. After an initial cell-mediated adjustment of the pH in the culture medium during the first day after transfer (from 5.3 to 5.6) the pH remained fairly constant up to the 30th day (Figure 2c). In

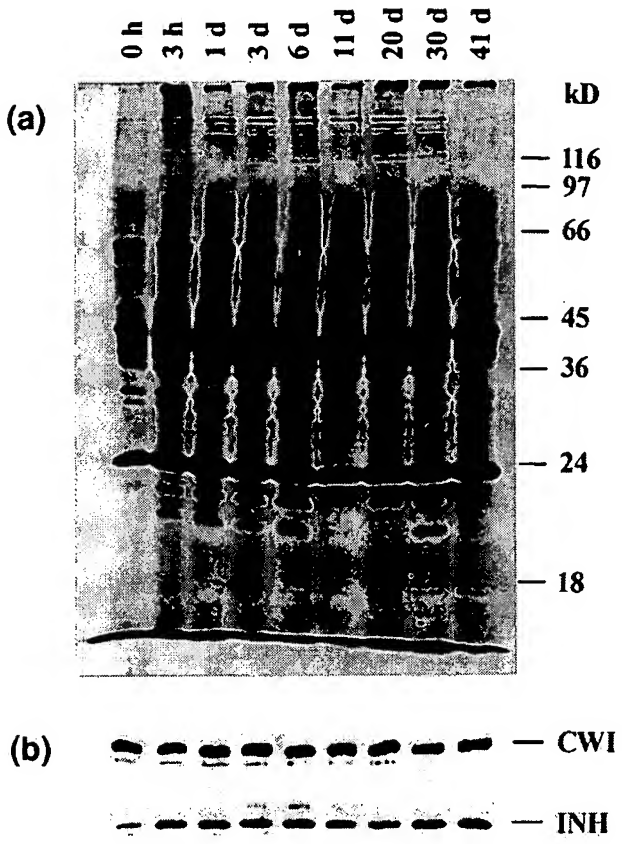

Figure 1. SDS–PAGE analysis of apoplasmic protein fractions (a), and Western blot analysis of CWI and INH expression (b) in TSCC at different culture stages.
Proteins were silver-stained. Immunological detection was performed with polyclonal antisera directed against carrot CWI (a gift from A. Sturm) and tobacco INH (Sander *et al.*, 1996). For (a) and (b) 20 µg cell wall protein was loaded per lane. Total cell wall protein per g fresh weight remained unchanged during the culture period.

Table 1 the pH-dependence of CWI activity is compared with the pH-dependence of CWI inhibition by INH. The maximum inhibition is obtained at pH 4.5, but even at pH 5.5 a significant *in vitro*-inhibition is observed. With respect to the local pH value in the cell wall it is important to note that the pH in the Donnan free space may in fact be significantly lower than the bulk pH of the culture medium.

To monitor complex formation between CWI and INH we have chromatographed cell wall protein fractions on ConA-Sepharose, based on the assumption that the non-glycosylated INH (Weil *et al.*, 1994) is recovered in the ConA-Sepharose-bound fraction only when bound to CWI. A comparison of the amounts of free INH with CWI-bound INH (Figure 3) revealed that during both early and late culture stages a major portion of INH was recovered in the ConA-Sepharose-bound fraction. In the bound fraction the ratio of CWI and INH immunosignals remained apparently constant, suggesting a fixed stoichiometry between INH and CWI. The amounts of free INH recovered in the non-bound fractions from both 4 and 28 days old cells showed

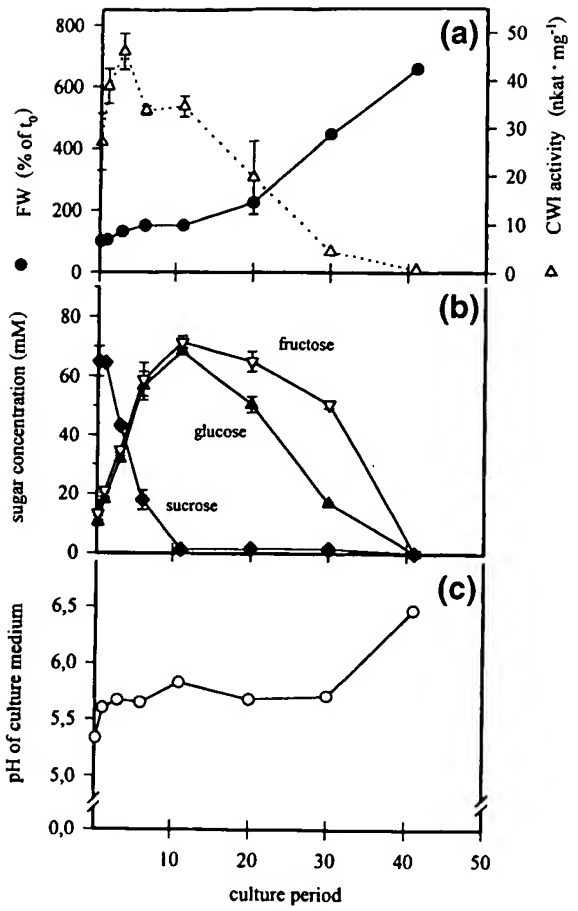

Figure 2. Fresh weight increase and apparent CWI activity (a), concentration of sucrose, glucose and fructose (b), and pH of culture medium (c) during the culture period of TSCC.
Apparent CWI activity was determined in the salt-eluted cell wall protein fraction after desalting on Sephadex G25. Under these conditions complexes between CWI and INH formed *in vivo* do not dissociate (Weil *et al.*, 1994).

Table 1. Relative CWI activities and percentage of inhibition by INH (pre-incubation in the absence of sucrose) *in vitro*. Data are calculated from Weil *et al.* (1994)

pH	Percent CWI activity in the absence of INH	Percent CWI inhibition in the presence of INH
4.5	100	100
4.75	83	78
5.5	50	63
6.5	21	33

no significant difference. This result indicates that INH, although associated with CWI throughout the culture period, becomes inhibitory only during later stages.

To exclude the possibility that in the ConA-bound fraction INH was associated with proteins other than CWI, we have determined the specificity of INH binding to CWI by native

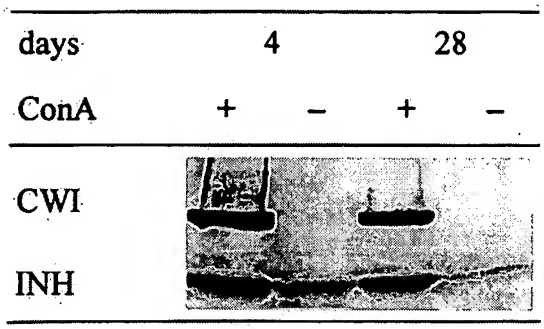

Figure 3. Evidence for the presence of CWI–INH complexes in the apoplasmic protein fractions from TSCC at different culture stages (4 and 28 days after transfer).
Cell wall proteins were chromatographed on ConA–Sepharose. INH is retained in the ConA–Sepharose(+)-bound fraction only when associated with CWI. CWI and INH were detected in the bound (+) or non-bound (–) fractions by Western blot analysis.

cathodic gel electrophoresis. The ConA-bound fraction of cell wall proteins, containing INH and CWI, and the ConA-nonbound fraction, containing only free INH, from cells 4 days after transfer (see Figure 3) were separated on a native cathodic gel and subsequently electroblotted to a PVDF membrane under only mildly denaturing conditions (1.3 mM SDS, 20% methanol). The detection of both proteins with their respective antisera (Figure 4) demonstrated that (i) free INH had a much higher mobility than INH co-eluting with CWI in the ConA-bound fraction, (ii) the mobility of INH in the ConA-bound fraction was identical with the mobility of CWI, and (iii) the immunosignal intensity of INH in the ConA-bound fraction was much weaker than the signal of free INH, although analysis by SDS–PAGE and Western blot indicated that the amount of INH in the ConA-bound fraction was even higher than in the non-bound fraction. This reduced immunosignal strongly suggests that in the CWI–INH complex not all INH epitopes were exposed for antibody binding. Separation of the entire gel lane of the ConA-bound fraction by SDS–PAGE in the second dimension (Figure 4) further confirmed the existence of specific CWI–INH complexes. The positions of immunosignals for INH and CWI, the latter represented by the intact protein (69 kDa) and the previously described specific 28 kDa splitting product (Weil and Rausch, 1994), showed perfect correlation, and no other INH signals appeared, excluding the binding to (and shielding by) other proteins in the ConA-bound fraction.

As a coordinate expression of INH with CWI could modulate CWI activity during plant development we have isolated cell wall proteins from seedlings by salt-elution (Figure 5a) and whole cell proteins from different parts of adult, flowering tobacco plants (Figure 5b). Western blot analysis revealed the presence of both proteins in seedlings and in roots and senescent leaves of adult tobacco plants. In the latter tissues the antiserum directed against INH detects,

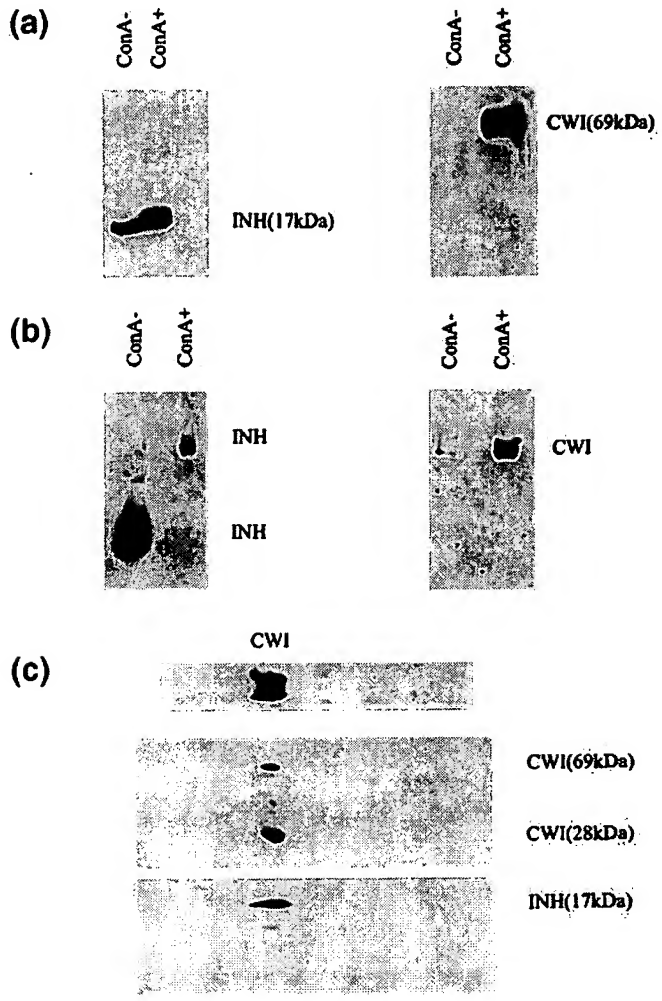

Figure 4. Demonstration of specific CWI–INH complexes by native cathodic gel electrophoresis in the ConA-bound (ConA+) fraction of cell wall proteins isolated from cells 4 days after transfer to fresh medium.
The ConA+ fraction from cells 28 days after transfer gave identical results (not shown).
(a) Analysis of ConA+ and ConA– (nonbound) fractions by SDS–PAGE and western blot with INH (left) and CWI (right) antiserum, respectively.
(b) Native cathodic gel electrophoresis of the same ConA+ and ConA– fractions (see a), followed by Western blot with INH (left) and CWI (right) antiserum under only mildly denaturing conditions.
(c) SDS–PAGE and Western blot analysis in the second dimension of the entire gel lane of the ConA+ fraction (see b), after initial separation by native cathodic gel electrophoresis.
Top: ConA+ lane (see b) from native cathodic gel electrophoresis (horizontal orientation).
Middle: Upper part of the Western blot after SDS–PAGE, developed with the CWI antiserum, giving signals for intact CWI (69 kDa) and its 28 kDa splitting product (Weil and Rausch, 1994).
Bottom: Lower part of the blot, developed with INH antiserum. Note that developing the upper part of the blot with INH antiserum or the lower part with CWI antiserum did not produce any immunosignals (data not shown).

in addition to INH, a protein with an apparent M_r of 19 kDa. In stem tissue and flower buds only INH could be detected, however, it is possible that here CWI expression is very low or, alternatively, another CWI isoform is expressed. In source and sink leaves both proteins were not detectable.

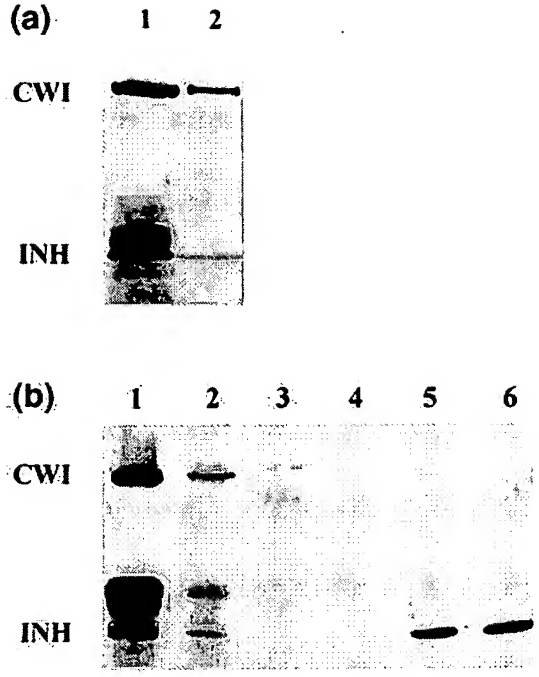

Figure 5. (a) Western blot analysis of CWI and INH expression in TSCC (1) and 10-day-old tobacco seedlings germinated in suspension (2); (b) expression of CWI and INH in different organs of 8-week-old tobacco plants: 1, root, 2, senescent leaf, 3, source leaf, 4, sink leaf, 5, stem, 6, flower bud. Antisera as described in Figure 1.

Discussion

The present study provides the first comparison of CWI and INH expression in a higher plant using specific immunodetection for both proteins. The results obtained for CWI and INH expression in TSCC indicate coordinate synthesis of both proteins in the same cell type. As both proteins are secreted into the apoplasmic space (Weil and Rausch, 1994; Weil *et al.*, 1994), it has to be assured that INH remains spatially close to CWI. Due to its strong positive charge (pI 9.5; Sturm and Chrispeels, 1990; Weil and Rausch, 1994) CWI is assumed to be firmly bound to the cell wall matrix. One possibility would be that both proteins are forming a loose complex during their transit through the secretory pathway.

The presented data show that complex formation between INH and CWI, as monitored by ConA-Sepharose chromatography, is independent of the culture stage. Thus, INH appears to be associated with CWI independently of its inhibitory effect. Furthermore, the analysis of the ConA-bound fraction of apoplasmic proteins by native cathodic polyacrylamide gel electrophoresis shows that (i) the major part of INH protein is complexed with CWI, and (ii) the binding to CWI is highly specific. The apparent shielding of INH by CWI indicates that INH may be partially buried in the protein-complex. It is important to note that previous work has identified the 28 kDa polypeptide, crossreacting

with the CWI antiserum, as a specific CWI splitting product resulting from intrinsic lability of CWI, and not from INH binding (Weil and Rausch, 1994). Its prominent appearance in Figure 4c may be due to the 60 min incubation in denaturing buffer before starting the second dimension SDS–PAGE step.

The transition from the non-inhibited to the inhibited conformation of the CWI–INH complex may be induced by lowering the sucrose concentration (Weil *et al.*, 1994; see below), but other as yet unknown factors could modulate this transition. The only gradual inactivation of CWI between 10 and 30 days after transfer of cells may result from the fact that during this period the sucrose concentration is still close to the concentration which provides half maximum substrate protection (1.2 mM; Weil *et al.*, 1994).

The observation that CWI and INH are also detected in seedlings and roots of adult plants emphasizes that inhibition of CWI by INH may have important implications for plant development, although it remains to be determined whether in the complex tissues of seedlings and adult plants both proteins are expressed in the same cell type. Thus, in addition to the recent discoveries of different CWI isoforms in several plant species showing very distinct spatial/developmental expression patterns, the regulation of CWI by an associated inhibitor provides another control mechanism. The existence of 'feast' and 'famine' isoforms of invertases suggested, that invertase expression is related to nutrient status (Koch, 1996, and references cited therein). The substrate protection of CWI against INH adds an additional facet to this emerging theme (Weil *et al.*, 1994; Sander *et al.*, 1996). The significance of INH expression in stem and flower buds of adult tobacco plants, where CWI could not be detected by Western blot, remains as yet unclear. The presence of CWI and INH in senescent leaves of adult plants might be due to a general stress response, as CWI has been shown to be induced upon wounding and infection (Sturm and Chrispeels, 1990; Herbers *et al.*, 1996).

For TSCC, and, possibly, other sink tissues the following model is proposed. In the presence of ample sucrose supply INH is loosely bound to CWI without affecting enzymatic activity (state I: feast condition). When sucrose falls below a threshold concentration ($\leq$1 mM), a conformational change of the CWI–INH complex leads to inactivation of idle CWI (state II: famine condition). On the assumption that apoplasmic hexoses may act as primary metabolic signals, which, after carrier-mediated uptake, are sensed by hexokinase (Jang and Cheen, 1994), a sucrose-sensitive conformational change in the CWI–INH complex would assure that the hexose signal is provided only at ample sucrose supply. In the intact plant high apoplasmic sucrose concentrations in sink tissues could result from apoplasmic phloem unloading and/or leakage from cells symplasmically supplied with sucrose.

Further elucidation of INH function depends on cloning the corresponding gene. Based on peptide sequences from tryptic digest we have recently cloned a cDNA for tobacco INH (Greiner *et al.*, 1998). Analysis of its function in transgenic *sense* and *antisense* plants will shed light on its role during plant development.

Experimental procedures

Plant material and extraction of cell wall proteins

Agrobacterium tumefaciens-transformed tobacco (*Nicotiana tabacum* cv. Petit Havana) suspension-cultured cells (TSCC) were grown in the dark, and apoplasmic proteins were eluted with 1.0 M NaCl solution without cell disruption as previously described (Weil and Rausch, 1990). Total apoplasmic proteins were precipitated with ammonium sulfate (45–85% fraction) and subsequently desalted on Sephadex G-25. Under these conditions CWI–INH complexes do not dissociate (Weil *et al.*, 1994).

Tobacco seedlings were grown from surface-sterilized seeds and cultivated in suspension in Murashige-Skoog medium in the dark at 25°C for 10 days on a rotary shaker at 120 *g*. Cell wall proteins were eluted with 1 M NaCl as described for TSCC. Tobacco plants were grown in soil in the greenhouse for 12 weeks until flowering. Whole cell proteins were extracted with 50 mM sodium acetate, pH 6.5, 500 mM NaCl, 1 mM EDTA, 5 mM DTT, 1 mM phenylmethylsulfonyl fluoride, and 5% (w/v) polyvinylpolypyrrolidone. Protein fractions were desalted on Sephadex G-25 prior to SDS–PAGE.

Detection of CWI–INH complexes by Concanavalin A-Sepharose chromatography

Desalted apoplasmic protein fractions were chromatographed on Con A-Sepharose as previously described (Weil *et al.*, 1994). Bound and non-bound fractions were ammonium sulfate-precipitated (90%), desalted on Sephadex G-25 minicolumns, and subjected to SDS–PAGE and Western blot analysis.

Native cathodic gel electrophoresis of apoplasmic proteins

Native cathodic gel electrophoresis of the ConA-bound and -nonbound fractions was performed on a 10% acrylamide gel according to Reisfeld *et al.* (1962). For the immunodetection of CWI and INH identical samples were run in triplicates in the same gel. One part of the gel was blotted to a Immobilon P membrane (Millipore, Eschborn, Germany), and CWI and INH were detected by their respective antisera. An identical total gel lane was cut from the native gel and equilibrated in denaturing buffer (4% SDS, 5 mM Na_2EDTA, 75 mM Tris–HCl, 20% (w/v) glycerine, 200 mM DTT, 1 mM PMSF, pH 6.8) for 60 min at RT. Thereafter, the entire gel lane was placed horizontally on top of a 15% denaturing gel and subjected to SDS–PAGE. After electroblotting to a Immobilon P membrane, CWI and INH were detected with the specific antisera in the top and bottom part, respectively, of the same blot.

Antisera and Western blot analysis

CWI was detected with a polyclonal antiserum (titer 1:2000) directed against carrot CWI (Chrispeels and Sturm, 1990; Weil and

Rausch, 1994). Tobacco INH, previously named p17, was purified to homogeneity according to Weil *et al.* (1994). A polyclonal antiserum was raised in rabbit (100 µg, single injection). The INH antiserum was used at a titer of 1:80000. After SDS–PAGE CWI and INH were detected by Western blot as previously described (Weil and Rausch, 1994).

Determination of CWI activity and of sugars in the growth medium

CWI activity was determined according to Weil and Rausch (1990). Sucrose, fructose and glucose from the growth medium were determined enzymatically (Jelitto *et al.*, 1992).

Acknowledgements

This work was supported by a grant of the Deutsche Forschungsgemeinschaft to T.R. (SFB 199, TP-C3). The antiserum against CWI from carrot was a gift from Arnd Sturm.

References

Bracho, G.E. and Whitaker, J.R. (1990) Purification and partial characterization of potato (*Solanum tuberosum*) invertase and its endogenous proteinaceous inhibitor. *Plant Physiol.* **92**, 386–394.

Cheng, W.-H., Taliercio, E.W. and Chourey, P.S. (1996) The *miniature1* seed locus of maize encodes a cell wall invertase required for normal development of endosperm and maternal cells in pedicel. *Plant Cell*, **8**, 971–983.

Delmer, D.P. and Amor, Y. (1995) Cellulose biosynthesis. *Plant Cell*, **7**, 987–1000.

Eschrich, W. (1989) Phloem unloading of photoassimilates. In *Transport of Photoassimilates* (Baker, D.A., Milburn, J.A., eds). New York: Longman Scientific & Technical, pp. 206–263.

Frommer, W.B. and Sonnewald, U. (1995) Molelcular analysis of carbon partitioning in solanaceous species. *J. Exp. Bot.* **46**, 587–607.

Greiner, S., Krausgrill, S. and Rausch, T. (1998) Cloning of a tobacco apoplasmic invertase inhibitor: Proof of function of the recombinant protein and expression analysis during plant development. *Plant Physiol.* in press.

Greiner, S., Weil, M., Krausgrill, S. and Rausch, T. (1995) A tobacco cDNA coding for cell-wall invertase. *Plant Physiol.* **108**, 825–826.

Herbers, K., Meuwly, P., Frommer, W.B., Métreaux, J.-P. and Sonnewald, U. (1996) Systemic acquired resistance mediated by ectopic expression of invertase: Possible hexose sensing in the secretory pathway. *Plant Cell*, **8**, 793–803.

Hofmann, B. and Kosegarten, H. (1995) FITC-dextran for measuring apoplast pH gradients between various cell types in sunflower leaves. *Physiol. Plant.* **95**, 327–335.

Jang, J.-C. and Sheen, J. (1994) Sugar sensing in higher plants. *Plant Cell*, **6**, 1665–1679.

Jelitto, T., Sonnewald, U., Willmitzer, L., Hajirezaei, M.R. and Stitt, M. (1992) Inorganic phosphate content and metabolites in leaves and tubers of potato and tobacco plants expressing *E.coli* pyrophosphatase in their cytosol. *Planta*, **188**, 238–244.

Koch, K. E. (1996) Carbohydrate-modulated gene expression in plants. *Annu. Rev. Plant Physiol. Plant Mol. Biol.* **47**, 509–540.

Krausgrill, S., Sander, A., Greiner, S., Weil, M. and Rausch, T. (1996) Regulation of cell wall invertase by a proteinaceous inhibitor. *J. Exp. Bot.* **47**, 1193–1198.

Miller, M.E. and Chourey, P.S. (1992) The maize invertase-deficient miniature-1 seed mutation is associated with aberrant pedicel and endosperm development. *Plant Cell*, **4**, 297–305.

Ovalle, R., Keyes, A.C., Ewing, E.E. and Quimby, F.W. (1995) Purification and characterization of the acid-stable proteinaceous inhibitor of potato tuber invertase by nonideal size exclusion chromatography. *J. Plant Physiol.* **147**, 334–340.

Pradel, K., Rezmer, C., Krausgrill, S., Rausch, T. and Ullrich, C. (1996) Evidence for a symplastic phloem unloading with concomittant high activity of acid cell wall invertase in *Agrobacterium tumefaciens*-induced plant tumors. *Bot. Acta*, **5**, 341–344.

Pressey, R. (1968) Invertase inhibitors from red beet, sugar beet, and sweet potato roots. *Plant Physiol.* **43**, 1430–1434.

Pressey, R. (1994) Invertase inhibitor in tomato fruit. *Phytochemistry*, **36**, 543–546.

Reisfeld, R.A., Lewis, U.J. and Williams, D.E. (1962) Disc electrophoresis of basic proteins and peptides on polyacrylamide gels. *Nature*, **4838**, 281–283.

Roitsch, T., Bittner, M. and Godt, D.E. (1995) Induction of apoplastic invertase of *Chenopodium rubrum* by D-glucose and a glucose analog and tissue-specific expression suggest a role in sink-source regulation. *Plant Physiol.* **108**, 285–294.

Ruan, Y.L. and Patrick, J.W. (1995) The cellular pathway of postphloem sugar transport in developing tomato fruit. *Planta*, **196**, 434–444.

Sander, A., Krausgrill, S., Greiner, S., Weil, M. and Rausch, T. (1996) Sucrose protects cell wall invertase but not vacuolar invertase against proteinaceous inhibitors. *FEBS Lett.* **385**, 171–175.

Schwimmer, S., Makower, R.U. and Romem, E.S. (1961) Invertase and invertase inhibitor in potato. *Plant Physiol.* **36**, 313–316.

Stitt, M. and Sonnewald, U. (1995) Regulation of metabolism in transgenic plants. *Annu. Rev. Plant Physiol. Plant Mol. Biol.* **46**, 341–368.

Sturm, A. and Chrispeels, M.J. (1990) cDNAcloning of carrot extracellular β-fructosidase and its expression in response to wounding and bacterial infection. *Plant Cell*, **2**, 1107–1119.

Sturm, A., Sebkova, V., Lorenz, K., Hardegger, M., Lienhard, S. and Unger, C. (1995) Development- and organ-specific expression of the genes for sucrose synthase and three isoenzymes of acid b-fructofuranosidase in carrot. *Planta*, **195**, 601–610.

Weber, H., Borisjuk, L., Heim, U., Buchner, P. and Wobus, U. (1995) Seed coat-associated invertases of fava bean control both unloading and storage functions: Cloning of cDNAs and cell type-specific expression. *Plant Cell*, **7**, 1835–1846.

Weil, M. and Rausch, T. (1990) Cell wall invertase in tobacco crown gall cells: enzyme properties and regulation by auxin. *Plant Physiol.* **94**, 1575–1578.

Weil, M. and Rausch, T. (1994) Acid invertase in *Nicotiana tabacum* crown-gall cells: Molecular properties of the cell-wall isoform. *Planta*, **193**, 430–437.

Weil, M., Krausgrill, S., Schuster, A. and Rausch, T. (1994) A 17 kDa *Nicotiana tabacum* cell-wall peptide acts as an *in vitro* inhibitor of the cell-wall isoform of acid invertase. *Planta*, **193**, 438–445.

Zrenner, R., Salanoubat, M., Willmitzer, L. and Sonnnewald, U. (1995) Evidence of the crucial role of sucrose synthase for sink strength using transgenic potato plants (*Solanum tuberosum* L.). *Plant J.* **7**, 97–107.

Attachment
CV Thomas Rausch & Publication list

Prof. Dr. Thomas Rausch

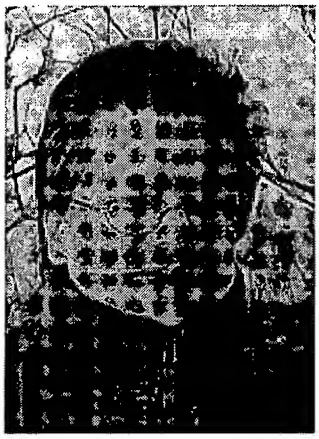

Heidelberg Institute of Plant Sciences (HIP)
University of Heidelberg
69120 Heidelberg, Germany

Phone: +49-(0)6221-54-6621
Fax:. +49-(0)6221-54-5859
E-mail: trausch@hip.uni-hd.de

22/07/1953, Frankfurt

SCIENTIFIC VITA

2003-2005	HIP Managing Director
2000-2003	Dean, Faculty of BioSciences
2001	Co-Founder of the Heidelberg Institute for Plant Sciences (HIP)
2000	Offer for full professorship, TU-Darmstadt; declined
since 1994	Full professor (C4), Director of Molecular Ecophysiology Lab, University of Heidelberg
1991-1993	Independent group leader, University of Frankfurt
1990	Habilitation in Botany, University of Frankfurt
1988-1989	Research fellow, Sinsheimer Lab, UCSC, USA
1986-1988	Independent Group leader, University of Frankfurt
1986	Guest scientist, Thimann Lab, UCSC, USA
1982-1985	Post doc, University of Frankfurt
1978-1981	PhD, Botanical Institute, University of Frankfurt
1972-1977	Biology & Chemistry Studies (1.Staatsexamen), University of Frankfurt

COORDINATING FUNCTIONS

2006-2009	Co-chairman of BMBF consortium BroCan
2000-2006	Coordinator of the German Plant Sulfur Group (DFG-funded)
1995-2000	Co-chairman of the SFB 199 *"Molecular Ecophysiology of Plants"*

FIELDS OF INTEREST

Molecular plant biology, genetic engineering of plant metabolism, stress physiology, cellular redox control.

CURRENTLY FUNDED PROJECTS

DFG-project on GSH1 structure; DFG-project on seed filling in maize (HD-excellence cluster CellNetworks); BMBF-BroCan; 3 industry-funded projects on engineering plant C-metabolism.

PUBLICATIONS (1999-2007):

Vogel R, Viereck R, Murmann A, Rausch T (1999) Cloning of a higher plant elongation factor 2 cDNA: Expression of eEF2 and α subunit of eEF1B in sugar beet cells during phosphate and carbohydrate starvation. J Plant Physiol 154: 192-196

Lehr A, Kirsch M, Viereck R, Schiemann J, Rausch T (1999) cDNA and genomic cloning of sugar beet V-type H^+-ATPase subunit A and c isoforms: Evidence for coordinate expression during plant development and coordinate induction in response to high salinity. Plant Mol Biol 39: 463-475

Heiss S, Schäfer HJ, Haag-Kerwer A, Rausch T (1999) Cloning sulfur assimilation genes of *Brassica juncea* L.: Cadmium differentially affects the expression of a putative low affinity sulfate transporter and isoforms of ATP sulfurylase and APS reductase. Plant Mol Biol 39: 847-857

Gabriel R, Schäfer L, Gerlach C, Rausch T, Kesselmeier J (1999) Factors controlling the emissions of volatile organic acids from leaves of *Quercus ilex* (Holm oak). Atmospheric Environment 44: 1347-1355

Haag-Kerwer A, Schäfer HJ, Heiss S, Walter C, Rausch T (1999) Transpiration but not photosynthesis is affected by cadmium in *Brassica juncea* L.: Temporal coordination of Cd-uptake and phytochelatin synthesis. J Exp Bot 50: 1827-1835

Greiner S, Rausch T, Sonnewald U, Herbers K (1999) Ectopic expression of a tobacco invertase inhibitor homolog prevents cold-induced sweetening of potato tubers. Nature/Biotechnology 17: 708-711

Schneider T, Haag-Kerwer A, Maetz M, Niecke M, Povh B, Rausch T, Schüßler A (1999) Micro-PIXE studies of elemental distribution in Cd-accumulating *Brassica juncea* L. Nuclear Instruments and Methods in Physics Research B

Greiner S, Köster U, Lauer K, Rosenkranz H, Vogel R, Rausch T (2000) Plant invertase inhibitors: Expression in cell culture and during plant development. Australian J Plant Physiol, 27: 807-814

Rosenkranz H, Vogel R, Greiner S, Rausch T (2001) In wounded sugar beet (*Beta vulgaris* L.) tap-root, hexose accumulation correlates with the induction of a vacuolar invertase isoform. J Exp Bot, 52: 2381-2385

Holtorf, H., Hohe A., Hong-Liang Wang, Jugold, M., Rausch, T., Duwenig, E. and Reski, R. (2002) Promoter subfragments of the sugar beet V-type H+-ATPase subunit c isoform drive the expression of transgenes in the moss *Physcomitrella.* Plant Cell Rep 21: 341-346

Scognamiglio MA, Ciardiello MA, Tamburrini M, Carratore V, Rausch T, Camardella L (2003) The plant invertase inhibitor has the same disulfide bridges arrangement as the pectin methylesterase inhibitor. J Protein Chem 22: 363-369

Heiss S, Wachter A, Bogs J, Cobbett C, Rausch, T (2003) Phytochelatin synthase (PCS) from *Brassica juncea*: Enzyme activity of recombinant PCS protein and analysis of PCS expression in control and Cd-treated plants. J Exp Bot 54: 1833-1839

Bogs J, Bourbouloux A, Cagnac O, Wachter A, Rausch T, Delrot S (2003) Functional charaterization and expression analysis of a glutathione transporter, BjGT1, from *Brassica juncea:* Evidence for regulation by heavy metal exposure. Plant Cell Environ 26: 1703-1711

Wolf S, Grsic-Rausch S, Rausch T, Greiner S (2003) Identification of pollen-expressed pectin methylesterase inhibitors in *Arabidopsis.* FEBS Lett 555: 551-555

Hothorn M, Bonneau F, Stier G, Greiner S, Scheffzek K (2003) Bacterial expression, purification and preliminary X-ray crystallographic characterization of the invertase inhibitor Nt-CIF from tobacco. Acta Cryst D59: 2279-2282

Rausch T, Greiner S (2004) Plant protein Inhibitors of Invertase. Biochim Biophys Acta 1696: 253-261

Grsic-Rausch S, Rausch T (2004) A coupled spectrophotometric enzyme assay for the determination of pectin methylesterase activity and its inhibition by proteinaceous inhibitors. Anal Biochem 333/1: 14-18

Link M, Rausch T, Greiner S (2004) In *Arabidopsis thaliana*, the invertase inhibitors AtC/VIF1 and 2 exhibit distinct target enzyme specificities and expression profiles. FEBS Lett 573: 105-109

Wachter A, Wolf S, Steininger H, Bogs J, Rausch T (2005) Differential targeting of GSH1 and GSH2 is achieved by multiple transcription initiation: Implications for the compartmentation of glutathione biosynthesis in the Brassicaceae. Plant J 41: 15-30

Wachter A, Rausch T (2005) Regulation of glutathione (GSH) synthesis in plants: Novel insight from *Arabidopsis*. FAL Agricultural Research 283: 149-155

Jost R, Altschmied L, Bloem E, Bogs J, Gershenzon J, Haeh U, Haensch R, Hartmann T, Kopriva S, Kruse C, Mendel R, Reichelt M, Papenbrock J, Schnug E, Rennenberg H, Schmidt A, Textor S, Tokuhisa J, Wachter A, Wirtz M, Rausch T, Hell R (2005) Expression profiling of metabolic genes in response to methyl jasmonate reveals regulation of genes of primary and secondary sulfur-related pathways in *Arabidopsis thaliana*. Photosyn Res 86: 491-508

Mullineaux P, Rausch T (2005) Glutathione, photosynthesis and the redox regulation of stress-responsive gene expression. Photosyn Res 86: 459-474

Rausch T, Wachter A (2005) Sulfur metabolism: A versatile platform for launching defence operations. TIPS 10: 503-509

Hothorn M, Wachter A, Gromes R, Stuwe T, Rausch T, Scheffzek K (2006) Structural basis for the redox-control of plant glutamate cysteine ligase. J Biol Chem 281: 27557-27565

An Z, Li C, Zu Y, Du Y, Wachter A, Gromes R, Rausch T (2006) Expression of BjMT2, a metallothionein 2 from *Brassica juncea*, increases copper and cadmium tolerance in *Escherichia coli* and *Arabidopsis thaliana*, but inhibits root elongation in *Arabidopsis thaliana* seedlings. J Exp Bot 57: 3575-3582

Rausch T, Gromes R, Liedschulte V, Müller I, Bogs J, Galovic V, Wachter A (2007) Novel insight into the regulation of GSH biosynthesis in higher plants. Plant Biol, *in press*

Rausch, T (2007) When plant life gets tough sulfur gets going. Plant Biol, *in press*

Meyer A, Rausch T (2007) Biosynthesis, compartmentation and cellular functions of glutathione in plant cells. *in press (book chapter)*

Gromes R, Hothorn M, Scheffzek K, Müller I, Rausch T (2007) Activation of glutamate cysteine ligase by redox-regulated monomer-dimer transition is a plant invention. *submitted*

Patents (1998-2007)

Rausch, T., Krausgrill, S., Greiner, S. (1998) Invertase-Inhibitor. EP 0 956 357 (granted)

Rausch, T., Duwenig, E. (1999) Plant gene expression, controlled by constitutive plant V-ATPase promoters. EP 1 206 560 (granted)

Harms, K., Rausch, T., Greiner, Harling, H., Rosenkranz, H. (2000) Nucleic acids coding for vacuolar invertases, vegetal cells and plants containing said nucleic acids and the use thereof. International patent application. EP13523 20011121 (German patent granted)

Rausch, T. (2001) Transgenic plants and plant cells comprising a reduced expression of invertase inhibitors. US-Patent, Application No. 09/762,782 (granted)

Schirmer S, Harms K, Harling H, Greiner S, Rausch T (2003) Modified PPase expression in sugar beet. WO 004083440 (pending)

EXPERIENCE IN THE SUPERVISION OF DOCTORAL CANDIDATES

Coordinator of the Heidelberg Plant & Fungal Biology PhD program (http://ephedra.hip.uni-heidelberg.de/phd/)
Member of numerous thesis and thesis advisory committees
International reviewer of doctoral theses
Supervised 20 doctoral theses

SUPERVISED DISSERTATIONS (last 5 years)

Rolf Stratmann, PhD (2007) Pektin Methylesterasen (PMEs) und PME-Inhibitor-verwandte Proteine im Maispollen: Genexpression, subzelluläre Lokalisation und funktionelle Charakterisierung. University of Heidelberg.
Current occupation: BMBF, grant administration, Bonn.

Jan Eufinger, PhD (2006) Regulation of sucrose accumulation and stabilization in sugar beet: Influence of invertase inhibitors and occurence of mitochondrial energy-dissipating proteins. University of Heidelberg
Current occupation: Scientific administration, BIOQUANT, University of Heidelberg.

Zahide Neslihan Ergen, PhD (2006) A functional genomics approach to the plant soluble pyrophosphatase family. University of Heidelberg.
Current occupation: Postdoctoral fellow, Sabanci Universitesi, Muhendislik ve Doga Bilimleri Fakultesi, Orhanli koyu, Tuzla, Turkey.

Andreas Wachter, PhD (2005) Glutathion-Synthese und Kompartimentierung in der Pflanze: Nachweis komplexer Regulationsmechanismen. University of Heidelberg.
Current occupation: Postdoctoral fellow, Yale University, USA.

Markus Schirmer, PhD (2004) Klonierung, Charakterisierung und Überexpression von Pyrophosphatasen in *Beta vulgaris* L. University of Heidelberg.
Current occupation: Highschool teacher.

Manfred Jugold, PhD (2004) Zur Bedeutung der polyTC-Motive in den Promotoren und 5'UTR-Bereichen konstitutiv exprimierter Gene. University of Heidelberg.
Current occupation: Postdoctoral fellow, DKFZ, Heidelberg.

Michelle Pfister, PhD (2003) Ektopische Expression von NtCIF und NtVIF in Kartoffelpflanzen: Posttranslationale Inhibition der wundinduzierten ZWI- und VI-Aktvitäten. University of Heidelberg.
Current occupation: not known.

Markus Kiefer, PhD (2002) Zum antioxidativen Verteidigungssystem bei *Mesembryanthemum crystallinum.* University of Heidelberg,
Current occupation: Postdoctoral fellow, HIP, Heidelberg.

An Invertase Inhibitor from Maize Localizes to the Embryo Surrounding Region during Early Kernel Development

Nicholas J. Bate*, Xiping Niu, Yuwen Wang, Kellie S. Reimann, and Timothy G. Helentjaris

Agronomic Traits, Trait and Technology Development, Pioneer Hi-Bred International, 7250 N.W. 62nd Avenue, Johnston, Iowa, 50131-0552

Invertase activity is thought to play a regulatory role during early kernel development by converting sucrose originating from source leaves into hexoses to support cell division in the endosperm and embryo. Invertases are regulated at the posttranslational level by small protein inhibitors, INVINHs. We found that in maize (*Zea mays*), an invertase inhibitor homolog (*ZM-INVINH1*) is expressed early in kernel development, between 4 and 7 d after pollination. Invertase activity is reduced in vitro in the presence of recombinant ZM-INVINH1, and inhibition is attenuated by pre-incubation with sucrose. The presence of a putative signal peptide, fractionation experiments, and ZM-INVINH1::green fluorescent protein fusion experiments indicate that the protein is exported to the apoplast. Moreover, association of ZM-INVINH1 with the glycoprotein fraction by concanavalin A chromatogaphy suggests that ZM-INVINH1 interacts with an apoplastic invertase during early kernel development. *ZM-INVINH1* was localized to the embryo surrounding region by in situ analysis, suggesting that this region forms a boundary, compartmentalizing apoplast invertase activity to allow different embryo and endosperm developmental rates.

Kernel development in maize (*Zea mays*) proceeds through a series of tightly regulated, overlapping stages. After double fertilization, during the prestorage phase, two distinct cell types are established: the triploid endosperm and the diploid embryo. Despite clearly different cell fates, the embryo and endosperm both rely upon photosynthate from source leaves transported through the maternal pedicel region of the developing kernel, ending at the terminal phloem cells. The presence of Suc-hydrolyzing enzymes, which produce hexose sugars from Suc, have been identified as critical for the establishment of the prestorage phase of seed development, and Suc hydrolysis is an important component of realizable plant yield (Cheng and Chourney, 1999; Weschke et al., 2003). The "invertase control hypothesis," largely based on work from dicots (Wobus and Weber, 1999), is supported in maize by the presence of a cell wall invertase, INCW2, localized to the basal endosperm transfer layer (Talercio et al., 1999). Mutations in this gene result in miniature kernels (the *mn1* mutation) and have a severely reduced endosperm (Cheng et al., 1996; Vilhar et al., 2002). Recently, the association of a IVR2, a soluble invertase expressed during early kernel development, with seed yield under conditions of limiting photosynthesis suggests that soluble invertases also play a significant role in providing hexose sugars to support cell division during the prestorage phase (Andersen et al., 2002), as has been previously suggested (Zinselmeier et al., 1999).

Invertases exhibit complex regulation at the transcriptional and posttranscriptional levels in response to developmental, environmental, and carbohydrate signals (Sturm, 1999). In addition, small (<20-kD) inhibitor proteins (INVINH) have been associated with invertase preparations in a number of dicot plant species (Pressey, 1994; Weil et al., 1994; Krausgrill et al., 1996, 1998; Greiner et al., 1998, 2000) since their first biochemical characterization (Pressey, 1966; Jaynes and Nelson, 1971). Recently, the first gene encoding an INVINH was characterized from tobacco (*Nicotiana tabacum*) and was shown to have inhibitory activity by assaying the effect of recombinant protein on invertase activity in vitro (Greiner et al., 1998). Transgenic studies, ectopically expressing tobacco *NtINVINH1*, demonstrated that overexpression reduces invertase activity in vivo and reduces the cold-induced sweetening of potato (*Solanum tuberosum*) tuber (Greiner et al., 1999). In addition, the activity of apoplastic versions of INVINH can be attenuated by the addition of low concentrations of Suc (Sander et al., 1996), suggesting the existence of a three-way regulatory switch involving invertase, INVINH, and Suc that serves to regulate sink strength and carbohydrate partitioning in plants (Krausgrill et al., 1998).

Here, we present the characterization of an invertase inhibitor from maize and demonstrate inhibitory activity by reducing invertase activity in vitro with recombinant ZM-INVINH1. Characterization of ZM-INVINH1 reveals that it is an early kernel-specific,

* Corresponding author; e-mail nic.bate@pioneer.com; fax 515-334-4788.

Article, publication date, and citation information can be found at www.plantphysiol.org/cgi/doi/10.1104/pp.103.027466.

embryo surrounding region (ESR)-localized, and apoplast-targeted protein. The role of ZM-INVINH1 may be to compartmentalize invertase activity within the early kernel to allow the endosperm and embryo to follow different rates of cell division and distinct developmental programs.

RESULTS

Identification of ZM-INVINH1

To identify invertase inhibitor homologs from maize, we screened DuPont/Pioneer databases with previously characterized dicot INVINH protein sequences. Three distinct sequences had a similar size and shared sequence homology with dicot INVINH proteins. One contig had an expressed sequence tag (EST) representation that suggested it was kernel specific, with two EST sequences originating from coencytic embryo sac libraries 4 d after pollination (DAP). Full-length sequence analysis revealed an open reading frame of 528 nucleotides, with a deduced amino acid sequence of 176 residues (Fig. 1). The other two *INVINH*-related genes in maize were restricted to either tassel libraries or libraries constructed from maize cell culture (GenBank accession nos. AX214357 and AX214336, respectively). On the basis of protein size and homology, these sequences represent the closest maize homologs to dicot INVINH proteins present in the public and our proprietary databases. To more clearly define the role of invertase inhibitor proteins in seed development, we concentrated on the EST with a library distribution limited to early kernel development and designate it as *ZM-INVINH1*.

ZM-INVINH1-deduced protein sequence has an apparent signal peptide sequence of 22 amino acid residues resulting in a mature protein of 17.7 kD, a size that is in keeping with other INVINH-related proteins (Pressey, 1994; Weil et al., 1994). Analysis of the full-length protein sequence by PSORT (http://psort.nibb.ac.jp/) suggests that the protein is targeted to the apoplast. Comparison of ZM-INVINH1 protein sequence with other INVINH-related gene products from dicots shows the conservation of four Cys residues as well as other amino acids spaced throughout the protein (Fig. 2).

Comparison of ZM-INVINH1 with the closest homologs in grass species reveals a higher degree of similarity, approaching 50% across the entire protein region. In the most recent public rice (*Oryza sativa*) sequence, three INVINH-related sequences exist, and we have identified an additional sequence (CAC69344). Two of the rice INVINH1-like sequences are in close proximity on chromosome four, separated by 1,437 bp, suggesting duplication (AL606658). The fourth rice sequence is present on chromosome 2 (AP004069). Two wheat (*Triticum aestivum*) INVINH-related sequences have also been identified in libraries from floral tissue 3 and 7 DAP (Fig. 2).

Effect of Recombinant ZM-INVINH1 on Maize Invertase Activity

To determine whether ZM-INVINH1 functions as an invertase inhibitor in vitro, we produced ZM-INVINH1 recombinant protein and assayed its ability to reduce invertase activity in a crude insoluble enzyme preparation from 10-DAP kernels. Figure 3 demonstrates that increasing the concentration of inhibitor in invertase reactions results in a quantitative decrease in invertase activity. The presence of 20 pmol of inhibitor protein reduces invertase activity by approximately 3-fold. A characteristic feature of

```
   1  GAATTCGCCC TTGGTAGATG TCTAGATGAC CTATTCTACT TTTCCTAAGA TTTTCTCTGT ATGAGTAACC TGTCATAATT
                                                  M  K  L  L  Q  A  L  C  P  L  V  I  L  L  A  C  S  T
  81  TAACTTGTGA GATCTTGCCG ATATAAAAAA AAAACGCCAG TCATTTATGG TACGGGATTA ATAGGTTCCA AGAACCAGCC
                S  N  A  S  V  L  Q  D  A  C  K  S  F  A  A  K  I  P  D  T  G  Y  A  Y  C  I
 161  ACAATCCATT TATTAGTTTC ATATAAATGT CATAAATTTT TACTAAAATT TTCTCTGTAT AGTAACATGT CATAACTGAA
      K  F  F  Q  A  D  R  G  S  A  G  A  D  K  R  G  L  A  A  I  A  V  R  I  M  G  A
 241  CTTGTGAGAA AAACGCCAGT TATTTATGGT ACGGGATTAA TAGGTTCCAA AAACCAGCCG TAACCTATTT ATATTAGGGT
      A  A  K  S  T  A  S  H  I  A  A  L  R  A  S  E  K  D  K  E  R  L  A  C  L  S  D
 321  ACTTTAAGCT GGTGCCCTCA GTTTTGTTGG TGTCTTCGTT TTTAAACTTA GTTGTATTTT TTTTCTTAGT TCTGTCCTTC
      C  S  E  V  Y  A  Q  A  V  D  Q  T  G  V  A  A  K  G  I  A  S  G  T  P  R  G
 401  TAGTGTTATA GAGCATAAGG ACAAAATTGA GCAAAAAATG ACTAAGGATA AAAATGAGGA TATCAGAAAG GGCAGCAGCT
      R  A  D  A  V  M  A  L  S  T  V  E  D  A  P  G  T  C  E  Q  G  F  Q  D  L  S  V
 481  TAAAAAACCT TTTATATTAG TTCAAAAGGA CACCAGTCTA TAAAAAGTAT ACTCCAAGCA CATTTGAATT TGGATTTGCA
      R  S  P  L  A  S  E  D  A  G  F  R  K  D  A  S  I  A  L  S  V  T  A  A  L
561  TTGTCAGTCA GGCCAGTCAA GGGGACCATG AAGCTTCTGC AAGCTCTGTG CCCTCTCGTC ATCCTCCTCG CCTGCTCCAC
641  GTCCAACGCT TCCGTCCTAC AAGACGCGTG CAAGTCCTTC GCCGCTAAGA TCCCGGACAC CGGCTACGCC TACTGCATCA
721  AGTTCTTCCA GGCCGACAGG GGAAGCGCCG GCGCGGACAA GCGTGGCCTC GCCGCCATCG CCGTGAGGAT CATGGGGGCA
801  GCCGCCAAGA GCACCGCCAG TCACATCGCC GCCCTGCGGG CCTCCGAGAA GGACAAGGAG CGGCTGGCGT GCCTCAGCGA
881  TTGCTCCGAG GTGTACGCGC AGGCCGTGGA CCAGACCGGC GTGGCGGCGA AGGGCATCGC CTCGGGCACG CCCCGGGGCC
961  GCGCGGACGC GGTGATGGCG CTCAGCACGG TGGAGGATGC CCCCGGCACC TGTGAGCAGG GGTTCCAGGA CCTGAGCGTG
1041 CGTTCGCCGC TGGCCTCGGA GGACGCCGGG TTCCGGAAGG ATGCGTCCAT CGCGCTGTCT GTAACGGCCG CGTTGTAAGC
1121 AAAGGTGTAT AATCCTTTTC GATATAGGTT AAAAATGAAT AAAAAAAAAA AAAAAGGGCG GCCGC
```

Figure 1. Nucleotide and deduced amino acid sequence of the *ZM-INVINH1* gene, including 587 bp upstream of the ATG. The deduced amino acid sequence is presented above the DNA sequence. Putative TATA sites are underlined, and the site of the longest cDNA clone is indicated by a double underline.

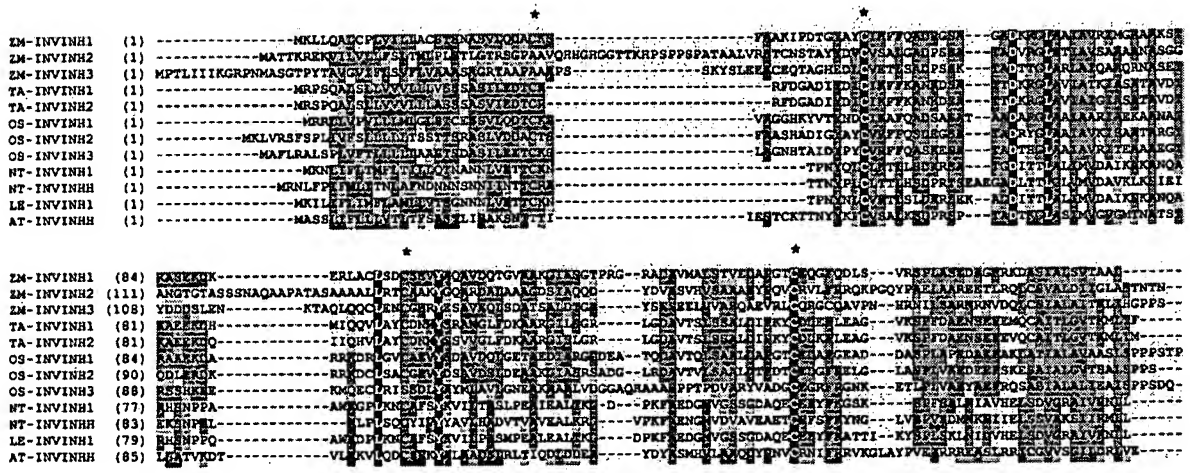

Figure 2. Comparison of ZM-INVINH1 with other invertase inhibitor-like proteins. Alignment of the deduced amino acid sequence of INVINH-like proteins from maize (ZM-INVINH1, ZM-INVINH2, and ZM-INVINH3), wheat (TA-INVINH1 and TA-INVINH2), rice (OS-INVINH1, OS-INVINH2, and OS-INVINH3), as well as previously published sequences from tobacco (NT-INVINH1 and NT-INVINHH), tomato (*Lycopersicon esculentum*; LE-INVINH1), and Arabidopsis (AT-INVINHH). Conserved Cys residues are indicated by asterisks.

invertase inhibitor proteins is that their inhibitory activity is reduced by the presence of Suc in the reaction. In Figure 3B, we demonstrate that inclusion of Suc concentrations as low as 1 mM has a significant attenuating effect on the reduction of invertase activity in vitro. In a separate experiment, we compared the ability of recombinant ZM-INVINH1 to reduce the activity of soluble and insoluble invertase activity (Table I). In this experiment, 20 pmol of recombinant ZM-INVINH1 reduced kernel soluble invertase activity by 5.3-fold and insoluble invertase by approximately 7-fold.

Localization of ZM-INVINH1

An apparent signal peptide suggests that ZM-INVINH1 is partitioned to the apoplast, where it targets apoplastic invertase. Apoplastic invertase is ionically bound to the cell wall and can be extracted with high-salt buffers, such as 1 M NaCl. We therefore used high-salt extraction, combined with western blotting to confirm the partitioning of ZM-INVINH1 in the cell wall fraction. Figure 4A shows that ZM-INVINH1 is present in significant proportion in the high-salt fraction and present in lower levels in the particulate fraction after the salt wash. Another diagnostic feature of invertases is *N*-glycosylation (Sturm, 1999), and association of non-glycosylated INVINH proteins with invertase has been indirectly shown by affinity purification with conconavalin A (ConA) chromatography (Weil et al., 1994; Greiner et al., 2000). Figure 4B demonstrates that ConA chromatography partitions ZM-INVINH1 into the glycosylated protein fraction, providing further evidence for a physical interaction between ZM-INVINH1 and invertase enzymes in maize. A high molecular mass protein, with an apparent size of approximately 75 kD, is present in western blots with ConA preparations, and a faint band of similar size appears in western-blot analysis of total protein preparations (Fig. 4A, lanes 1 and 2).

To further characterize the intercellular location of ZM-INVINH1, we used green fluorescent protein (GFP) targeting by bombardment of a ZM-INVINH1::GFP fusion into onion epidermal cells. GFP alone, under the control of a constitutive promoter, fluoresces throughout the cell, including the nucleus (Fig. 5, A and B). A higher magnification clearly shows cytoplasmic streams (Fig. 5B), indicating that the protein is partitioned to the cytoplasm as has been previously discussed (Scott et al., 1999). GFP fused to the C terminus of ZM-INVINH1 has a distinct pattern of fluorescence: No signal is detectable in the nucleus or vacuole, no cytoplasmic streams are evident, and ZM-INVINH1-targeted GFP fluorescence is restricted to the outer edges of the onion cells (Fig. 5, C–F). Fluorescent signal was shown to spread to adjacent cells as shown in Figure 5F, which is a diagnostic feature of small, nonanchored apoplastic proteins. In addition, a strong fluorescence signal required incubation of the bombarded cells with neutral pH, further suggesting that the fusion is targeted to the apoplast, where a low pH quenches the fluorescence signal (Scott et al., 1999).

Expression and Localization of ZM-INVINH1

EST distribution for *ZM-INVINH1* was restricted to 4-DAP libraries and suggests a low level of expression because only two ESTs are present. Consistent with this, expression was not reliably detected by northern-blot analysis. To verify the restricted spatial and temporal pattern of expression, we performed reverse transcriptase (RT)-PCR using RNA isolated from leaf,

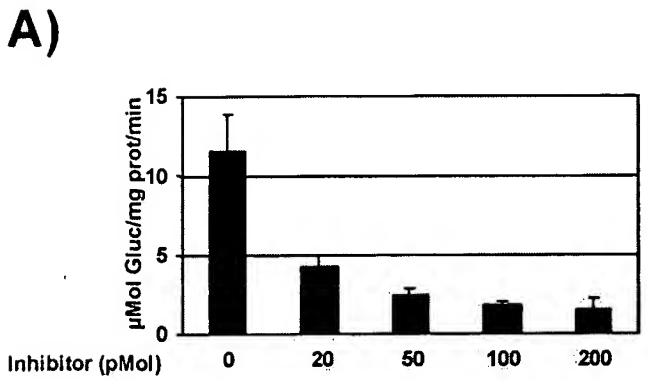

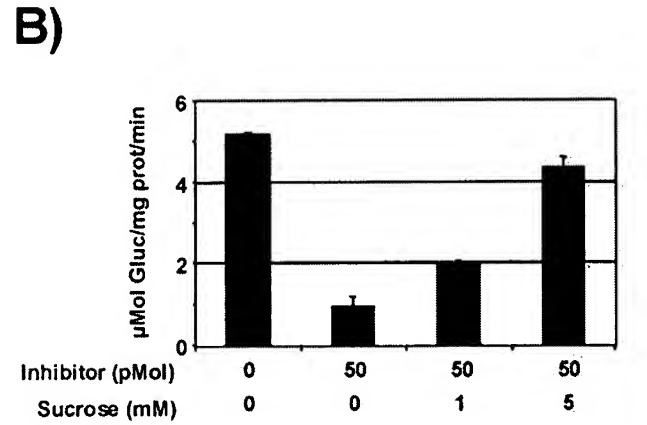

Figure 3. Recombinant ZM-INVINH1 inhibits invertase activity in vitro. ZM-INVINH1 produced in *Escherichia coli* was pre-incubated with an enzyme extraction from maize kernels harvested at 10 DAP. A, Invertase activity measured after pre-incubation with 20 to 200 pmol of recombinant ZM-INVINH1. B, Effect of Suc on ZM-INVINH1 inhibition of invertase activity. Pre-incubation of 10-DAP kernel enzyme extract with 50 pmol of ZM-INVINH1 and 1 or 5 mM Suc. The data are presented as a mean ± SD of three reactions.

root, and tassel tissues, as well as from a range of early kernel development time points (Fig. 6). No message was detectable by RT-PCR in any tissue other than early kernel development, and *ZM-INVINH1* transcript accumulation decreased dramatically after 4 DAP to almost undetectable levels by 10 DAP.

To further characterize the role of ZM-INVINH1 in the invertase-mediated control of early kernel development, we used in situ analysis to determine the spatial pattern of *ZM-INVINH1* expression. In situ analysis was performed on 5-DAP kernels because this is close to the peak of expression as determined by RT-PCR (Fig. 6). Figure 7 demonstrates that expression of *ZM-INVINH1* is restricted to a very defined region surrounding the embryo. This region, called the ESR, has been previously characterized as one of the four cell types of the developing endosperm (Olsen, 2001). Previously, a group of small proteins with a similar pattern of expression in maize have been characterized (ESR1–3; Opsahl-Ferstad et al., 1997; Benello et al., 2000), suggesting the ESR is a

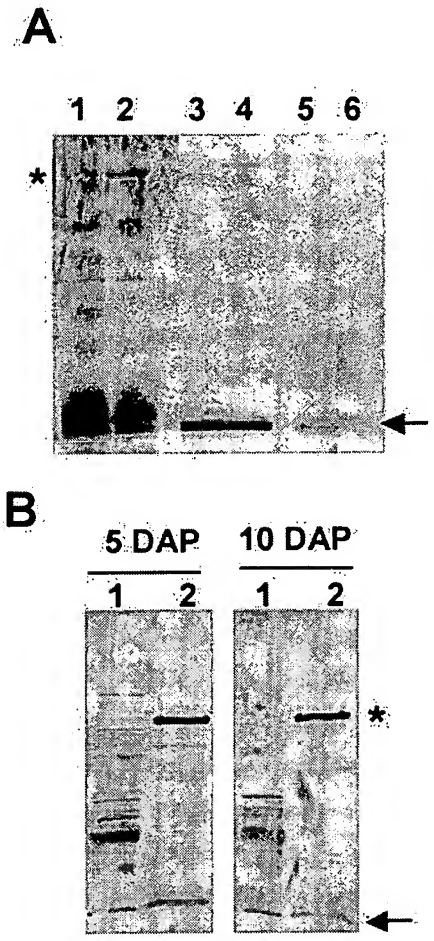

Figure 4. Fractionation of ZM-INVINH1. A, Proteins isolated from 5-DAP (odd lanes) and 10-DAP (even lanes) kernels were fractionated into soluble (lanes 1 and 2), high-salt wash (lanes 3 and 4), and insoluble fractions (lanes 5 and 6) and subjected to western-blot analysis with antibody raised against ZM-INVINH1. Fifty micrograms of total soluble protein and 20 µg of high-salt and insoluble protein were separated by SDS-PAGE, and western-blot analysis was performed with ZM-INVINH1 antibody. B, ZM-INVINH1 associates with the glycoprotein fraction in maize kernels. Glycoproteins were isolated from 5- and 10-DAP kernels by ConA chromatography, and ZM-INVINH1 was detected by western-blot analysis. Lanes 1 and 2 correspond to ConA chromatography flow through and eluate, respectively. A large arrow represents ZM-INVINH1, and an asterisk indicates a high M_r cross-reacting protein.

Table I. *Effect of recombinant invertase inhibitor on soluble and insoluble invertase activity from maize (n = 3). Twenty picomoles of recombinant invertase inhibitor was pre-incubated with soluble and insoluble preparations of kernel protein.*

Protein Preparation	Invertase Activity		
	−Inh	+Inh	-Fold Reduction
	µmol reducing sugar mg^{-1} protein min^{-1}		
Maize soluble	0.21	0.04	5.3
Maize insoluble	8.7	1.23	7.1

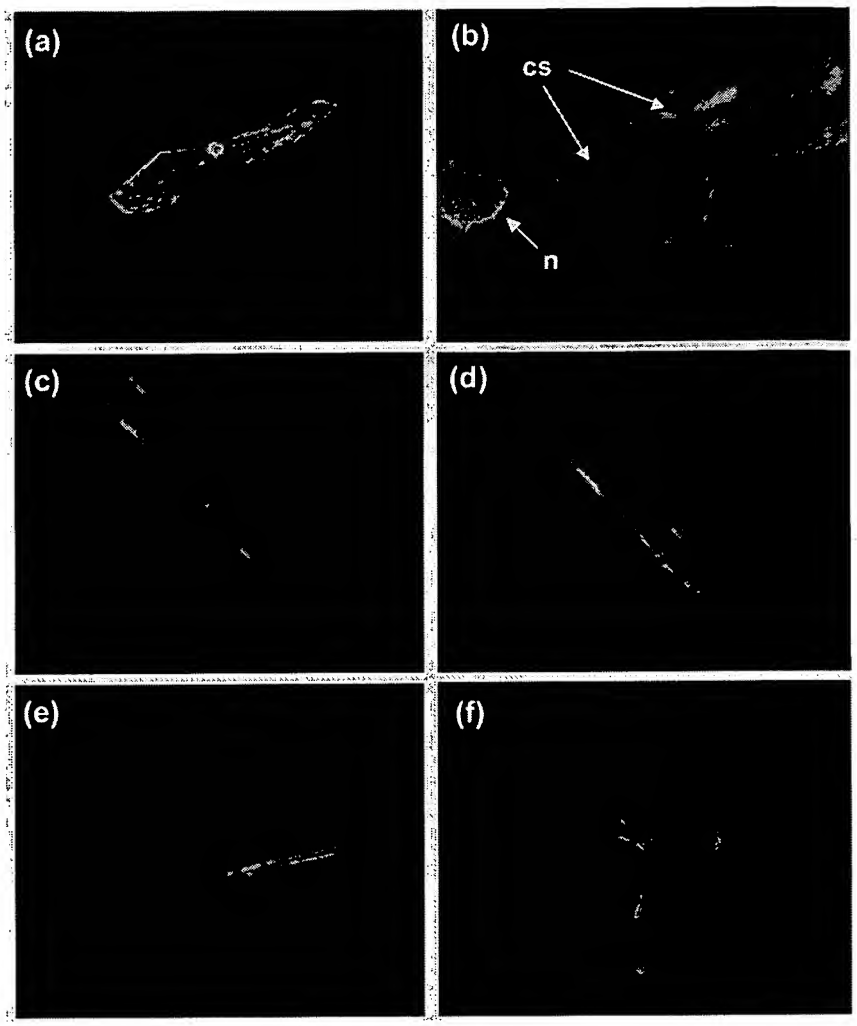

Figure 5. ZM-INVINH1 is targeted to the apoplast. Particle bombardment into onion epidermal cells was performed with GFP alone (A and B) or fused to ZM-INVINH1 at the C terminus (E and F) under the control of the maize ubiquitin promoter. Cytoplasmic streams and the nucleus evident in GFP bombardments are indicated by cs and n, respectively.

distinct compartment important for endosperm and embryo development (Bommert and Werr, 2001).

DISCUSSION

Invertase inhibitor proteins were first characterized biochemically as copurifying proteins in invertase enzyme preparations (Pressey, 1966; Jaynes and Nelson, 1971) and dicot genes encoding INVINH proteins with demonstrated activity in vitro (Greiner et al., 1998) and in vivo (Greiner et al., 1999) were recently characterized. Analysis of sequences from maize and other monocots indicates that there are at least two to three INVINH-related proteins in these species as well. Furthermore, phylogenetic tree analysis indicates that individual sequences share a greater degree of homology across species than exists for INVINH-related sequences within either species alone. Taken together, sequence analyses suggest that there are distinct classes of INVINH-related sequences within each species, potentially reflecting distinct invertase inhibitory activities or function. Identification is further complicated by structurally related proteins that have been demonstrated to have

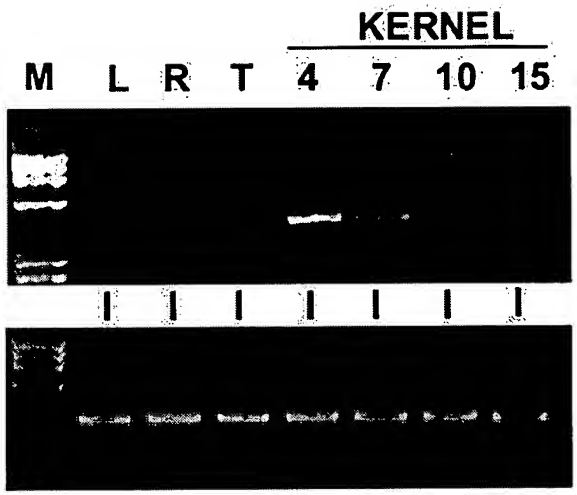

Figure 6. Expression analysis of *ZM-INVINH1* by RT-PCR. Top, Total RNA isolated from mature leaf (L), root (R), and tassel (T), as well as from whole kernels harvested 4, 7, 10, and 15 DAP was subjected to RT-PCR to amplify the *ZM-INVINH1* transcript. A M_r marker (M) is included. Bottom, A control reaction using primers designed to amplify maize tubulin was also performed.

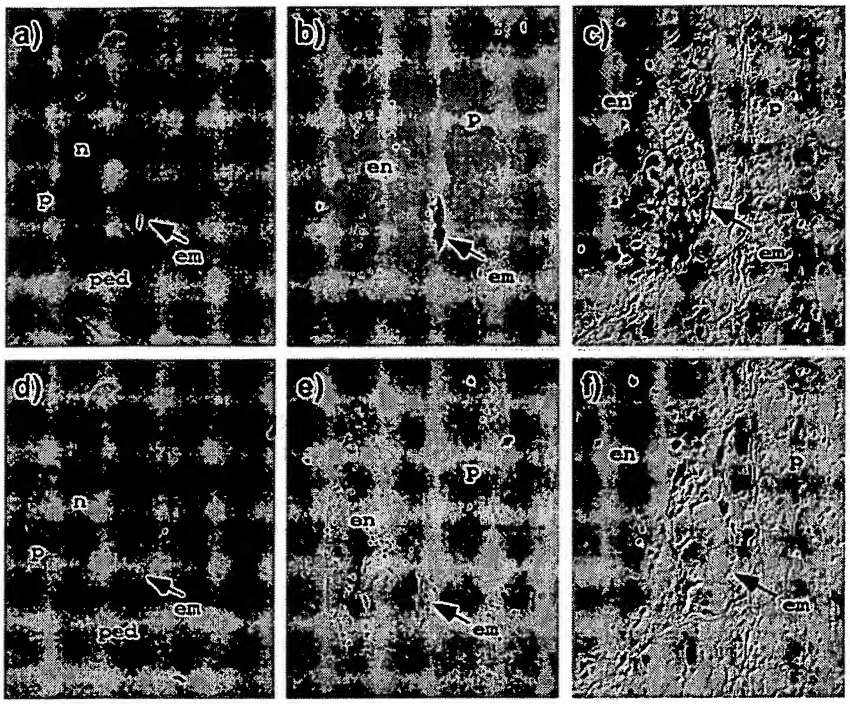

Figure 7. In situ analysis of *ZM-INVINH1* in 5-DAP kernels. Embedded and longitudinal kernel sections were hybridized with an antisense (A–C) or sense transcript (D–F) generated from *ZM-INVINH1*. ped, pedicel; n, nucellus; p, pericarp; en, endosperm; em, embryo.

distinct inhibitory activity (Camardella et al., 2000). Recombinant INVINH protein expression and in vitro demonstration of inhibitory activity may be the most definitive means to distinguish INVINH proteins from those with similar structure but distinct function.

ZM-INVINH1 produced as a recombinant protein inhibits maize invertase in a dose-dependent manner, establishing it as an invertase inhibitor. Similar to other INVINH proteins with demonstrated inhibitor activity, inhibition is attenuated by the presence of low Suc concentrations. In addition, ZM-INVINH1 associates with the glycoprotein fraction despite having no obvious glycosylation sites, as has been demonstrated for dicot INVINH proteins (Sander et al., 1996; Krausgrill et al., 1998; Greiner et al., 2000). Taken together, biochemical characterization indicates that *ZM-INVINH1* is the first invertase inhibitor gene identified from a monocot species.

ZM-INVINH1 is an early kernel, ESR-localized, apoplastic protein. The question therefore arises: Which invertase is ZM-INVINH1 inhibiting? At least three possible invertase targets for ZM-INVINH1 can be envisioned. First, ZM-INVINH1 could be inhibiting INCW2 present at low levels in the ESR region. INCW2 has been localized to the basal endosperm transfer layer by immunolocalization (Cheng et al., 1996) and in situ analysis (Talercio et al., 1999). However, it is possible that INCW2 may be present in the ESR at levels undetectable by either of these methods. A second possibility is that vacuolar-targeted IVR2, present in the ESR, is mis-localized to the cell wall. IVR2 has been localized to the pedicel region by in situ analysis (Andersen et al., 2002), and we have demonstrated a strong in situ hybridization signal for IVR2 transcript in the ESR at 5 DAP (Y. Wang and N.J. Bate, unpublished data). A third possibility is that ZM-INVINH1 functions to inhibit an as yet uncharacterized apoplastic invertase (INCW). In addition to INCW2, there are at least three cell wall invertases (INCW1, INCW3, and INCW4) that all have expression detectable in early kernels (Talercio et al., 1999; Comparot et al., 2003), albeit at very low levels relative to INCW2 and IVR2. Another related possibility is that ZM-INVINH1 functions as insurance against the activity of any apoplastic invertase activity in the cells surrounding the embryo, whether derived from INCW activity or mis-directed IVR activity. The ability of ZM-INVINH1 to inhibit both soluble and insoluble invertase activities suggests that this may be the case.

The importance of Suc/hexose ratio and the role of invertases in development has been well documented. Transported Suc acts as a carbon source for both the developing embryo and endosperm, yet these two cell types have distinct developmental programs and rates of cell division. By 4 DAP, the embryo has between eight and 32 nuclei, whereas the endosperm develops much more rapidly, having approximately 250 nuclei at the same stage (Randolph, 1936). Furthermore, the basal endosperm cells begin to differentiate at approximately 6 DAP (Kiesselbach, 1949), whereas embryo cells differentiate later. ZM-INVINH1 may therefore serve as a barrier to protect the slower developing embryo from hexoses supplied from an apoplastic invertase early post-pollination, allowing the proper developmental rate of the embryo. The transient presence of ZM-INVINH1 sug-

gests that by 7 to 10 DAP, the inhibitory barrier to invertase is no longer necessary.

The ESR is a region of cells within the endosperm, and three highly related proteins have been localized to the ESR by in situ localization and promoter::GUS fusion experiments (Opsahl-Ferstad et al., 1997; Benello et al., 2000). ESR1–3 are small proteins with some structural homology to the developmental ligand CLV3 from Arabidopsis (Brand and Simon, 2000), suggesting the possibility that ESR proteins play a developmental role in maize. ESR-localized ZM-INVINH1, which is about 2-fold larger than ESR1–3, share several features, most notably their ESR localization and apoplast targeting. Interestingly, a mammalian protein, uterglobin (also known as Clara2 and blastokinin), is a small protein that plays a signaling role and also serves as an enzyme inhibitor (Mukherjee et al., 1999). An intriguing possibility is that ZM-INVINH1 has a dual-function: as an invertase inhibitor and also performing a signaling role as has been suggested for the ESR1–3 proteins. Despite similar temporal and spatial expression, there is little similarity between ESR upstream regulatory regions and the 587 bp of *ZM-INVINH1* upstream sequence presented here (Fig. 1). Repeated sequences conserved between ESR1–3 promoters are absent, for example. Alignment of *ESR1-3* and *ZM-INVINH1* promoter regions identifies two small conserved sequences: AGCATA and T(A/T) AAAAT, present at −170 and −100, relative to the translational start site of *ZM-INVINH1*. More detailed analysis of the *ZM-INVINH1* and *ESR1-3* promoters will determine whether these sequences are important for ESR-localized expression.

Identification of *ZM-INVINH1* represents the first monocot invertase inhibitor gene to be characterized. In addition, the work presented here provides a bridge between invertase activity, known to be important for the control of carbohydrate partitioning, and the regulation of events during early kernel development by showing expression of *ZM-INVINH1* in the ESR, an important and intriguing cluster of cells surrounding the embryo. *ZM-INVINH1* therefore also provides a useful marker for early events in the establishment of the embryo and endosperm.

MATERIALS AND METHODS

Gene Isolation and Characterization

To characterize invertase inhibitor homologs from maize (*Zea mays*), we screened Pioneer/DuPont EST databases using a consensus sequence generated from alignment of previously characterized invertase homologs from dicot species. Full-length sequence for three maize invertase homologs were generated, and effort was concentrated on one homolog, designated *ZM-INVINH1*, present only in EST libraries from 4-DAP kernels. Rice (*Oryza sativa*) and wheat (*Triticum aestivum*) INVINH1-like cDNAs were characterized by screening Pioneer/DuPont EST databases using the *ZM-INVINH1* sequence.

Expression by RT-PCR

Mature leaves from 12-leaf (V12) plants, whole roots from 18-leaf (V18) plants, and preshed tassel or kernels 4, 7, 10, or 15 DAP were excised from field-grown public inbred (B73) plants. Total RNA was isolated using the Plant RNeasy kit from Qiagen (Valencia, CA). Total RNA (1 μg) was treated with amplification grade DNase (Invitrogen, Carlsbad, CA), according to the manufacturer's instructions, and RT reactions were performed using the Thermoscript kit according to manufacturer's instructions (Invitrogen) using an oligo(dT) primer. Primers specific to *ZM-INVINH1* were generated for RT-PCR: CCAGTCAAGGGGACCATGAA and ATGCATTGGAACCCCTGCTCACAGGTGC. Primers designed to maize tubulin were used as a control for loading and amplification. PCR conditions were optimized, and amplification was cycled 25 times.

Recombinant Protein Expression and Invertase Activity

Recombinant protein was produced using the pET expression system from Novagen (Madison, WI) by cloning the *Hin*dIII site immediately downstream of the ATG start, in frame with the poly-His tag of pET28. *Not*I from the *ZM-INVINH1* vector was used at the 3′ end. Recombinant protein was produced in BL21 (Lys) cells according to standard protocols, and affinity chromatography was performed using a cesium column and FPLC. Protein purity was estimated at >75%, and protein concentration determined using Coomassie PLUS (Pierce, Rockford, IL) using bovine serum albumin as a standard. Recombinant protein was dialyzed against 50 mM Tris-HCl (pH 7.5), 100 mM NaCl, and 1 mM phenylmethylsulfonyl fluoride. For long-term storage, recombinant protein preparations were combined with an equal volume of 50% (w/v) glycerol, aliquoted into working volumes, and stored at −80°C.

Inhibition of invertase activity was measured using protein preparations from 10-DAP kernels from a public inbred (B73), isolated as described by Cheng et al., 1996. Excised kernels, ground in liquid nitrogen and stored at −80°C, were mixed with cold isolation buffer (10 mM Tris, pH 7.5, and 1 mM phenylmethylsulfonyl fluoride) in a 1:4 (w/v) ratio. The slurry was centrifuged in an Eppendorf centrifuge at full speed for 10 min, the supernatant was removed (soluble fraction), and the pellet was washed five times with cold isolation buffer by resuspension and centrifugation. Washed pellet fractions were incubated for 30 min on ice with isolation buffer plus 1 M NaCl. After centrifugation, the supernatant was dialyzed overnight against isolation buffer using micro-slide-a-lyzer dialysis units from Pierce. Protein was quantified by Bradford reagent (Bio-Rad Laboratories, Hercules, CA). Invertase activity was measured by adapting a protocol of the Nelson's assay (Jaynes and Nelson, 1971) for 96-well plates. Fifty microliters of soluble or insoluble enzyme preparation was incubated with 2% (w/v) Suc at 37°C for 30 min before transfer to Somagyi's reagent and heating to 100°C for 10 min. After addition of Nelson's reagent to the mixture, reducing sugars were measured by A_{520} in a spectrophotometer (SpectraMax 190, Molecular Devices, Sunnyvale, CA). ZM-INVINH1 and Suc treatments were performed by pre-incubation of the reaction mixture with known concentrations of recombinant protein or Suc for 10 min before addition of 2% (w/v) Suc.

In Situ Analysis

Greenhouse-grown inbred maize (public inbred B73) was grown in a greenhouse in Johnston, Iowa. Kernels were taken from the middle of ears harvested at 5 DAP. Longitudinal median sections containing embryos were obtained and immediately fixed in 4% (w/v) paraformaldehyde (in phosphate-buffered saline [PBS; 100 mM sodium phosphate and 100 mM NaCl, pH 7.5]), which was prepared in diethyl pyrocarbonate-treated deionized, distilled water. Fixation, sectioning, and in situ conditions were as published previously (Woo et al., 2001). Digoxigenenin (DIG)-labeled sense and antisense RNA probes were synthesized in vitro by transcription of linearized pBluescript II KS+ plasmids with T3 or T7 RNA polymerase (Roche Diagnostics). For *ZM-INVINH1*, a *Hin*dIII/*Sma*I fragment was used to reduce nonspecific binding from the poly(A) sequence present in the cDNA. After hybridization, slides were washed three times in 50% (v/v) formamide, 2× SSC (1× SSC is 0.15 M NaCl and 0.015 M sodium citrate) and 0.2× SSC for a total of 120 min. Between these stringent washes, the slides were treated with 10 μg mL^{-1} RNase A for 30 min at 37°C. DIG-labeled probes were detected with anti-DIG antibody conjugated with alkaline

phosphatase (AP) and an AP color reaction (Roche Diagnostics), which produces a red precipitate.

GFP Localization

To visualize subcellular localization of ZM-INVINH1, we used GFP imaging as has been previously described (Scott et al., 1999). A control plasmid (GFP) and the ZM-INVINH1 fusion plasmid (the entire coding sequence fused in-frame to GFP), both under the control of the maize ubiquitin promoter, were bombarded into onion epidermal cells with 1-μm Tungsten particles using a Biolistic 100 (Bio-Rad Laboratories; placed onto Murashige and Skoog plates, with 10 mg L^{-1} L-ascorbic acid) at 650 pounds per square inch. Bombarded cells were incubated for 48 h before incubation with 20 mM PIPES buffer pH 7.0 (Scott et al., 1999) for 3 h. GFP fluorescence was visualized by epifluorescence microscopy using a microscope (SMZ1500, Nikon, Tokyo).

Protein Isolation and Analysis

For fractionation studies, the lower one-third of 5- and 10-DAP kernels was ground in liquid nitrogen and stored at −80°C. Total proteins were extracted by grinding frozen tissue with 4 volumes (v/w) of extraction buffer (50 mM Tris, pH 8.0, 100 mM KCl, 5% [w/v] glycerol, 10 mM dithiothreitol, 2% [w/v] polyvinylpolypyrrolidone, 1 mM EDTA, and 4 mM PefaBloc [Roche Diagnostics]) before centrifugation at full speed in an Eppendorf microfuge at 4°C. Total soluble proteins were removed, and the pellet was washed by adding 10 volumes of extraction buffer, mixing, and centrifuging as above for a total of five times. The insoluble pellet was incubated for 1 h at 4°C in three volumes of 1 M NaCl and 50 mM Tris, pH 7.5, before centrifugation. Pellets from this fraction represent the insoluble fraction. Sodium chloride wash fractions were dialyzed overnight at 4°C as for invertase enzyme assays. Fifty micrograms of total soluble protein and 20 μg of high-salt and insoluble fractions were separated by SDS-PAGE for western analysis.

For affinity purification of the glycoprotein fraction, proteins were subjected to ConA chromatography. Whole-kernel fresh frozen tissue was incubated with extraction buffer (50 mM citric acid, pH 4.6, 500 mM NaCl, 5 mM dithiothreitol, and 1 mM Pefabloc [Roche Diagnostics]), filtered through four layers of cheesecloth, and centrifuged for 10 min at 10,000 rpm in a JA17 rotor (Beckman Coulter, Fullerton, CA). The supernatant was removed, and NH_4SO_4 added to 90% (w/v) and stirred on ice for 90 min. After centrifugation as above, the pellets were resuspended in 2 mL of column buffer (50 mM sodium acetate, pH 6.3, 500 mM NaCl, 1 mM $CaCl_2$, 1 mM $MgCl_2$, 1 mM $MnCl_2$, and 1 mM Pefabloc). The resuspended proteins were dialyzed overnight against two changes of column buffer using Slide-A-lyzer dialysis membranes (3000-D molecular weight cut-off, Pierce). Hi-Trap ConA columns (Pharmacia, Uppsala) were equilibrated with 10 mL of column buffer using a syringe. Samples were added to the column at a rate of one drop every 2 to 3 s. An aliquot was removed from the column flow-through for analysis before washing immobilized proteins with five column volumes of column buffer. Proteins were eluted with 3 mL of 15% (w/v) methyl-α-glucopyranoside and concentrated in a centricon-10 microconcentrator (Ambion, Austin, TX). Thirty micrograms of protein from flow through and affinity-purified fractions was used for western-blot analysis.

Antibodies were raised against recombinant ZM-INVINH1 in New Zealand White rabbits at HTI Bioproducts (Ramona, CA), raised on a maize-free diet. Affinity-purified His tag fusions of ZM-INVINH1 were denatured in 5 M urea for 5 min at 100°C and used as antigens. Antibody titer was determined using purified antigen, and crude serum was used as a 1:2,000 (v/v) dilution in western-blot experiments.

For western-blot analysis, proteins were separated by SDS-PAGE, blotted onto PVDF membranes (Bio-Rad Laboratories), and blocked according to standard protocols issued by the manufacturer, using either 5% (w/v) nonfat milk or Superblocker (Pierce). Primary antibody was diluted 1:2,000 in PBS with 0.1% (v/v) Tween 20 for several hours to overnight. Blots were washed several times in PBS with 0.1% (v/v) Tween 20 before incubating with a secondary antibody (goat anti-rabbit, AP conjugated, Sigma-Aldrich, St. Louis) for 1 h. Blots were subsequently washed before visualizing immunoreactive signal by AP color development.

Distribution of Materials

Novel materials described in this publication may be available for noncommercial research purposes upon acceptance and signing of a material transfer agreement. In some cases, such materials may contain or be derived from materials obtained from a third party. In such cases, distribution of material will be subject to the requisite permission from any third-party owners, licensors, or controllers of all or parts of the material. Obtaining any permissions will be the sole responsibility of the requestor.

ACKNOWLEDGMENTS

We are grateful to Gabrielle Tordensen and Tom Davis and the protein production facility at Pioneer for working with us to produce functional recombinant ZM-INVINH. Odd-Arne Olsen and Cunxi Wang provided helpful and insightful discussion. Virginia Crane and Jeanne Sandahl helped with bombardment, and Bill Gordon-Kamm helped with GFP localization. In addition, we are grateful to Jeff Mullen, Chris Zinselmeier, and other members of the Yield Stability Group for helpful suggestions and productive collaboration.

Received May 27, 2003; returned for revision August 12, 2003; accepted October 10, 2003.

LITERATURE CITED

Andersen MN, Asch F, Wu Y, Jensen CR, Næsted H, Mogensen VO, Koch KE (2002) Soluble invertase expression is an early target of drought stress during the critical, abortion-sensitive phase of young ovary development in maize. Plant Physiol **130:** 591–604

Benello J-F, Opsahl-Ferstad H-G, Perez P, Dumas C, Rogowsky PM (2000) *Esr* genes show different levels of expression in the same region of maize endosperm. Gene **246:** 219–227

Bommert P, Werr W (2001) Gene expression patterns in the maize caryopsis: clues to decisions in embryo and endosperm development. Gene **271:** 131–142

Brand U, Simon R (2000) Dependence of stem cell fate in Arabidopsis on a feedback loop regulated by CLV3 activity. Science **289:** 617–619

Camardella L, Carrotore V, Ciardiello MA, Servillo L, Balestrieri C, Giovane A (2000) Kiwi protein inhibitor of pectin methylesterase amino-acid sequence and structural importance of two disulfide bridges. Eur J Biochem **267:** 4561–4565

Cheng WH, Chourney P (1999) Genetic evidence that invertase-mediated release of hexoses is critical for appropriate carbon partitioning and normal seed development in maize. Theor Appl Genet **98:** 485–495

Cheng W-H, Taliercio EW, Chourey PS (1996) The Miniature1 seed locus of maize encodes a cell wall invertase required for normal development of endosperm and maternal cells in the pedicel. Plant Cell **8:** 971–983

Comparot S, Lingiah G, Martin T (2003) Function and specificity of 14-3-3 proteins in the regulation of carbohydrate and nitrogen metabolism. J Exp Bot **54:** 595–604

Greiner S, Koster U, Lauer K, Rosenkranz H, Vogel R, Rausch T (2000) Plant invertase inhibitors: expression in cell culture and during plant development. Aust J Plant Physiol **27:** 807–814

Greiner S, Krausgrill S, Rausch T (1998) Cloning of a tobacco apoplasmic invertase inhibitor: proof of function of the recombinant protein and expression analysis during plant development. Plant Physiol **116:** 733–742

Greiner S, Rausch T, Sonnewald U, Herbers K (1999) Ectopic expression of a tobacco invertase inhibitor homolog prevents cold-induced sweetening of potato tubers. Nat Biotechnol **17:** 708–711

Jaynes TA, Nelson OE (1971) An invertase inactivator in maize endosperm and factors affecting inactivation. Plant Physiol **47:** 629–634

Kiesselbach TA (1949) The Structure and Reproduction of Corn. Cold Spring Harbor Laboratory Press, Cold Spring Harbor, NY

Krausgrill S, Greiner S, Koster U, Vogel R, Rausch T (1998) In transformed tobacco cells the apoplasmic invertase inhibitor operates as a regulatory switch of cell wall invertase. Plant J **13:** 275–280

Krausgrill S, Sander A, Greiner S, Weil M, Rausch T (1996) Regulation of cell wall invertase by a proteinaceous inhibitor. J Exp Bot **47:** 1193–1198

Mukherjee AB, Kundu GC, Mantile-Selvaggi G, Yuan CJ, Mandal AK, Chattopadhyay S, Zheng F, Pattabiraman N, Zhang Z (1999) Uteroglobin: a novel cytokine? Cell Mol Life Sci **55:** 771–787

Olsen O-A (2001) Endosperm development: cellularization and cell fate specification. Annu Rev Plant Physiol Plant Mol Biol **52:** 233–267

Opsahl-Ferstad H-G, Le Deunff E, Dumas C, Rogowsky PM (1997) ZmEsr, a novel endosperm-specific gene expressed in a restricted region around the maize embryo. Plant J **12:** 235–246

Pressey R (1966) Separation and properties of potato invertase and invertase inhibitor. Arch Biochem Biophys **113:** 667–674

Pressey R (1994) Invertase inhibitor in tomato fruit. Phytochemistry **36:** 543–546

Randolph LF (1936) Developmental morphology of the caryopsis in maize. J Agric Res **53:** 881–916

Sander A, Krausgrill S, Greiner S, Weil M, Rausch T (1996) Sucrose protects cell wall invertase but not vacuolar invertase against proteinaceous inhibitors. FEBS Lett **385:** 171–175

Scott A, Wyatt P-L, Tsou D, Robertson D, Stromgren A (1999) Model system for plant cell biology: GFP imaging in living onion epidermal cells. Biotechniques **26:** 1125–1132

Sturm A (1999) Invertases: primary structures, functions, and roles in plant development and sucrose partitioning. Plant Physiol **121:** 1–7

Talercio E, Kim J-Y, Mahe A, Shaker S, Choi J, Cheng W-H, Prioul J-L, Chourey PS (1999) Isolation, characterization and expression analyses of two cell wall invertase genes in maize. J Plant Physiol **155:** 197–204

Vilhar B, Kladnik A, Blejec A, Chourey PS, Dermastia M (2002) Cytometrical evidence that the loss of seed weight in the miniature1 seed mutant of maize is associated with reduced mitotic activity in the developing endosperm. Plant Physiol **129:** 23–30

Weil M, Krausgrill S, Schuster A, Rausch T (1994) A 17-kDa *Nicotiana tabacum* cell-wall peptide acts as an in-vitro inhibitor of the cell-wall isoform of acid invertase. Planta **193:** 438–445

Weschke W, Panitz R, Gubatz S, Wang Q, Radchuk R, Weber H, Wobus U (2003) The role of invertases and hexose transporters in controlling sugar ratios in maternal and filial tissues of barley caryopses during early development. Plant J **33:** 395–411

Wobus U, Weber H (1999) Sugars as signal molecules in plant seed development. Biol Chem **380:** 937–944

Woo YM, Hu DW, Larkins BA, Jung R (2001) Genomics analysis of genes expressed in maize endosperm identifies novel seed proteins and clarifies patterns of zein gene expression. Plant Cell **13:** 2297–2317

Zinselmeier C, Jeong B-R, Boyer JS (1999) Starch and the control of kernel number in maize at low water potential. Plant Physiol **121:** 25–35

The Plant Journal (2003) **33**, 395–411

The role of invertases and hexose transporters in controlling sugar ratios in maternal and filial tissues of barley caryopses during early development

Winfriede Weschke*, Reinhard Panitz, Sabine Gubatz, Qing Wang†, Ruslana Radchuk, Hans Weber and Ulrich Wobus
Institut für Pflanzengenetik und Kulturpflanzenforschung (IPK), D-06466 Gatersleben, Germany

Received 1 July 2002; revised 26 September 2002; accepted 25 October 2002.
*For correspondence (Fax +49 39482 5138; E-mail weschke@ipk-gatersleben.de).
†Present address: Universität Hamburg, Institut für Allgemeine Botanik, Ohnhorststraße 18, D-22609 Hamburg, Germany.

Summary

To analyse carbohydrate metabolism and its role during early seed development of barley we characterised genes encoding two cell wall-bound invertases (HvCWINV1 and HvCWINV2) and two putative hexose transporter-like genes (*HvSTP1* and *HvSTP2*). No typical vacuolar invertase gene could be identified. Instead, a gene encoding sucrose:fructan 6-fructosyltransferase (*HvSF6FT1*), an enzyme with soluble acid invertase activity, was isolated and characterised. Furthermore, enzyme activities and sugar levels were measured. *HvSF6FT1*-mRNA levels and acid soluble invertase activity are highest in the maternal pericarp 1–2 days after flowering (DAF). *HvSF6FT1* is strongly expressed in regions flanking the main vascular bundle and to a lower extent in filial endospermal transfer cells, which persist until maturity and never accumulate starch. In contrast, cell wall-bound invertase HvCWINV2 is expressed early in development mainly in the style region and later on in pericarp areas which transiently accumulate starch and undergo degradation later in development. The hexose transporter HvSTP2 shows a temporal and spatial expression pattern similar to HvCWINV2. Transcripts of *HvCWINV1* have been localised within the first row of endospermal cells and in the outermost area of the nucellar projection as well as in endospermal transfer cells before starch filling; the same regions of the endosperm are labelled with a hexose transporter *HvSTP1*-probe. *HvSTP1* is expressed at very low levels within the pericarp but much higher in the syncytial endosperm at 3 DAF and in endospermal transfer cells 7 DAF. The temporal and spatial association of *HvCWINV1* and *HvSTP1* expression indicates that hexoses liberated by the invertase within the endospermal cavity are taken up by the transporter to be delivered into the central uncellularised space of the endosperm to supply mitotically active endosperm cells with hexoses. The results are discussed and compared with published data on the role of soluble sugars as signal molecules in seed developmental processes.

Keywords: barley seed development, sugar levels, invertase activity, seed-specific EST collection, invertase and hexose transporter isoforms, endospermal transfer cells.

Introduction

In sink organs sucrose hydrolysis is catalysed by sucrose synthases and/or invertases. Sucrose synthase in seeds is often associated with starch synthesis (Doehlert, 1990; Heim *et al.*, 1993; Weber *et al.*, 1996a; Weschke *et al.*, 2000). Invertases, on the other hand, have been correlated with developmental processes with highest activities measured before storage processes start (Sturm and Tang, 1999; Weber *et al.*, 1995). They can control developmental processes by regulating the sucrose to hexose ratio. For instance, differentiation in carrot cells is induced when acid invertase activity decreases (Silva and Ricardo, 1992) whereas its persistence at certain stages can delay differentiation by reducing the level of sucrose (Sturm, 1999).

At present, different roles are discussed for cell wall-bound and vacuolar (soluble) acid invertases. However, functions of different invertase classes are actually very similar and are distinguished mainly based on whether apoplastic or symplastic transport is involved. Cell wall-bound isoforms of invertase are most active in apoplastic sinks such as developing seeds and fungal symbionts where they facilitate unloading by increasing the concentration gradient of sucrose (Eschrich, 1989). Moreover, they

can be involved in sucrose partitioning (Eschrich, 1989), osmoregulation (Meyer and Boyer, 1981) and wound response (Matsushita and Uritani, 1974; Sturm and Chrispeels, 1990). In contrast, vacuolar or soluble acid invertases regulate hexoses/sucrose levels in vacuoles (Sturm, 1999; Winter and Huber, 2000). They are most active in growing zones and extending tissues such as root tips, internodes, and developing leaves. A large number of genes and cDNAs annotated as encoding acid soluble and cell wall-bound invertases have been cloned from different species. The sequences are characterised by N-terminal signals responsible for either vacuolar or apoplastic targeting. The two groups of enzymes are encoded by different small gene families (Sturm, 1999; Tymowska-Lalanne and Kreis, 1998).

Closely related to invertases are fructosyltransferases which, until recently, have been classified by BLASTX as soluble vacuolar invertases at least in the case of the northern grasses wheat and barley, possibly due to high sequence homologies between barley and wheat fructosyltransferase ESTs and the vacuolar invertase sequences of maize and rice. Fructosyltransferases most probably evolved from the acid soluble invertases (Van der Meer *et al.*, 1998; Wei and Chatterton, 2001). They synthesise fructans. As proposed by Edelman and Jefford (1968), the enzyme sucrose:sucrose 1-fructosyltransferase (1-SST; EC 2.4.1.99) catalyses the transfer of fructosyl residues to another sucrose molecule resulting in the formation of the trisaccharide 1-ketose and glucose. In a second step, fructan:fructan 1-fructosyltransferase (EC 2.4.1.100) transfers fructosyl residues from one fructan to another, producing a mixture of fructans with different chain length. In barley, the fructan molecule bifurcose is produced. This molecule is composed of (2–1)- and (2–6)-linked β-D-fructosyl units linked to sucrose (Vijn and Smeekens, 1999). The β-2(r)6-linkage of fructosyl residues is probably brought about by sucrose:fructan 6-fructosyltransferase (6-SFT; EC 2.4.1.10), an enzyme which acts mainly as an invertase if only sucrose is available as a substrate (Sprenger *et al.*, 1995, 1997).

Fructans are synthesised and stored often in replacement of starch. They accumulate to high levels especially in the northern grasses including barley, wheat, oat and rye (Hendry, 1993), probably due to the insensitivity of their synthesis against low temperatures and the failure of fructans to feed-back inhibit photosynthesis in contrast to sucrose (for review, see Pollock, 1986; Vijn and Smeekens, 1999).

Extensive studies on the role of sugars in developing legume seeds led to the postulate (the invertase control hypothesis of seed development), that invertases generate a specific sugar status which is important for early development whereas the developmental and cell-specific decline in invertase activity allows the necessary switch to the sucrose synthase-dependent pathway of storage product accumulation during seed maturation (Weber *et al.*, 1997a). Three different invertase genes are expressed in isoform-specific patterns in *Vicia faba* seed coats (Weber *et al.*, 1995). *VfCWINV1* and *VfCWINV2* represent cell wall-bound gene isoforms; *VfVCINV* encodes a soluble acid isoform. The expression of *VfCWINV1* mainly in the unloading area of the seed coat (thin-walled parenchyma) leads to cleavage of incoming sucrose within the apoplast at a stage when mitotic activity proceeds in the embryo. Thus, VfCWINV1 is critical to provide fast dividing seed tissues with hexoses which in turn may act as a developmental signal. In addition, VfCWINV1 might establish sink strength by increasing the sucrose gradient. The importance of cell wall-bound invertase to regulate seed development is underlined by mutant analysis in maize. The *miniature1 (mn1)* mutant has a decreased invertase content in both pedicel and endosperm and is inhibited at early stages of kernel growth. The *mn1* mutation causes reduction in expression of an endosperm-specific isoform of cell wall-bound invertase, INCW2 (Cheng *et al.*, 1996).

Hexoses liberated by invertases are often taken up by associated hexose transporters. These proteins are encoded by large gene families described in *R. communis* (Weig *et al.*, 1994), *Chenopodium rubrum* (Roitsch and Tanner, 1994) and *Arabidopsis* (Sauer *et al.*, 1994). The single members show tissue-specific expression patterns (Sauer *et al.*, 1994). Co-ordinated expression of a hexose transporter and an invertase (Ehness and Roitsch, 1997) indicates that such co-operation efficiently provides sink tissues with hexoses. In *V. faba* the *VfSTP1* hexose transporter gene is expressed early in cotyledon development. Levels of mRNA then decrease rapidly and remain very low throughout seed maturation (Borisjuk *et al.*, 2002). This suggests that VfSTP1, together with VfCWINV1, plays an important role during the pre-storage phase.

Assimilate unloading and post-phloem transport within cereal seeds have been described mainly for the starch-filling phase (see Patrick and Offler, 2001; for review). In wheat and barley unloading is restricted to vascular bundles within the pericarp. Other pathways are prevented by cuticles within the integument layer surrounding the lateral and the dorsal region of the endosperm (Zee and O'Brien, 1970). From the crease vein assimilates are transported symplastically inwards and are released into the endospermal cavity by the nucellar projection cells proximal to the endosperm. Physiological data suggest that sucrose moves symplastically from sieve tube to endospermal cavity without energised membrane transport (Wang and Fisher, 1995). No evidence for an invertase-mediated unloading at least during storage product accumulation has been provided (Thorne, 1985). The cells of the endosperm at the ventral region adjacent to the crease are differentiated into transfer cells (Wang *et al.*, 1994), and these cells express a sucrose transporter gene involved in solute uptake into the endosperm (Weschke *et al.*, 2000).

In the work presented, we show the expression of sucrose:fructan 6-fructosyltransferase, cell wall-bound invertases and hexose transporter genes during early seed development of barley to allow comparisons with the data and working hypotheses established in grain legume seeds (Weber *et al.*, 1997a; Wobus and Weber, 1999). Based on the cellular localisation of transcripts, enzyme activity profiles and changing sugar levels in maternal and filial tissues, specific metabolic and developmental functions of enzymes with invertase activity and hexose transporter isoforms for the early development of the barley seed are discussed.

Results

A brief recapitulation of early caryopsis development

Spring barley variety *Hordeum vulgare* cv. Barke was grown in growth chambers as described in experimental procedures. During early development (pre-storage phase, 1–6 DAF), the caryopsis grows mainly longitudinally, whereas later on thickness increases because of the deposition of mainly starch within the filial endosperm. Endosperm development allows detailed definition of stages. At 2 DAF nucellus remnants but no endospermal cells are evident (cf. Figure 9a). The cellularisation of the starchy endosperm starts around 3 DAF and leads to the formation of a continuous layer of cells (cf. Figure 5a and Figure 9b). At 4 DAF, the endosperm is completely cellularised leaving a recognisable line at the meeting boundary of cell walls from the ventral and dorsal parts of the tissue (cf. Figure 5b, arrowhead). One day later, internal cell divisions mainly in the wings of the caryopsis produce a high number of smaller cells (cf. Figure 7a). The wings as well as the middle part of the endosperm are the first places of starch deposition, which starts 6 DAF (Weschke *et al.*, 2000; Figure 8(i). Detailed histological descriptions of barley endosperm development (but at a different time scale) have been published by Olsen *et al.* (1992, 1999).

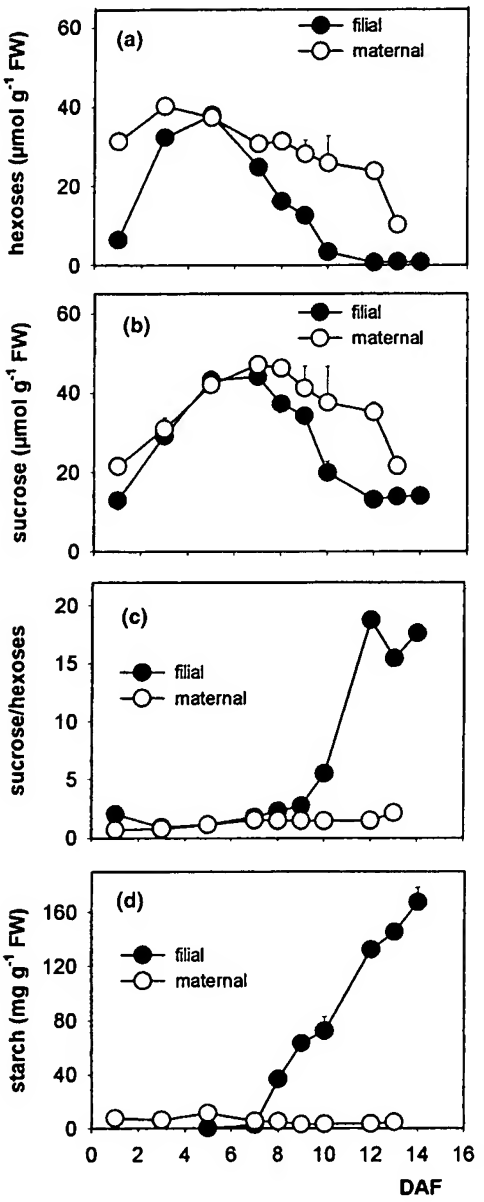

Figure 1. Accumulation of hexoses (a), sucrose (b) and starch (d) as well as sucrose/hexoses ratios (c) in the maternal and the filial fraction of young developing barley caryopses (0–14 DAF). Standard deviations (SD), resulting from three-fold repetition of measurements, are given but were in most cases smaller than FW, the circle symbol. FW, fresh weight.

Free sugars and starch within the maternal and the filial seed fraction

To analyse the dynamics of free sugars and starch within seed tissues especially during the pre-storage phase, we measured hexoses, sucrose and starch content of the maternal (mostly pericarp) and the filial tissue fraction (mostly endosperm and embryo) of developing caryopses. Hexose levels (Figure 1a) within the maternal fraction remained at about 30 µmol g^{-1} FW throughout development and decreased only after 12 DAF when the maternal tissues degrade. In the filial fraction levels increased from low values at 1 DAF, reached highest levels at 5 DAF and decreased to very low levels after 10 DAF. Sucrose levels (Figure 1b) within the maternal and the filial fraction increased from approximately 20 µmol g^{-1} FW at 1 DAF to a maximum of approximately 50 µmol g^{-1} FW at 7 DAF. Thereafter sucrose levels of the filial tissues decreased within the following 3 days to approximately 20 µmol g^{-1} FW and afterwards remained constant at about 15 µmol g^{-1} FW. Within the maternal tissues levels decreased slowly between 7 and 12 DAF and more rapidly thereafter. The sucrose/hexose ratio revealed major differences (Figure 1c).

Low ratios (approximately 1) were calculated for both the maternal and the filial fraction up to 9 DAF. Starting around 10 DAF, a nearly linear increase was detected in the endosperm/embryo with a maximum value of nearly 20 at 12 DAF. In contrast, the sucrose/hexose ratio in the maternal tissues remained constantly low. Starch content (Figure 1d) in the maternal fraction was low compared to the filial tissues with a small transient accumulation between 4

Table 1 Isoforms of fructoyltransferases, cell wall-bound invertases and putative hexose transporters identified by STACKPACK analysis (Christoffels *et al.*, 1999; Miller *et al.*, 1999) in a collection of 45 000 caryopsis-specific ESTs

Gene designation	EST ID	EST source	Highest homology to	Acc. no.
Fructosyl transferases				
HvSS1FT 1	HZ42J03 HZ60C23 HZ44H21	Early pericarp (0–7 DAF)	*T. aestivum* SS1FT (96%)	AB029888
HvFT 2	HZ39I13	Early pericarp (0–7 DAF)	*L. perenne* FT 2 (88%)	AY082350
HvSF6FT 2	HF11K03	Whole caryopsis (16–25 DAF)	*L. perenne* SF6FT (71%)	AF069309
Cell wall-bound invertases				
HvCWINV 1	HB25B07	Early embryosac (0–7 DAF)	*Z. mays* INCW2[1] (83%)	AF165181
HvCWINV 2	HZ01D05 HZ47P18 HZ43H14 HZ57H19 HZ58A09 (HZ37F12)	Early pericarp (0–7 DAF)	*O. sativa* INV 1 (third exon of a genomic sequence) (85%) (80% – bad sequence quality)	AF155121
HvCWINV 3?	HZ63H15		*O. sativa* INV 1, *Z. mays* Incw 4, (mainly 3'NTR, score <40)	AF155121 AF043347
Hexose transporters				
HvSTP 1 (cluster 1)	HA24B20 HA10F09 HB13L04 HB29B12 HF03E01 HF04O01 HF11I09 HF19J23 HF13M11	Early embryosac (0–7 DAF) Whole caryopsis (8–15 DAF) Whole caryopsis (16–25 DAF)	*O. sativa* chromosome 10; BAC clone, score ≥ 200	AC073166
(cluster 2)	HZ58P18 HB11M04 HF22E20	Early pericarp (0–7 DAF) Whole caryopsis (8–15 DAF) Whole caryopsis (16–25 DAF)	*O. sativa* chromosome 10; BAC clone, score ≥ 200	AC073166
HvSTP 3	HB23F17 HB22G03	Whole caryopsis (8–15 DAF)	*Z. mays* (hexose transport sequence); (86%)	AF215854
HvSTP 4?	HA15M17	Early embryosac (0–7 DAF)	*O. sativa* chromosome 10; BAC clone, score 75.8	AC018727
HvSTP 5?	HZ58P05	Early pericarp (0–7 DAF)	*O. sativa* chromosome 1 BAC clone; score 77.8	AP004365.2
HvSTP 6?	HB26N24	Whole caryopsis (8–15 DAF)	*A. thaliana* (putative sugar transporter); score 81.8	AY080624

ESTs were generated from cDNA libraries representing transcripts of the maternal (HZ, 12 500 ESTs) as well as the filial part (HA, 12 500 ESTs) of young developing caryopses (0–7 DAF), further from cDNA libraries specific for whole caryopses 8–15 DAF (HB, 10 000 ESTs) and 16–25 DAF (HF, 10 000 ESTs). Isoforms whose designation is given in italics have been further analysed; the results are presented in this paper. The highest homology of every single EST to a known sequence (column 4) is given either in percentages of identity (%) or if only small pieces of homologous sequences could be identified, score values are given instead. Because the score values of different sequences is lower than 100, functional assignment of these ESTs is not sure. These isoforms are labelled by question marks in column 1 (Gene designation). They were not analysed further.

[1]Carlson *et al.*, 2000.

and 6 DAF. The starch content increased in filial tissues beginning at 7 DAF, followed by a steady increase with highest accumulation rates between 10 and 13 DAF. The overall values depicted in Figure 1(c,d) show that the sucrose/hexose ratio increases rapidly about 2 days later than starch accumulation starts. However, the increase of the sucrose/hexose ratio at 10 DAF coincides with the major second phase of starch accumulation after a certain lag period around 9 DAF (Figure 1d and Weschke *et al.* 2000; Figure 7d).

Invertase activities in developing barley caryopses

The enzyme assay used to measure the activity of soluble acid invertase is based on the substrate sucrose. Because the purified barley 6-SFT retains considerable invertase activity when incubated with sucrose alone (Sprenger *et al.*, 1995), the measured soluble acid invertase activity may originate from vacuolar invertase and 6-SFT as well. However, because only cDNAs encoding different fructosyltransferases were identified by both, RT–PCR library screening and EST analysis (see Table 1), the measured activity probably originates only from 6-SFT.

Soluble acid invertase activity was highest in the maternal fraction at 1–2 DAF and decreased continuously afterwards. Activity in the filial tissues was generally lower. It increased from very low values at 1–2 DAF to a maximum at 5 DAF and decreased afterwards (Figure 2a).

Enzyme activity of cell wall-bound invertase was again highest in the maternal tissues at 1–2 DAF but decreased rapidly by 60–70% at 3 DAF and remained relatively constant until 10–12 DAF when it decreased to very low values. In the filial fraction, activity increased from 3 DAF onwards reaching a maximum at 6–7 DAF and decreased to practically zero at 12 DAF (Figure 2b).

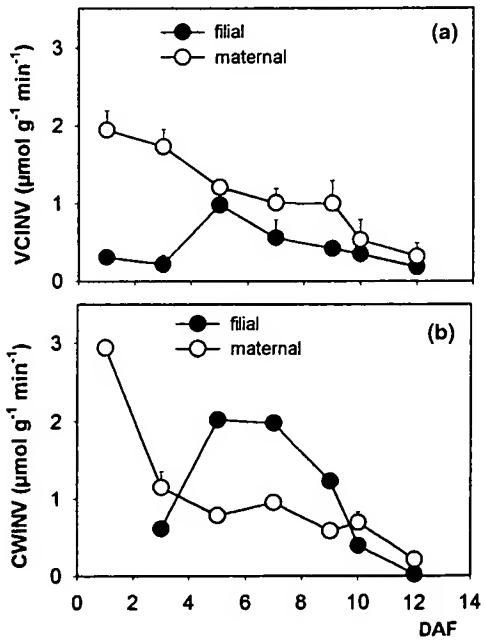

Figure 2. Activities of vacuolar (a) and cell wall-bound invertases (b) in the maternal and the filial fraction of young developing caryopses (0–14 DAF). SD as in Figure 1.

Isoforms of fructosyltransferases, cell wall-bound invertases and hexose transporters expressed in developing caryopses

Sucrose-cleaving enzymes and hexose transporters are known to exist in different isoforms which often differ in expression pattern suggesting different functions. We based our choice of genes for detailed studies mainly on a careful analysis of a large barley EST collection from four different libraries. These libraries represent cDNA fragments expressed between 0 and 7 DAF in the maternal (HZ) and the filial part of the caroypsis (HA) as well as in whole developing caryopses between 8 and 15 DAF (HB) and 16 and 25 DAF (HF). A total of 45 000 clones (12 000 from HZ, 12 500 from HA, 10 000 from HB, 10 000 from HF) were randomly chosen and subjected to 5′-sequencing. The resulting ESTs were clustered, and the clusters representing ESTs encoding isoforms of fructosyltransferases, cell-wall bound invertases and hexose transporters were selected.

Fructosyltransferases

A gene designated *HvSF6FT1* was isolated from a λZAP2 cDNA library. The full-length cDNA fragment showed 100% identity to an already described sucrose:fructan 6-fructosyltransferase (HVSF6FT) of *Hordeum vulgare* (Sprenger *et al.*, 1995). This gene, represented by 15 independent cDNA clones, was selected for further analysis because of its preferred expression during early caryopsis development and because of its ability to work as a vacuolar invertase if only sucrose is available as substrate (Sprenger *et al.*, 1995). Three ESTs showing highest homology (96%) to a SS1FT sequence from *Triticum aestivum* were identified in the EST-collection specific for the early pericarp (Table 1). A second fructosyltransferase EST was found in the same collection. This EST shows a lower degree of homology (88%) to a non-specified fructosyltransferase from *Lolium perenne*. During later development of the whole caryopsis, a second SF6FT isoform, HvSF6FT 2, is expressed. The homology to an SF6FT sequence from *L. perenne* is relatively low (71%; Table 1). Remarkably, no EST could be identified showing highest homology to one of the vacuolar invertase sequences known from maize or rice.

Cell wall-bound invertases

Eight ESTs were identified encoding cell wall-bound invertases (HvCWINV). Seven of them originate from young maternal tissue (Table 1). Five of the seven ESTs encode the same isoform whereas the identity of one of the two

other ESTs remains unclear (Table 1). The only EST found in the young filial tissue library (HB25B07) is most similar (83% identity) to the *Zea mays* cell wall invertase (*INCW2*)-mRNA (Acc. number AF165181) mapped at the *mn1* locus (Carlson *et al.*, 2000). Full-length cDNAs for both isoforms were again isolated from the λZAP2 library, designated *HvCWINV2* and *HvCWINV1*, respectively, and used for further analysis.

Hexose transporters

Seventeen ESTs were identified encoding putative hexose transporters. Nine of them form one unequivocal cluster representing a gene designated *HvSTP1*. The clones originate from the early filial library (HA) and from the early and mid-term caryopses libraries (HB and HF, respectively). A second cluster contains three further hexose transporter candidates found in three different libraries (Table 1). Sequences contained in both clusters show highest homology to a BAC clone from *Oryza sativa* chromosome 10 (AC073166). Cluster 3 is represented by only two sequences from the HB-library with 86% identity to a hexose transporter sequence from *Z. mays* (AF215854). Furthermore, three singletons were identified with the homologies given in Table 1. HZ15M17 may encode a different part of the cluster 1- and 2-genes since it shows highest homology to the same rice BAC sequence.

Before the 45 000 EST collection became available two seed-specific isoforms of putative hexose transporters were selected from a smaller set of ESTs described by Michalek *et al.* (2002). The respective full-length cDNAs were directly amplified from the phage inserts. They posses open reading frames of 2175 and 2234 bp encoding 744 and 755 amino acids, respectively, and were designated *HvSTP1* and *HvSTP2* (Figure 3a). *HvSTP1* is 100% homologous to the sequences represented in cluster 1 described above. Surprisingly, *HvSTP2* was not represented at all in the 45 000 EST collection. This could be explained by the high instability of this sequence in common *E. coli* vector plasmids (cf. Material and methods). Because *HvSTP1* and *HvSTP2* had been pre-characterised by Northern blotting as being highly expressed in either filial or maternal tissue, they were chosen for further analysis. Additional isoforms seem to be expressed at relatively low level during later development (*HvSTP3*) or the sequences were too short to give a secure assignment of a putative function (Table 1). These candidates were not included in the present study.

The putative amino acid sequences of HvSTP1 and HvSTP2 were aligned with the deduced protein sequences of all putative and functionally characterised hexose transporters currently available. Among them, 47 sequences with a common alignment pattern showed relatively high identity (alignment score 80–200) in the 5′- and the coding 3′-region but no homology in the middle part of the protein. Those sequences originating mostly from mammals were excluded from further alignment studies. As shown in Figure 3(b), the two putative hexose transporters HvSTP1 and HvSTP2 form a somewhat outstanding sub-branch in the phylogenetic tree. HvSTP1 shows highest homology (90.1%) to a putative hexose transporter from *O. sativa*, and,

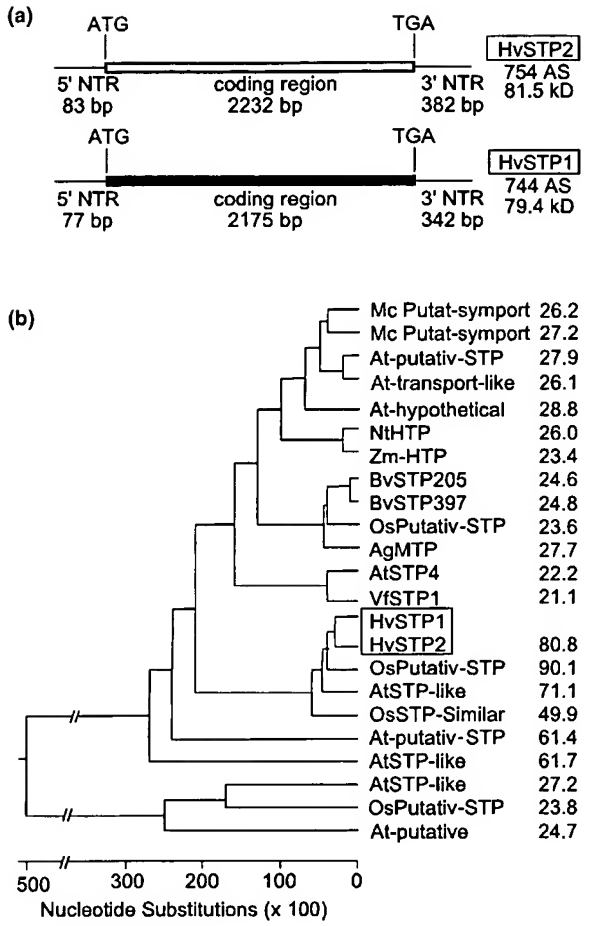

Figure 3. Schemes of *HvSTP1* and *HvSTP2* cDNAs (a) and comparison of a selection of monocot and dicot hexose transporter amino acid sequences (b). (a) cDNA organisation of *HvSTP1* and *HvSTP2* genes. Length in base pairs (bp) is given for the known parts of the 5′-non-translated regions (5′ NTR), the coding regions and the 3′-non-translated regions (3′ NTR). The coding sequences were conceptually translated resulting in the numbers of amino acid residues (AS) and the molecular weight of the peptides given (in kDa). (b) Dendrogram of alignment of hexose transporter sequences. The order of branching within the dendrogram indicates statistical similarities between hexose transporters from different plant species. The amino acid sequence of HvSTP1 was aligned with the corresponding hexose transporters as follows (the numbers given refer to EMBL data base accession numbers): *Apium graveolens* (AgMTP, AAG43998); *Arabidopsis thaliana* (At_putativ STP 27.9%, NP_181117; At_transport_like, NP_193381; At_hypothetical, NP_174313; AtSTP4, S25009; AtSTP_like 71.1%, NP_195256; At_putativ_STP 61.4%, NP_173508; AtSTP_like 61.7%, NP_190717; AtSTP_like 27.2%, NP_195385; At_putativ_STP 24.7%, NP_188513); *Beta vulgaris* (*B. vulgaris* STP205, T14606; *B. vulgaris* STP397, T14617); *Hordeum vulgare* (HvSTP2); *Mesembryanthemum crystallinum* (McPutat_symport 26.2%, AAF91431; McPutat_symport, AAF91432); *Nicotiana tabacum* (NtHTP, AAF74566); *Oryza sativa* (OsPutativ-STP, AAL14615; OsPutativ-STP 90.1%, AAG46115; OsSTP_Similar, BAA85398; OsPutativ-STP 23.8%, AAD27676); *Vicia faba* (VfSTP1, CAB07812); *Zea mays* (Zm-HTP, AAF74568).

surprisingly, more than 60% identity to a collection of sequences resulting from the *Arabidopsis* cDNA sequence program. Those sequences may be expressed in *Arabidopsis* seeds. As expected, all the highly homologous proteins are of nearly the same length (around 740 amino acid residues). The homology between HvSTP1 and HvSTP2 amounts to 80.8%.

Transcript levels of SF6-fructosyltransferase and cell wall-bound invertases in developing caryopses

Due to the existence of several isoforms (Table 1), we used the 3′-non-translated regions of *HvSF6FT1* and *HvCWINV1* and a 1-kb *Sph*I fragment covering the highly specific middle part of the *HvCWINV2* cDNA sequence as gene-specific probes in RNA gel blot experiments. Transcripts homologous to all three fragments were found in both the maternal and the filial fraction. However, the relative abundance differed between tissues and developmental stages. *HvSF6FT1*-mRNA levels were highest in maternal tissues at 1–2 DAF and decreased continuously by 80–90% until 10 DAF (Figure 4a). In filial tissues, the *HvSF6FT1*-specific transcript levels were very low at 1–3 DAF, increased to moderate levels at 5–7 DAF and decreased again at 9 DAF (Figure 4a).

Transcript levels of the cell wall-bound invertase *HvCWINV2* were highest in the maternal fraction at 2 DAF, decreased by about 50% at 6 DAF, followed by a second smaller maximum at 10 DAF. In the filial fraction, the *HvCWINV2*-mRNA level remained low. Detectable levels appeared at 4 DAF, reached a small maximum at 10 DAF and decreased again (Figure 4b). In contrast, levels of *HvCWINV1*-mRNA were highest in the filial tissues increasing from 2 DAF to a maximum at 6–8 DAF and decreasing afterwards. *HvCWINV1* transcripts in the maternal tissues revealed a similar pattern compared to the filial tissues but levels were lower between 6 and 8 DAF (Figure 4c).

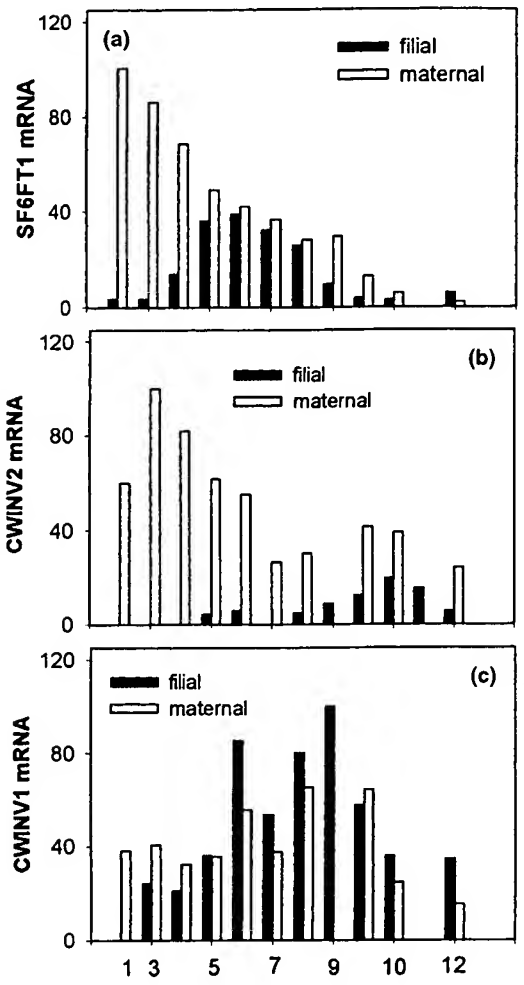

Figure 4. Transcript levels of sucrose:fructan 6-fructosyltransferase1 and different cell wall-bound invertase isoforms in the maternal and the filial fraction of young developing caryopses (0–12 DAF).
(a) sucrose:fructan 6-fructosyltransferase (HvSF6FT1).
(b, c) cell wall-bound invertases *HvCWINV2* and 1, respectively. Accumulation of *HvCWINV1* and 2 as well as *HvSF6FT1* mRNA was sequentially detected on the same blot. The complete experimental series was repeated twice. Results are presented from one out of two independent sets of phytochamber-grown plant material (for further explanations see Material and Method section). For quantification of the hybridisation signals see Experimental procedures.

Spatial expression patterns of SF6-fructosyltransferase and cell wall-bound invertases

According to Northern blotting experiments HvSF6FT and cell wall-bound invertases within developing barley seeds are mainly active early in development. Between 3 and 6 DAF, the pericarp (P) represents the main part of the caryopsis and is composed mostly of enlarged vacuolated cells (Figure 5a–c). It contains the main vascular bundle or crease vein (MVT) and three smaller veins (VT), two at the lateral sides and one on the dorsal side (Figure 6a). The pericarp-enclosed endosperm/embryo is surrounded by different cell layers, the outer (OI) and the inner integument (II), each composed of two cell rows and the mono-layered nucellar epidermis (NE). Assimilates reaching the pericarp via the main vascular bundle are unloaded into the nucellar projection (NP) and pass the endosperm cavity (EC) to be taken up by the opposite endospermal transfer cells (ET) to finally reach the endosperm which is cellularising at about 3 DAF (see Figure 5a) and completely cellularised about 6 DAF (Figure 5c).

Cell type-specific expression was analysed by *in situ* hybridisation using gene-specific probes of *HvSF6FT1*, *HvCWINV1* and *HvCWINV2*. At 3 DAF, the *HvSF6FT1*-specific label is distributed over most of the pericarp cells with highest intensities in the highly vacuolated cells of the dorsal region attached to the integument (small arrowhead in Figure 5d) and in the ventral regions (large arrowheads in Figure 5d). At 4 DAF, the label was mainly found in the cells

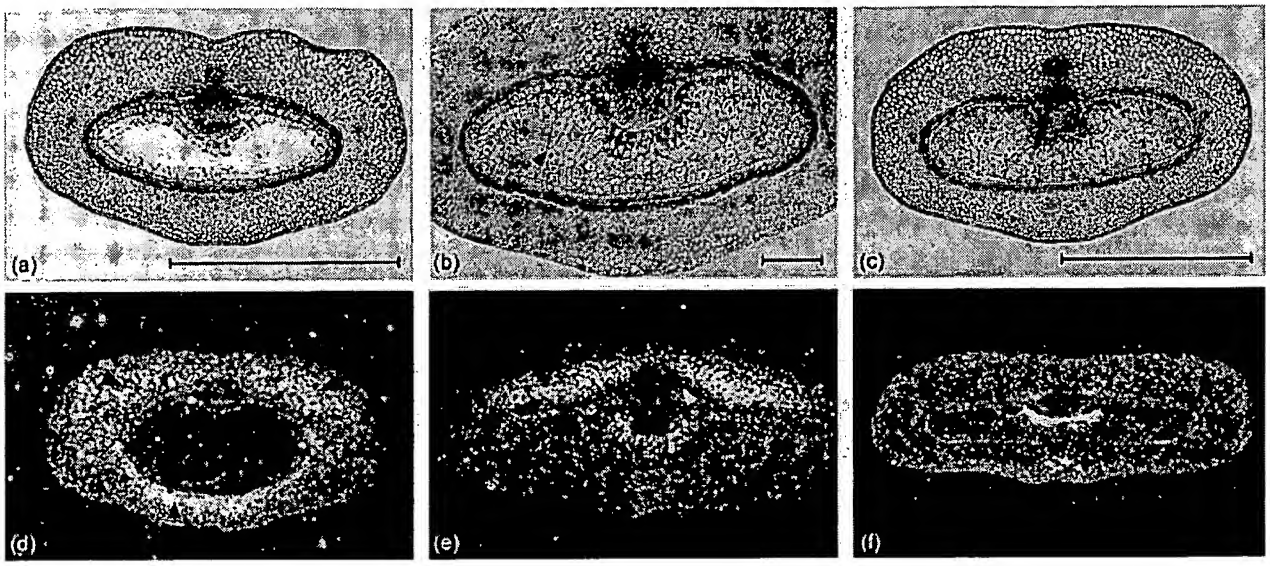

Figure 5. Tissue-specific accumulation of sucrose:fructan 6-fructosyltransferase *HvSF6FT1*-mRNA in transverse sections of young developing caryopses as shown by *in situ* hybridisation.
(a–c) Transverse section from the middle part of a caryopsis 3, 4 and 6 DAF, respectively; toluidene blue staining.
(d) 3 DAF: mRNA is localised in the pericarp. Most intense label is found over the inner cell rows on the dorsal side (small arrowhead) and ventral cells flanking the main vascular bundle (large arrowheads); dark field image.
(e) 4 DAF: mRNA is mainly localised in the ventral part of the pericarp and in the endospermal transfer cells. Note that those cells immediately flanking the main vascular bundle are completely free of label (white arrowhead); dark field image.
(f) 6 DAF: Intense labelling is now nearly exclusively found in the endospermal transfer cells; dark field image. For a schematic representation of the histological organisation of a barley caryopsis see Figure 6(a). Bars = 1000 μm in (a, c); 200 μm in (b).

of the ventral pericarp, which flank the crease vein. At that stage label is present also in the developing endospermal transfer cells. No signal was detected in the cells flanking the crease vein (Figure 5e, white arrowhead) and the nucellar projection. At 6 DAF, some *HvSF6FT1*-specific label was found equally distributed across the pericarp, whereas a very strong signal characterised the now fully differentiated endospermal transfer cells (Figure 5f).

When we used a *HvCWINV1* sequence to probe 3 DAF caryopses, high amounts of label were found in that first cell row of the endosperm flanking the nucellar projection (Figure 6b). Due to the close proximity of the filial endosperm cells to the outermost cell row of the nucellar projection, *HvCWINV1* may also be expressed in these maternal cells. Two days later (5–6 DAF), median-longitudinal sections of the developing caryopsis revealed that the endosperm cavern is build up of sub-caverns (lower arrow in Figure 6c) interrupted by layers of cylindrical cells orientated perpendicular to the transfer cells (upper arrow in Figure 6c). These cylindrical cells are rich in plasmodesmata (visible at higher magnification; not shown). In Figure 6(d,e), results of *in situ* hybridisation of the *HvCWINV1*-specific fragment to two transversal sections of the same caryopsis are shown, one through the region of the cylindrical cells (Figure 6d) and the other one through the subcavern region (Figure 6e). In Figure 6(d,e), *HvCWINV1*-specific label is clearly visible in both, the endospermal transfer cells and the outermost region of the nucellar projection, i.e. in the filial as well as the maternal tissue. Signals specific for *HvCWINV2* at 5 DAF were detected mainly in the dorsal pericarp and over the endospermal transfer cells (Figure 7b).

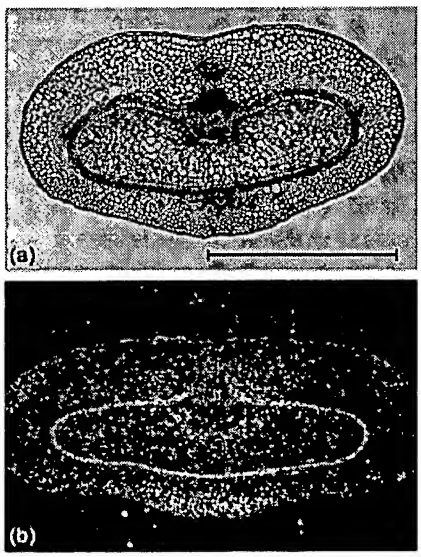

Figure 7. Tissue-specific accumulation of cell wall-bound invertase *HvCWINV2*-mRNA in median cross sections of a barley caryopsis at 5 DAF as shown by *in situ* hybridisation. Bars = 1000 μm.
(a) Transverse section from the middle part of the caryopsis.
(b) Localization of *HvCWINV2*-mRNA in the most dorsal part of the pericarp next to the vascular bundle and in the endospermal transfer cells.

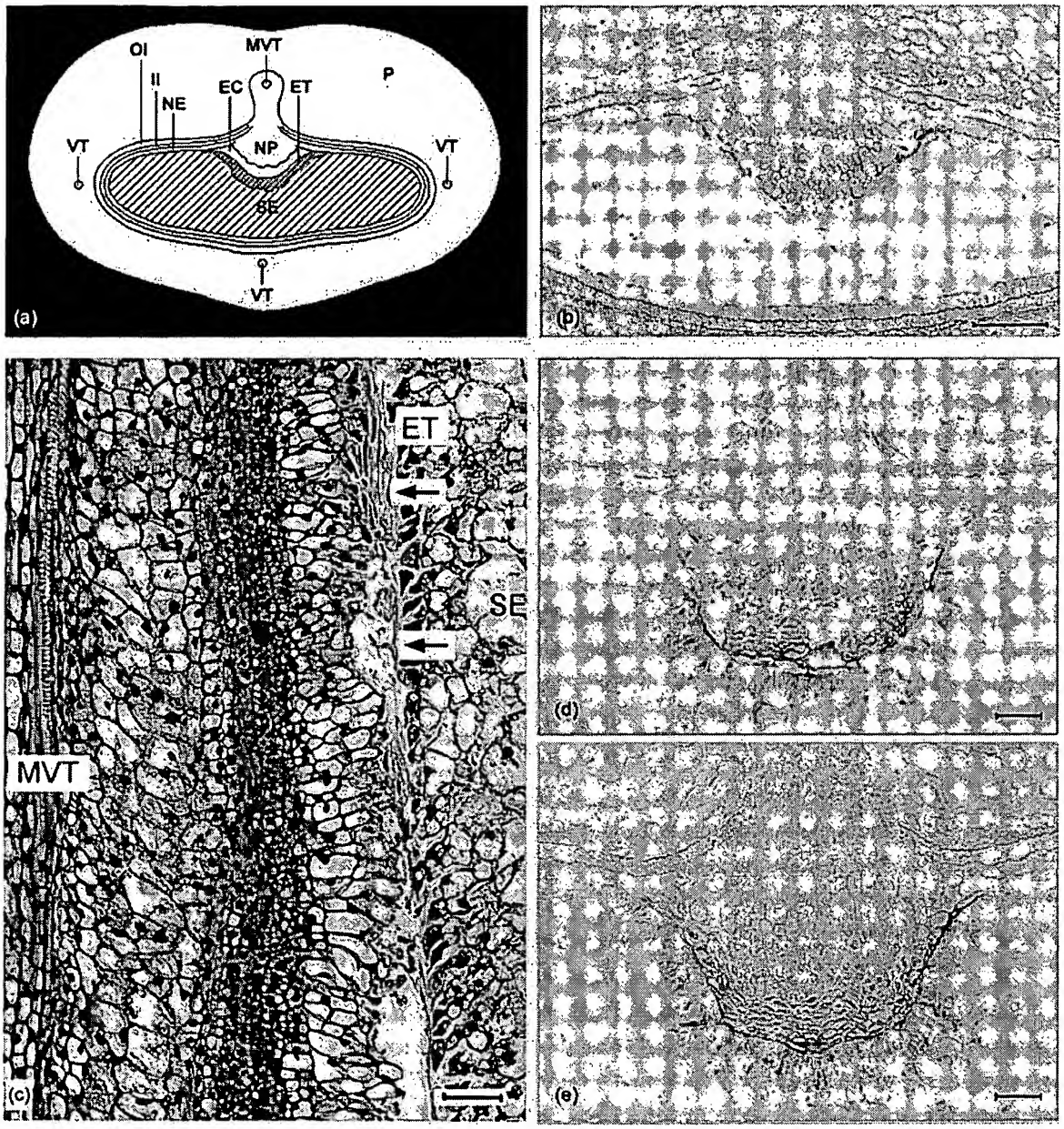

Figure 6. Tissue-specific accumulation of cell wall-bound invertase *HvCWINV1*-mRNA in transverse sections of young developing caryopses as shown by *in situ* hybridisation.
(a) Schematic representation of the histological organisation of a barley caryopsis; median cross section.
(b) 3 DAF: Localisation of *HvCWINV1*-mRNA in the first endospermal cell rows facing the left and right part of the nucellar projection; DIG labelling.
(c) Median-longitudinal section of a developing caryopsis 5/6 DAF; toluidine-blue staining. The arrows label the position of the transversal sections shown in (d) (lower arrow) and (e) (upper arrow). Notice patches of destroyed cells within the sub-caverns (compare to the structure visible in the transversal section in (d)].
(d, e) 5/6 DAF: Localisation of *HvCWINV*-mRNA in both the endospermal transfer cells and in parts of the nucellar projection. Bars = 100 μm in (b); 50 μm in (c–e).

Taken together, expression of *HvSF6FT1* as well as the measured acid soluble invertase activity are mainly confined to the early pericarp before the onset of transient starch accumulation. The two isoforms of cell wall invertases exhibit different expression patterns. Although overlapping, HvCWINV2 is mainly active in the pericarp whereas HvCWINV1 is preferentially expressed in the maternal–filial boundary with a main phase of activity immediately before the endospermal starch-filling phase.

Transcript levels and cell-type specific expression of hexose transporters in developing caryopses

Gel blot analysis of RNA from whole caryopses provided first information on the expression of *HvSTP1* and *HvSTP2* genes. *HvSTP2*-mRNA levels were highest in young caryopses (1–4 DAF) and decreased thereafter by around 50%. Significant transcript levels were also detected in vegetative tissues (Figure 8a). In contrast, *HvSTP1* tran-

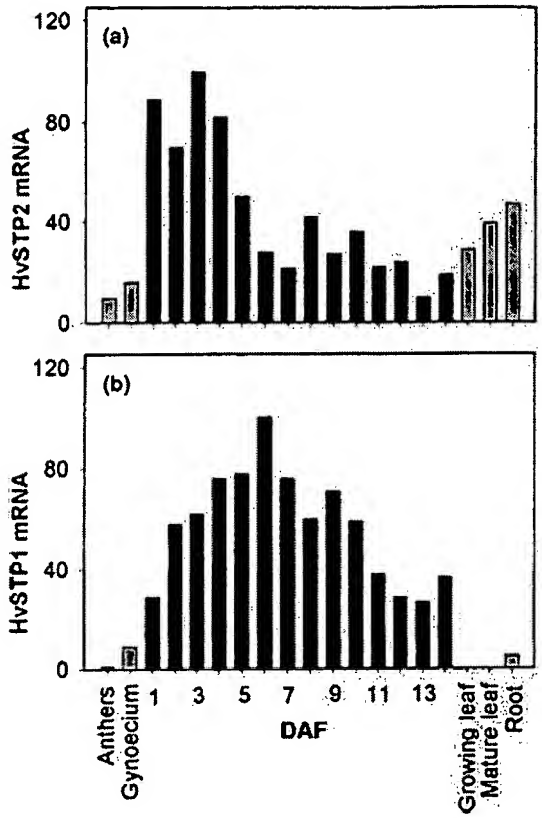

Figure 8. Analysis of hexose transporter *HvSTP1* and *HvSTP2* transcripts in young developing caryopses (1–14 DAF) and other plant tissues.
(a) *HvSTP1*-mRNA;(b) *HvSTP2*-mRNA. Accumulation of both transcripts was sequentially detected on the same blot. The complete experimental series was repeated twice. Results are presented from one out of two independent sets of phytochamber-grown plant material (for further explanations see Material and method section). For quantification of the hybridisation signals see Experimental procedures.

scripts accumulated from 1 DAF reaching a maximum at 6 DAF and decreased steadily until 14 DAF. Its RNA levels in tissues other than caryopses were very low (Figure 8b).

Cell type-specific expression of *HvSTP1* and *HvSTP2* was analysed by *in situ* hybridisation using transversal sections of caryopses at 2 (Figure 9a), 3 (Figure 9b) and 7–8 DAF (Figure 9c). *HvSTP2*-specific signals were present in most of the pericarp cells at 2 DAF with strongest labelling of the dorsal region and around the lateral veins (Figure 9d; see especially labelling of some cell rows flanking the outer integument, small arrowheads). At 3–4 DAF labelling was generally weak (Figure 9e). At 7–8 DAF, *HvSTP2*-specific signals were present mainly within the endospermal transfer cells and in cells surrounding the crease vein (Figure 9f). In contrast, label specific for *HvSTP1*-mRNA was very low in pericarp at 2 DAF (Figure 9g). Later on at 3–4 DAF, a strong signal could be detected in the syncytial endosperm layer. Some label was also present in the inner region of the pericarp and the integuments (Figure 9h, white arrowhead). At 7–8 DAF, a strong signal occurred in endospermal transfer cells (Figure 9i) similar but much stronger than that of *HvSTP2*-mRNA (Figure 9f).

The results show, that the two isoforms of hexose transporters exhibit a different temporal and spatial mode of expression. HvSTP1 is nearly endosperm-specific with preference to the syncytial stage and, later in development, fully differentiated transfer cells. On the other hand, HvSTP2 shows a broader range of expression and is mainly active in the young pericarp.

Discussion

Barley seeds consist of the maternal tissues (mainly pericarp) and the filial embryo/endosperm. Whereas early development (pre-storage phase) is dominated by pericarp growth and cellularisation processes in the early endosperm, the maturation or storage phase is determined by storage product accumulation in the endosperm and development of the embryo proper. We have shown earlier in developing legume seeds that gradients of soluble sugars and changes in hexoses/sucrose ratios are an important prerequisite for normal seed development, especially for the transition between the pre-storage and storage phase of cotyledons. Accordingly, highly specific expression patterns of major genes of carbohydrate metabolism as invertases, sucrose synthases as well as sugar transporters exert important controlling functions in legume seed development (see Weber *et al.*, 1997a; Wobus and Weber, 1999; for reviews). The aim of the work presented here was to analyse in a developing cereal seed tissue-specific and developmental expression patterns of invertases/fructosyl transferases and hexose transporters together with invertase enzyme activities and sugar levels in a further attempt to better understand the role of sugars in cereal seed development (see also Weschke *et al.*, 2000).

Maternal tissues represent the main sink of the grain during early caryopsis development and are characterised by high acid soluble invertase activity

During caryopsis development the content of hexoses in the maternal fraction is high (Figure 1a) most probably due to high acid soluble (vacuolar) invertase activity (Figure 2a). Contrary to maize where two isoforms of vacuolar invertase have been described in kernels (Xu *et al.*, 1996), different fructosyltransferases but no vacuolar invertases were identified in barley caryopses by RT–PCR library screening as well as BLASTX and STACKPACK analysis (Table 1). HvSF6FT1 as well as HvSS1FT are expressed in maternal tissues early in development (0–7 DAF). A second SF6FT isoform, HvSF6FT2, was found in a cDNA library specific for the later phase of barley grain development (HF, 16–25

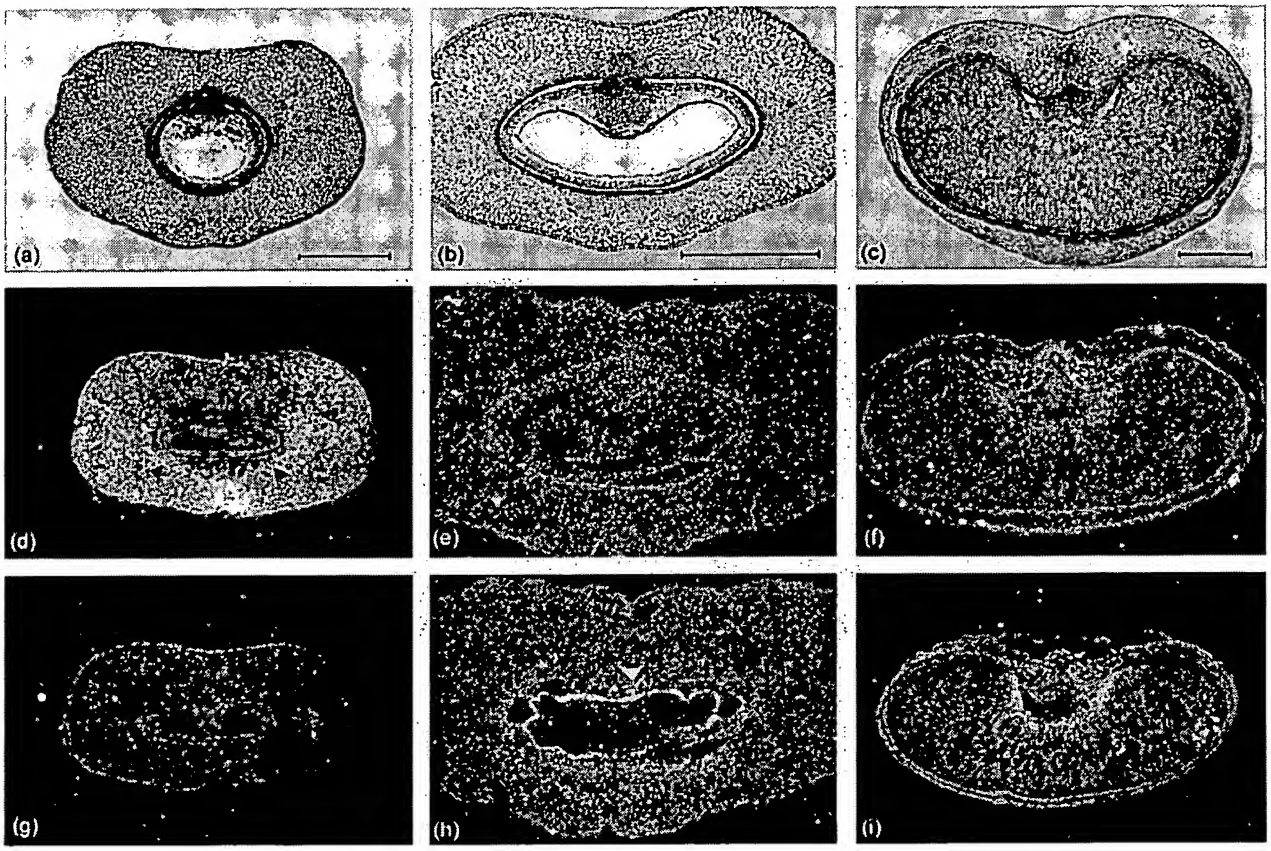

Figure 9. Tissue-specific accumulation of hexose transporter *HvSTP1*- and *HvSTP2*-mRNA in transverse sections of young developing caryopses as shown by *in situ* hybridisation.
(a–c) Transverse section from the middle part of a barley caryopsis 2, 3 and 7/8 DAF, respectively; toluidene blue staining.
(d) 2 DAF: Localisation of *HvSTP2*-mRNA in the pericarp. Labelling is found mainly in the region of the dorsal vascular bundle, weaker labelling in some cell rows surrounding the dorsal part of the embryo sac (small arrowheads) and in the region of the lateral vascular bundles; dark field image.
(e) 3 DAF: No *HvSTP2*-mRNA-specific labelling is seen, neither in the pericarp nor in the first syncytial cell row of the developing endosperm; dark field image.
(f) 7/8 DAF: Localisation of *HvSTP2*-mRNA in the endospermal transfer cells and in the parenchyma cells of the main vascular bundle (small arrowhead); dark field image.
(g) 2 DAF: The maternal tissues are free of any *HvSTP1*-mRNA-specific labelling; dark field image.
(h) 3 DAF: Localisation of *HvSTP1*-mRNA is found in the first syncytial cell rows of the developing endosperm, weaker labelling of the integuments (small arrowheads) and the nucellar projection (large arrowhead); dark field image.
(i) 7/8 DAF: Localisation of *HvSTP1*-mRNA in the endospermal transfer cells; dark field image. Bars = 500 μm.

DAF); it needs further investigation. For the present study, we selected the maternal-specific HvSF6FT1 isoform showing high mRNA-abundance.

Both, soluble acid invertase and SF6FT cleave sucrose and release glucose in *in vitro* assays using sucrose as substrate, i.e. these act as invertases. The fructosylransferase activity of SF6FT is activated only when the trisaccharid 1-kestose, produced by the enzyme SS1FT, is present in the vacuole (Sprenger *et al.*, 1995). Soluble invertase activity and high expression levels of *HvSF6SFT1*-mRNA in most parts of the pericarp at around 3 DAF (Figure 5d) are indicative of strong sink activity. At the tissue level, *HvSF6SFT1*-mRNA is mainly localised within cells of the dorsal and ventral regions (Figure 5d) whereas regions of transient starch accumulation (see Weschke *et al.* 2000) are less labelled. Only 1 day later, at 4 DAF, expression becomes restricted to enlarged vacuolated cells of the ventral region flanking the main vascular bundle (Figure 5e). Generally, *HvSF6FT1*-mRNA in the pericarp is found early in development in young enlarging cells and is later confined to cells flanking the main vascular bundle, i.e. those regions which persist during further development because these are involved in assimilate transport until the end of the maturation phase.

cDNA fragments of *SS1FT* and *SF6FT* were found predominantely in the maternal HZ cDNA library (Table 1) suggesting induction of gene activities in the early pericarp. Remarkably, no transcript encoding a typical vacuolar invertase could be identified, neither in 45 000 seed specific ESTs nor in a caryopsis-specific phage library screened with a specific fragment produced by RT–PCR. An extended BLASTX2 search for vacuolar invertase sequences of *T. aestivum* has shown that the two sequences available in the net and annotated as vacuolar invertases exhibit highest

homology to fructosyltransferases. Based on the data discussed we conclude that expression of vacuolar invertase genes is low or missing in developing barley grains. Possibly, this conclusion can be extended to northern grasses in general. However, since hexose levels (Figure 1a) as well as *HvSF6FT1*-mRNA levels (Figure 4a) are high in the maternal tissues of the young barley grain we assume that HvSF6FT has vacuolar invertase activity. In which way the ratio of the two possible activities of this enzyme is influenced by the sucrose concentration increasing later in development, is not known. However, fructans should be produced in addition to hexoses because SS1FT, producing the SF6FT-substrate 1-kestose, is expressed in the young pericarp too.

The irreversible cleavage of incoming sucrose in hexoses assures high turgor and cell integrity and guarantees a high sucrose influx (Eschrich, 1989). In barley caryopses both, the production of hexoses and soluble fructans is most probably realised by the enzyme HvSF6FT and thus points to a role of SF6FT in phloem unloading of the young grain. Contrary to cell wall-bound invertases, contributions of acid soluble invertase activity to phloem unloading have received comparatively little attention due to: (a) their more widely known role in sugar balance of maturing fruits (Sturm, 1999); (b) their role in the control of intracellular sugar composition, cell enlargement and osmoregulation; (c) the prominence of cell-wall invertases in maize kernel development [as per Shannon's original hypothesis (Shannnon and Dougherty, 1972)]; and (d) the apparently limited evidence of a vacuolar site of sucrose hydrolysis in phloem unloading, particularly with respect to a symplastic path of import. Recent studies by Fisher and Cash-Clark (2000a,b) extended earlier work by Wang and Fisher (1994) on the post-phloem transport path in wheat grains exhibiting structural features similar to barley. Their data indicate that phloem unloading and the maternal portion of the post-phloem transport path are symplastic. Thus, sucrose transversing the cell wall through plasmodesmata would be physically isolated from cell-wall bound invertase until reaching a site of apoplastic transfer. Therefore, HvSF6FT activity apparently provides the predominant path for metabolisation of imported sucrose leaving the phloem during early development. Our localisation of *HvSF6FT1*-mRNA in pericarp cells flanking the vascular tissue is compatible with data from wheat grain tissues (discussion in Fisher and Cash-Clark, 2000b). Because only these pericarp cells stay alive during nearly the complete caryopses development, fructan production may be helpful to withstand high osmotic stress during later development.

Besides its presence in the pericarp, *HvSF6FT1*-mRNA has been localised in filial endospermal transfer cells beginning at 4 DAF and culminating at 6 DAF when all other tissues are nearly free of label (Figure 5e, f). Expression occurs in the developing as well as functionally active transfer tissue. A possible role of the enzyme in transfer cells could be to assure high levels of soluble fructans and/or hexose which in faba bean seeds prevents further differentiation into storage cells (Weber *et al.*, 1996b).

In the pericarp, the spatial expression pattern of cell wall-bound invertase 2 is different from that of HvSF6FT1 but correlates with the expression of the hexose transporter HvSTP2

Besides the *HvSF6FT1* gene two cell wall-bound invertase genes are expressed in the pericarp. Whereas the expression of *HvCWINV2* within the seed is nearly pericarp-specific (Figure 4b), *HvCWINV1*-mRNA is found at comparable levels in both the maternal fraction and in the endosperm/embryo (Figure 4c). Like in the faba bean maternal seed coat, where VfCWINV2 is likely to have a seed coat-specific function (Weber *et al.*, 1995), HvCWINV2 is postulated to serve the pericarp. We noted that its temporal and spatial expression pattern correlates roughly with the expression of the putative hexose transporter *HvSTP2* (cf. Figure 4b with Figures 8a, and Figure 7b with Figure 9d) suggesting that hexoses generated by the cell wall-bound invertase are immediately transported into the respective cells.

Invertases and hexose transporters are expressed in endospermal transfer cells and thus potentially control the sugar status of the filial tissues during early caryopsis development

Photoassimilates are imported into the seed through the crease phloem, the vascular parenchyma, pigment strand and nucellar projection from where these are released into the apoplastic endospermal cavity to be finally taken up by the endospermal transfer cell layer (see Patrick and Offler, 1995, 2001; for review). It is remarkable that around 5–6 DAF practically all the genes described here, i.e. a fructosyl transferase, two cell wall-bound invertases and two putative hexose transporters, are expressed in the endospermal transfer cell layer. This is also true for two sucrose transporters described earlier (Weschke *et al.*, 2000). The data underline the importance of these cells for regulating the endosperm development. With respect to gene expression the endospermal transfer cell tissue is similar to the faba bean coenocytic endosperm layer in which also all types of investigated invertases as well as hexose and sucrose transporters are expressed (Weber *et al.*, 1995; 1997b). Contrary to the active transport into the filial tissues, sucrose movement through the maternal cells of the nucellar projection, exhibiting pronounced transfer cell morphology (see Weschke *et al.*, 2000 for barley and Wang *et al.*, 1994 for wheat) and release into the apoplastic endospermal cavity, is less well defined but seems to be mainly passive as revealed by physiological experiments (Wang and Fisher, 1995).

A high hexose level rapidly decreasing during development is characteristic for the prestorage phase of the filial tissues

Whereas pollination initiates the development of the filial embryo/endosperm, maternal tissues are differentiated already before anthesis. Thus, at 1 DAF levels of hexoses are already high in the maternal fraction (Figure 1a) to energise ongoing cell division and elongation processes. On the other hand, the hexose level in the filial tissues is very low immediately after fertilisation, increases rapidly when the first syncytial cell rows appear in the endosperm (3 DAF) and reaches its maximum when internal cell division as well as elongation processes take place. Afterwards the level drops to nearly zero between 10 and 12 DAF. Since the same hexose profile has been found in pre-storage legume cotyledons (Borisjuk *et al.*, 2002; Borisjuk *et al.*, 1998; Weber *et al.*, 1995) it can be regarded as a typical feature of the cell division/early cell elongation phase (=pre-storage phase) of seed development.

In principle, sucrose levels in the maternal and the filial fraction show a temporal pattern comparable to that of the hexoses with the only difference that in both tissues sucrose peaks 7 DAF, 2 days later than hexoses (Figure 2b). However, the sucrose/glucose ratio, which is very low (approximately 1) and consistent from 1 to 13 DAF in the maternal tissues but strongly increasing from 9 DAF onwards in the filial fraction (Figure 1c), clearly indicates differences in the carbohydrate metabolism within the two caryopsis parts.

Invertase HvCWINV1, a homologue of INCW2 reduced in the maize mn1 mutant, is expressed together with HvSTP1

In the filial tissues both, the *HvCWINV2* and the *HvCWINV1* gene are expressed but HvCWINV1 represents the isoform with preference for this tissue. The *HvCWINV1* transcript was localised 3 DAF in the first endospermal transfer cells flanking the nucellar projection (Figure 6b). More intensive label was found 5–6 DAF within the endospermal transfer cell layer and in cells of the nucellar projection bordering the endosperm cavity (Figure 6c,d). Northern blotting revealed maximal transcription immediately before the starch-filling phase (5–6 DAF, cf. Figure 4c).

Biochemical and physiological studies provide evidence that cell wall-bound invertases are most active at sites of sugar transport within rapidly importing apoplastic sinks (see Tymowska-Lalanne and Kreis, 1998; for review). Accordingly, transcriptional activity of *HvCWINV1* is highest within the filial tissue during the rapid growing phase. In *V. faba* seeds, cell wall-bound invertases are active within the inner thin-walled parenchyma of the seed coat creating a sucrose gradient across the unloading area (Weber *et al.*, 1995). Thereby, a high hexose status is created which is thought to promote mitotic activity within the embryo (Borisjuk *et al.*, 1998; Weber *et al.*, 1996b). A similar mode of regulation was reported for maize seed development. The kernel-specific cell wall-bound invertase INCW2 is expressed temporarily coincident with endospermal cell division. It was concluded that the metabolic release of hexoses is critical to provide a sugar-sensing signal (Cheng and Chourey, 1999). Functionally analogous to the situation in faba bean seeds, the maize *INCW2* gene is expressed in cells, which are involved in assimilate transfer from the maternal to the filial part, i.e. at the base of the kernel. The loss of invertase, due to the *mn1* mutation, causes severely reduced kernel weight (Cheng *et al.*, 1996).

HvCWINV1 of barley is at the sequence level highly similar to maize invertase *INCW2* and therefore probably represents the orthologue isoform. *HvCWINV1* is mainly expressed in the endospermal transfer cells but also in the outermost area of the nucellar projection, at the maternal–filial boundary (Figure 6d,e). Recently, high expression of cell wall invertase OsCIN1 during early development of the rice caryopsis was reported (Hirose *et al.* 2002). However, the *in situ* hybridisation patterns of *OsCIN1* and *HvCWINV1* mRNAs as well as sequence comparisons hint to different isoforms; *OsCIN1* shows highest homology to the *Z. mays* invertase gene *INCW1* not to *INCW2*.

According to Hirose *et al.* (2002), the invertases discussed above belong to the group I cell wall-bound invertases, whereas VfCWINV2, OsINV1 and ZmInv4 belong to group II. Based on sequence homology, HvCWINV2, the second isoform of cell wall-bound invertases presented in this paper should also belong to the latter group (cf. Table 1). Group II invertases may represent, according to Kim *et al.* (2000), an unique type of cell wall invertase unbound in the apoplast. Group I invertases obviously participate in creating sucrose gradients in unloading areas, either in the vascular parenchyma of rice grains (Hirose *et al.* 2002), at the base of the maize kernel (Cheng *et al.*, 1996), in the thin-walled parenchyma of the *V. faba* seed coat (Weber *et al.*, 1996b) or at the maternal–filial boundary of the developing barley caryopsis as shown in this paper. Contrary to the legume system, where sucrose is mostly broken down in the inner layers of the maternal seed coat, sucrose destined to the filial tissues of the barley caryopsis seems to enter the endospermal cavity uncleaved and is broken down afterwards at the surface of both, nucellar projection and endospermal transfer cells. Although *HvCWINV1* is expressed in the major transport pathway for sugar movement into the endosperm, sucrose levels within the endosperm/embryo are high and sucrose/glucose ratios are low at least 6–10 DAF (cf. Figure 1b,c). This contradictory finding can be explained by the expression of the high affinity sucrose transporter HvSUT1 (Weschke *et al.* 2000), competing with HvCWINV1 in such a way that the sucrose cleavage- to

transport ratio is regulated during development by the activity/expression ratio of the enzyme/transporter, respectively. Whether parts of the sucrose measured within the filial fraction result from re-synthesis via sucrose phosphate synthase cannot be decided yet.

Already at early stages, the maternal–filial boundary of the barley caryopsis is most probably involved in transfer of glucose. Accordingly, the hexose levels within the embryo sac are highest at this stage (Figure 1a). We conclude therefore that in barley caryopses cell wall-bound invertases, especially HvCWINV1, are responsible for providing fast dividing endosperm cells with hexoses.

There is evidence that hexose transporter gene expression is co-ordinately induced together with that of extracellular invertases. This regulatory mechanism results in higher tissue uptake of sucrose, due to the apoplastic invertase activity, and of hexoses, due to the hexose transporter activity (Ehness and Roitsch, 1997). Accordingly, expression of the barley *HvSTP1* gene is temporally and spatially associated with the expression of *HvCWINV1* (compare Figure 6 with Figure 9), indicating that hexoses generated by the HvCWINV1 enzyme within the endospermal cavity are taken up by the putative HvSTP1 transporter into the central uncellularised space of the endosperm. An analogous situation was described earlier for *V. faba* seeds. Expression of the hexose transporter *VfSTP1* in the cotyledonary epidermis during mid-cotyledon stage is confined to epidermal cells covering developmentally younger, mitotically active regions at the abaxial tip of the cotyledons (Weber *et al.*, 1997b). Opposite this region across the apoplast a cell wall-bound invertase is expressed in the thin-walled parenchyma of the seed coat (Weber *et al.*, 1995). Again, such co-operation between invertases and hexose transporters most probably provides growing sink tissues with hexoses.

Experimental procedure

Plant material and tissue preparation

Plants from a two-rowed spring barley (*H. vulgare* cv. Barke) were cultivated in growth chambers. During the generative phase of development the plants were grown under a 16-h light/20°C and 8 h dark/14°C regime. Days after flowering were determined and harvesting of seed material was done as described (Weschke *et al.*, 2000). The maternal (mostly pericarp) and the filial grain fraction (mostly endosperm/embryo) were hand-dissected and isolated (for discussion see Sreenivasulu *et al.*, 2001).

Isolation of cDNA clones specific for sucrose:fructan 6-fructosyltransferase and cell wall-bound invertases

By using primers specific for a barley sucrose:fructan 6-fructosyltransferase (accession number X83233), a fragment was amplified by RT–PCR from total RNA isolated from developing caryopses (1–15 DAF). After sub-cloning and sequencing, the fragment was used to screen a λZAP2 cDNA library specific for developing caryopses (1–15 DAF). Fifteen independent positive clones were isolated and sequenced, and all found to be identical to the known barley sequence HVSF6FT.

To isolate cell wall-bound invertase-specific cDNA clones a cDNA from a root-specific invertase isoform (HW07B12) was used to screen the above-mentioned λZAP2 cDNA library under low-stringency conditions. 6 independent positive phages were identified and two of them contained a complete coding region showing highest homology (83% identity) to the *Z. mays* cell wall invertase *Incw*-sequence (accession number AF 165181). This cDNA clone was named *HvCWINV1* (EMBL/GenBank/DDBJ accession number AJ534447).

By evaluation of the BLASTX results of ESTs specific for the caryopses library, a cDNA clone (HY01G12) was identified coding for a second isoform of cell wall-bound invertase and named *HvCWINV2*. It shows highest homology (85% identity) to the third exon of a genomic sequence specific for an apoplastic invertase from rice (accession number AF 155121).

Together with the complete set of caryopsis-specific ESTs, the ESTs with the identification codes HW07B12 and HY01G12 (see above) have been deposited in the EMBL sequence database and can also be obtained from the IPK web-server (http://www.pgrc.ipk-gatersleben.de).

Isolation and sequence analysis of putative hexose transporter cDNAs

From the caryopsis-specific λZAP2 cDNA library an EST collection was generated from the 5′ as well as the 3′-end of about 3500 genes (Michalek *et al.* 2002). By using BLASTX search, cDNA clones were identified containing mainly the 3′ part of two different putative hexose transporter cDNAs. Specific fragments of these clones were used to screen the λZAP2 cDNA library, and recombinant plasmids were isolated from positive phages by *in vivo* excision. However, all recombinant plasmids contained only parts of the two different putative hexose transporter cDNAs and were highly unstable. By using one primer specific for the 3′-end of each of the putative hexose transporters and one primer representing a part of the vector sequence flanking the 5′-end of the cDNA, amplification of fragments more than 2 kb in length was possible from the recombinant phages. These fragments were used directly in sequence analysis to get the full-length sequence of the two putative hexose transporter cDNAs named HvSTP1 and HvSTP2. (EMBL/GenBank/DDBJ accession numbers AJ534445 and AJ534446, respectively).

RNA extraction and hybridisation procedures

Whole developing caryopses (1–14 DAF) as well as the maternal (pericarp) and the filial part (endosperm/embryo) of the grain were used for preparation of total RNA as described by Heim *et al.* (1993). Additionally, total RNA was extracted from anthers, the female part of the flower immediately before anthesis, growing and mature leaves and roots by using the same procedure. RNA (10 μg lane^{-1}) was separated on an agarose gel and blotted. One membrane was sequentially hybridised according to Church and Gilbert (1984) using the following probes: two cDNA fragments 511 bp (nucleotides 1916–2427) and 406 bp (nucleotides 2063–2469) in length, representing parts of the 3′ region of *HvSTP1* and *HvSTP2*, respectively. A second filter was hybridised by using fragments specific for *HvCWINV1* (380 bp in length, generated

from the 3′-NTR by using the primers 5′-CCTAAGGGGGAAATGACCCCTTCG-3′ and 5′-GGCAAGATATCTCTGAGAAGCCTG-3′ for PCR amplification), HvCWINV2 (a *Sph*I-fragment 1 kb in length covering the highly specific middle part of the cDNA sequence) and HvSF6SFT1 (283 bp in length, generated from the 3′NTR by using the primers 5′-GTTTATTAGGCAAACCAGATCGG-3′ and 5′-GGACGATGGCATGTATCTCC-3′ for PCR amplification). In a fourth hybridisation round, this membrane was hybridised to a 26S rDNA fragment for estimation of RNA loading (data not shown). The hybridisation signals were quantified as described by Weber *et al.* (1996a) and are given in relative units.

Radioactive *in situ* hybridisation was performed according to Panitz *et al.* (1995) using the fragments described above labelled by ^{33}P. As a control, slides were treated with RNase before hybridisation. No labelling of any cell type by any probe was seen (data not shown). For digoxigenin (DIG)-based *in situ* hybridisation fragments were labelled using the DIG High prime reaction (Roche, Mannheim, Germany). The specific activity of the labelled product was tested as recommended by the manufacturer. Sections (5 μm) were prepared from BMM (butyl-methyl methacrylate) embedded material. After de-embedding in acetone, sections were treated with protease and hybridised as described above. DIG-labelled hybrids were detected as described by DeBlock and Debrouwer (1996).

Determination of sugars and starch

Soluble carbohydrates from the maternal as well the filial fraction were extracted with 80% ethanol at 80°C for 1 h. Extracts were evaporated and dissolved in sterile water. Sucrose and glucose were determined enzymatically according to Bergmeyer *et al.* (1974), using sugar-determination kits (Boehringer, Mannheim, Germany). Because always nearly the same concentration was measured for the two hexoses glucose and fructose, twice the glucose concentration was used to calculate the total hexose level in all experiments. After boiling for 20 min in 0.2 M KOH (1 ml per 10 mg starting tissue) the pH was adjusted to 6, starch was hydrolysed with amyloglucosidase and determined enzymatically as glucose units using a starch-determination kit (Boehringer) [cf. Heim *et al.* (1993)].

Enzyme assay

Hexoses-producing enzymes (invertases, fructosyltransferases) were extracted from the tissues in a fivefold volume of 20 mM NaAc, pH 5.2. After centrifugation, the pellet was washed twice in 20 mM NaAc, pH 5.2, four times in destilled water, and used for the determination of cell wall-bound invertase. The assay buffer was 50 mM citric acid/Na_2HPO_4 pH 4.5, 100 mM sucrose, and the reaction was started with 150 μl of extract in a total volume of 300 μl for the soluble enzymes. The cell wall-bound invertase was determined by suspending 10 mg of cell wall material in 150 μl of 20 mM NaAc, pH 5.2. The reaction was started by adding 150 μl of assay buffer. After incubation for 20 min, 30°C, the reaction was stopped in a boiling water bath for 2 min, and an aliquot was used to determine the reducing sugars with a Boehringer kit (Boehringer, Mannheim, Germany [cf. Weber *et al.* (1996b)].

Histological methods

Caryopses were fixed overnight in 4% paraformaldehyde, 10 mM dithiothreitol (DTT) in PBS or 0.025 M phosphate buffer pH 7.0 with or without addition of sorbit. If necessary, caryopses were placed in buffer and cut in up to three pieces before fixation. After fixation, these were washed in PBS containing 10 mM DTT and dehydrated in an ethanol series containing 10 mM DTT. Samples were passed through a graded ethanol-methacrylate series as described in Baskin *et al.* (1992) and polymerised for at least 48 h in UV light at −20°C.

Using a Leica RM 2165 microtome the 3–5 μm sections were cut. The sections were stained with toluidine blue and examined in bright field using either a Zeiss Axioskop or a Nikon E 600 microscope. Pictures were taken with the Zeiss MC 80 DX or the Nikon UIII system using the Fujichrome 64 T or RVP 135 film. Slides were scanned and the images processed using Adobe Photoshop 5.5 software.

Reliability of the results

In general, all Northern blot analyses as well as measurements of invertase activity and estimations of sugar and starch content were repeated at least twice by using completely independent sets of hand-dissected material isolated from caryopses independently grown under the same growing conditions in different phytochambers. In all cases, the profiles of mRNA expression as well as invertase and sugar profiles were reproducible. However, small differences were found in the time scale of expression and in the activity values of the respective invertases as well as in sugar and starch levels, resulting from the slightly different development of caryopses in the independent experiments. All results presented in this paper were taken from one set of material. Therefore, SD given for sugar and starch levels as well as for invertase activities result from the threefold repetition of measurements using the same starting material. In case of the Northern blots, no standard deviation was shown because the same Northern blot was used to hybridise the different invertase isoforms to allow better comparison. A second Northern blot was prepared, using the same set of material, for hybridisation of the two hexose transporter fragments.

Acknowledgements

We are grateful to Wolfgang Michalek for his help in sequencing the hexose transporter cDNA fragments. We thank Hangning Zhang for STACKPACK analysis of the 45 000 EST collection and Angela Stegmann, Gabi Einert, Uta Siebert and Elsa Fessel for excellent technical assistance. An anonymous reviewer provided thoughtful comments (especially with respect to the possible role of vacuolar invertase in phloem unloading). This work was supported by the Land Sachsen-Anhalt (FKZ 2678/A/0087G). Figures 5(a–c), 6, 7(a) and 9(a–c) are based on experiments financed by a BMBF grant (GABI-SEED, FKZ 0312282).

References

Baskin, T.I., Busby, C.H., Fowke, L.C., Sammut, M. and Gubler, F. (1992) Improvements in immunostaining samples embedded in methacrylate: localisation of microtubules and other antigenes throughout developing organs in plants of diverse taxa. *Planta*, **187**, 405–413.

Bergmeyer, H.U., Bernt, E., Schmid, F. and Stark, H. (1974) *Methods of Enzymatic Analysis. 2nd edn. Verlag Chemie, Weinheim.*

Borisjuk, L., Walenta, S., Rolletschek, H., Müller-Klieser, W., Wobus, U. and Weber, H. (2002) Spatial analysis of plant development: sucrose imaging within *Vicia faba* cotyledons reveals specific development patterns. *Plant J.* **29**, 521–530.

Borisjuk, L., Walenta, S., Weber, H., Müller-Klieser, W. and Wobus, U. (1998) High resolution histographical mapping of glucose concentrations in developing cotyledons of *Vicia faba* in relation to mitotic activity and storage processes: glucose as a possible developmental trigger. *Plant J.* **15**, 583–591.

Carlson, S.J., Shankera, S. and Choarey, P.S. (2000) A point mutatin at the Miniature1 seed locus reduces levels of the encoded protein, but not its mRNA, in maize. *Mol. Gen. Genet.* **263**, 367–373.

Cheng, W.-H. and Chourey, P.S. (1999) Genetic evidence that invertase-mediated release of hexoses is critical for appropriate carbon partitioning and normal seed development in maize. *Theor. Appl. Gen.* **98**, 485–495.

Cheng, W.-H., Talliercio, E.W. and Chourey, P.S. (1996) The Miniature1 seed locus of maize encodes a cell wall invertase required for normal development of endosperm and maternal cells in the pedicel. *Plant Cell*, **8**, 971–983.

Christoffels, A., Miller, R. and Hide, W. (1999) STACK_PACK and STACK (Sequence Tag Alignment and Consensus Knowledgebase): a novel, comprehensive, hierarchical EST clustering and consensus generation and analysis system providing unique insight into the human genome. *Am. J. Hum. Genet.* **65**, 477.

Church, G.M. and Gilbert, W. (1984) Genomic sequencing. *Proc. Natl. Acad. Sci. USA* **81**, 1991–1995.

DeBlock, M. and Debrouwer, D. (1996) RNA–RNA *in situ* hybridization using DIG-labelled probes: the effect of high molecular weight polyvinyl alcohol on the alkaline phosphatase indoxyl-nitroblue tetrazolium reaction. In *Nonradioactive in Situ Hybridization Application Manual*, 2nd edn. Boheringer Mannheim: GmbH, pp. 141–145.

Doehlert, D.C. (1990) Distribution of enzyme activities within the developing maize (*Zea mays*) kernel in relation to starch, oil and protein accumulation. *Phys. Plant.* **78**, 560–567.

Edelman, J. and Jefford, T.G. (1968) The mechanism of fructosan metabolism in plants as exemplified in *Helianthus tuberosis*. *New Phytol.* **67**, 517–531.

Ehness, R. and Roitsch, T. (1997) Co-ordinated induction of mRNAs for extracellular invertase and a glucose transporter in *Chenopodium rubrum* by cytokinins. *Plant J.* **11**, 539–548.

Eschrich, W. (1989) Phloem unloading of photoassimilates. In *Transport of Photoassimilates* (Baker, D.A. and Milburn, J.A. eds). Harlow, UK: Longman Scientific & Technical, pp. 206–263.

Fisher, D.B. and Cash-Clark, C.E. (2000a) Sieve tube unloading and post-phloem transport of fluorescent tracers and protein injections into sieve tubes via severed aphid stylets. *Plant Physiol.* **123**, 123–137.

Fisher, D.B. and Cash-Clark, C.E. (2000b) Gradients in water potential and turgor pressure along the translocation pathway during grain filling in normally watered and water-stressed wheat plants. *Plant Phsiol.* **123**, 138–147.

Heim, U., Weber, H., Bäumlein, H. and Wobus, U. (1993) A sucrose-synthase gene of *Vicia faba L.* Expression pattern in developing seeds in relation to starch synthesis and metabolic regulation. *Planta*, **191**, 394–401.

Hendry, G.A.F. (1993) Evolutionary origin and natural functions of fructans – a climatological, biogeographic and mechanistic appraisal. *New Phytol.* **123**, 3–14.

Hirose, H., Takano, M. and Terao, T. (2002) Cell wall invertase in developing rice caryopsis: molecular cloning of *OsCIN1* and analysis of its expression in relation to its role in grain filling. *Plant Cell Physiol.* **43**, 452–459.

Kim, J.Y., Mahe, A., Guy, S., Brangeon, J., Roche, O., Chourey, P. and Prioul, J.L. (2000) Characterization of two members of the maize gene family, Incw3 and Incw4, encoding cell-wall invertases. *Gene* **245**, 89–102.

Matsushita, K. and Uritani, I. (1974) Change in invertase activity of sweet potato in response to wounding and purification and properties of its invertases. *Plant Physiol.* **54**, 60–66.

Meyer, R.F. and Boyer, J.S. (1981) Osmoregulation, solute distribution and growth in soybean seedlings having low water potentials. *Planta*, **151**, 482–489.

Michalek, W., Weschke, W., Pleissner, K.-P. and Graner, A. (2002) EST analysis in barley defines a unique set comprising 4000 genes. *Theor. Appl. Genet*, **104**, 97–103.

Miller, R.T., Christoffels, A.G., Gopalakrishnan, C., Burke, J., Ptitsyn, A.A., Brovaek, T.R. and Hide, W.A. (1999) A comprehensive approach to clustering of expressed human gene sequences: The sequence tag alignment and consensus knowledge base. *Genome Res.* **9**, 1143–1155.

Olsen, O.-A., Linnestad, C. and Nichols, S.E. (1999) Developmental biology of the cereal endosperm. *Trends Plant Sci.* **4**, 253–257.

Olsen, O.-A., Potter, R.H. and Kalla, R. (1992) Histo-differentiation and molecular biology of developing cereal endosperm. *Seed Sci. Res.* **2**, 117–131.

Panitz, R., Borisjuk, L., Manteuffel, R. and Wobus, U. (1995) Transient expression of storage proteins during early embryogenesis of *Vicia faba*: synthesis and metabolization of vicilin and legumin in embryo, suspensor and endosperm. *Planta*, **196**, 765–774.

Patrick, J.W. and Offler, C.E. (1995) Post-sieve element transport of sucrose in developing seeds. *Aust. J. Plant Physiol.* **22**, 681–702.

Patrick, J.W. and Offler, C.E. (2001) Compartmentation of transport and transfer events in developing seeds. *J. Exp. Bot.* **52**, 551–564.

Pollock, C.J. (1986) Fructans and the metabolism of sucrose in vascular plants. *New Phytol.* **104**, 1–24.

Roitsch, T. and Tanner, W. (1994) Expression of a sugar-transporter gene family in a photoautotrophic suspension culture of *Chenopodium rubrum* L. *Planta*, **193**, 365–371.

Sauer, N., Baier, K., Gahrtz, M., Stadler, R., Stolz, J. and Truernit, E. (1994) Sugar transport across the plasma membranes of higher plants. *Plant Mol. Biol.* **26**, 1671–1679.

Shannon, J.C. and Dougherty, C.T. (1972) Movement of ^{14}C-labelled assimilates into kernels of *Zea mays* L. Part II. Invertase activity of the pedicel and placento-chalazal tissues. *Plant Physiol.* **49**, 203–206.

Silva, M.P. and Ricardo, C.P.P. (1992) β-Fructosidases and *in vitro* dedifferentiation-redifferentiation of carrot cells. *Phytochemistry* **31**, 1507–1511.

Sprenger, N., Borlik, K., Brandt, A., Boller, T. and Wiemken, A. (1995) Purification, cloning, and functional expression of sucrose: fructan 6-fructosyltransferase, a key enzyme of fructan synthesis in barley. *Proc. Natl. Acad. Sci. USA* **92**, 11652–11656.

Sprenger, N., Schellenbaum, L., Van Dun, K., Boller, T. and Wiemben, A. (1997) Fructan synthesis in transgenic tobacco and chicory plants expressing barley sucrose: fructan 6-fructosyltransferase. *FEBS Lett.* **400**, 355–358.

Sreenivasulu, N., Altschmied, L., Panitz, R., Hähnel, U., Michalek, W., Weschke, W. and Wobus, U. (2002) Identification of genes specifically expressed in maternal and filial tissues of barley caryopses: a cDNA array analysis. *Mol. Genet. Genomics* **266**, 758–767.

Sturm, A. (1999) Invertases. Primary structure, functions, and roles in plant development and sucrose partitioning. *Plant Physiol.* **121**, 1–7.

Sturm, A. and Chrispeels, M.J. (1990) cDNA cloning of carrot extracellular β-fructosidase and its expression in response to wounding and bacterial infection. *Plant Cell*, **2**, 1107–1119.

Sturm, A. and Tang, G.-Q. (1999) The sucrose-cleaving enzymes of plants are crucial for development, growth and carbon partitioning. *Trends Plant Sci.* **4**, 401–407.

Thorne, J.H. (1985) Phloem unloading of C and N assimilates in developing seeds. *Ann. Rev. Plant Physiol.* **36**, 317–343.

Tymowska-Lalanne, Z. and Kreis, M. (1998) The plant invertases: Physiology, biochemistry and molecular biology. *Adv. Bot. Res.* **28**, 71–117.

Van der Meer, I.M., Koops, A.J., Hakkert, J.C. and Van Tunen, A.J. (1998) Cloning of the fructan biosynthesis pathway of Jerusalem artischoke. *Plant J.* **15**, 489–500.

Vijn, I. and Smeekens, S. (1999) Fructan: more than a reserve carbohydrate. *Plant Physiol.* **120**, 351–359.

Wang, N. and Fisher, D.B. (1994) The use of fluorescent tracers to characterize the post-phloem transport pathway in maternal tissues of developing wheat grains. *Plant Physiol.* **104**, 17–27.

Wang, N. and Fisher, D.B. (1995) Sucrose release into the endosperm cavity of wheat grains apparently occurs by facilitated diffusion across the nucellar cell membranes. *Plant Physiol.* **109**, 579–585.

Wang, H.L., Offler, C.E. and Patrick, J.W. (1994) Nucellar projection transfer cells in developing wheat grain. *Protoplasma* **182**, 39–52.

Weber, H., Borisjuk, L., Heim, U., Buchner, P. and Wobus, U. (1995) Seed coat-associated invertases of faba bean control both unloading and storage functions: cloning of cDNAs and cell-type specific expression. *Plant Cell*, **7**, 1835–1846.

Weber, H., Borisjuk, L., Heim, U., Sauer, N. and Wobus, U. (1997b) A role for sugar transporters during seed development: molecular characterization of a hexose and a sucrose carrier in fava bean seeds. *Plant Cell*, **9**, 895–908.

Weber, H., Borisjuk, L. and Wobus, U. (1996b) Controlling seed development and seed size in *Vicia faba*: a role for seed coat-associated invertases and carbohydrate state. *Plant J.* **10**, 823–830.

Weber, H., Borisjuk, L. and Wobus, U. (1997a) Sugar import and metabolism during seed development. *Trends Plant Sci.* **2**, 169–174.

Weber, H., Buchner, P., Borisjuk, L. and Wobus, U. (1996a) Sucrose metabolism during cotyledon development of *Vicia faba* L. is controlled by the concerted action of both sucrose-phosphate, synthase and sucrose synthase: expression patterns, metabolic regulation and implications for seed development. *Plant J.* **9**, 841–850.

Wei, J.-Z. and Chatterton, N.J. (2001) Fructan biosynthesis and fructosyltransferase evolution: expression of the 6-SFT (sucrose: fructan 6-fructosyltransferase) gene in crested wheat grass (*Agropyron cristatum*). *J. Plant Physiol.* **158**, 1203–1213.

Weig, A., Franz, J., Sauer, N. and Komor, E. (1994) Isolation of a family of cDNA clones from *Ricinus communis* L. with close homology to the hexose carriers. *J. Plant Physiol.* **143**, 178–183.

Weschke, W., Panitz, R., Sauer, N., Wang, Q., Neubohn, B., Weber, H. and Wobus, U. (2000) Sucrose transport into barley seeds: Molecular characterisation of two transporters and implications for seed development and starch accumulation. *Plant J.* **21**, 455–467.

Winter, H. and Huber, S.C. (2000) Regulation of sucrose metabolism in higher plants: localization and regulation of activity of key enzymes. *Crit. Rev. Plant Sci.* **19**, 31–67.

Wobus, U. and Weber, H. (1999) Sugars as signal molecules in plant seed development. *Biol. Chem.* **380**, 937–944.

Xu, J., Avigne, W.T., McCarty, D.R. and Koch, K.E. (1996) A similar dichotomy of sugar modulation and developmental expression affects both paths of sucrose metabolism: Evidence from a maize invertase gene family. *Plant Cell*, **8**, 1209–1220.

Zee, S.Y. and O'Brien, T.P. (1970) Studies on the ontogeny of the pigment strand in the caryopsis of wheat. *Aust. J. Biol.* **23**, 1153–1171.

[‡]Less extensive measurements published earlier (insert of Figure 9b in Weschke *et al.* 2000) provided similar data but symbols for pericarp and embryo sac values were interchanged by mistake.

Sugar import and metabolism during seed development

Hans Weber, Ljudmilla Borisjuk and Ulrich Wobus

During seed development, cell division is followed by elongation, differentiation and storage. In legumes, this sequence of events has been found to spread in a wave-like manner, creating a developmental gradient across the cotyledons. All these processes, including storage activities, appear to be subject to metabolic control. Sucrose is imported during seed development, and a sucrose breakdown pathway mediated by cell wall invertase operates in the seed coat during early development. The resulting high hexose state is associated with growth and mitotic activity. The storage/maturation phase is initiated following the developmentally controlled loss of invertase, and is accompanied by the formation of an active sucrose transport system. Invertases are therefore regarded as a control element in the changing carbohydrate status of seeds, and the invertase control hypothesis for seed development has emerged. Cotyledonary sucrose metabolism is controlled by a cycle of synthesis and breakdown involving sucrose-phosphate synthase and sucrose synthase, respectively; net breakdown for storage product synthesis involves sucrose synthase. The complex framework of interactions involved in these pathways is now being elucidated via a combination of biochemical, physiological and molecular methods.

Developing seeds are a well-defined system in which to analyze the transport of assimilates and sink metabolism. The large seeds of grain legumes and cereals, in particular, allow physiological and biochemical approaches to be combined with an analysis of the underlying developmental processes. In addition, a large number of mutants covering different aspects of development and metabolism are available in pea, maize and barley. Seeds from different species can accumulate the storage products starch, protein and oil in different proportions. In legume seeds, these products are synthesized in the cotyledons from sucrose imported during the later stages of seed development. This quality is of agronomic significance, and is one reason why legume seeds have become the subject of intensive investigation. This review summarizes recent progress in understanding sugar import and metabolism, and its relation to seed development, in legumes, and also includes comparable data from cereals.

Seed development – a series of differentiation events

Developing legume seeds are complex structures containing the embryo and several other tissues, including the seed coat, endosperm and suspensor. Development occurs in a series of specific temporal and spatial steps, with a phase of cell division, followed by differentiation and storage activity. The expression of storage protein genes is regarded as a marker for maturation, and a gradient of storage protein gene expression is generally detected in developing storage organs (although the spatial orientation can be species-specific). In soybean cotyledons, the expression of several storage protein genes is developmentally regulated, and the expression pattern appears to spread in a wave from the outer to the inner surface[1]. In pea cotyledons, a similar wave-like expression of vicilin starts at the adaxial region and spreads to the abaxial surface[2]. The pea vicilin gene is only expressed in regions that lack mitotic activity[2], suggesting that there is a negative correlation between mitotic activity and storage protein gene expression. In *Vicia faba* cotyledons, the expression of vicilin and legumin, as well as starch accumulation, starts at the adaxial region and spreads to the abaxial zone with increasing seed fresh weight. The pattern of storage protein gene expression is spatially distinct from the pattern of mitotic activity[3]. The developmental gradient that is generated across the cotyledons comprises younger, mitotically active cells in the abaxial region and older cells in the adaxial region undergoing elongation, endopolyploidization and storage product synthesis (Fig. 1). Several aspects of this process remain unclear, including how the activities of genes involved in seed development are programmed, how the observed developmental patterns are coordinated in space and time, and how metabolic signals are integrated.

Sugar transfer into developing seeds

It has often been assumed that post-phloem sugar transport to sink tissues is exclusively sink-controlled, involving a mechanism in which a high capacity to metabolize assimilates in the embryo lowers sugar concentrations and creates a gradient, which drives import. However, a growing body of evidence argues against this idea, favouring the view that assimilate partitioning is regulated by sink-located transfer and transport processes[4,5].

In developing seeds, the embryo is isolated from the maternal seed coat by the apoplast. On their way from the phloem to the embryo, assimilates must therefore pass at least two membranes. Active transport systems are present in different parts of the seed[6,7], and these could represent control points. In wheat, unloading is controlled at the level of transport through the maternal seed tissue[4]. The control of import is exercised by the rate of assimilate delivery through the chalazal plasmodesmata[4].

PII S1360-1385(97)01030-3

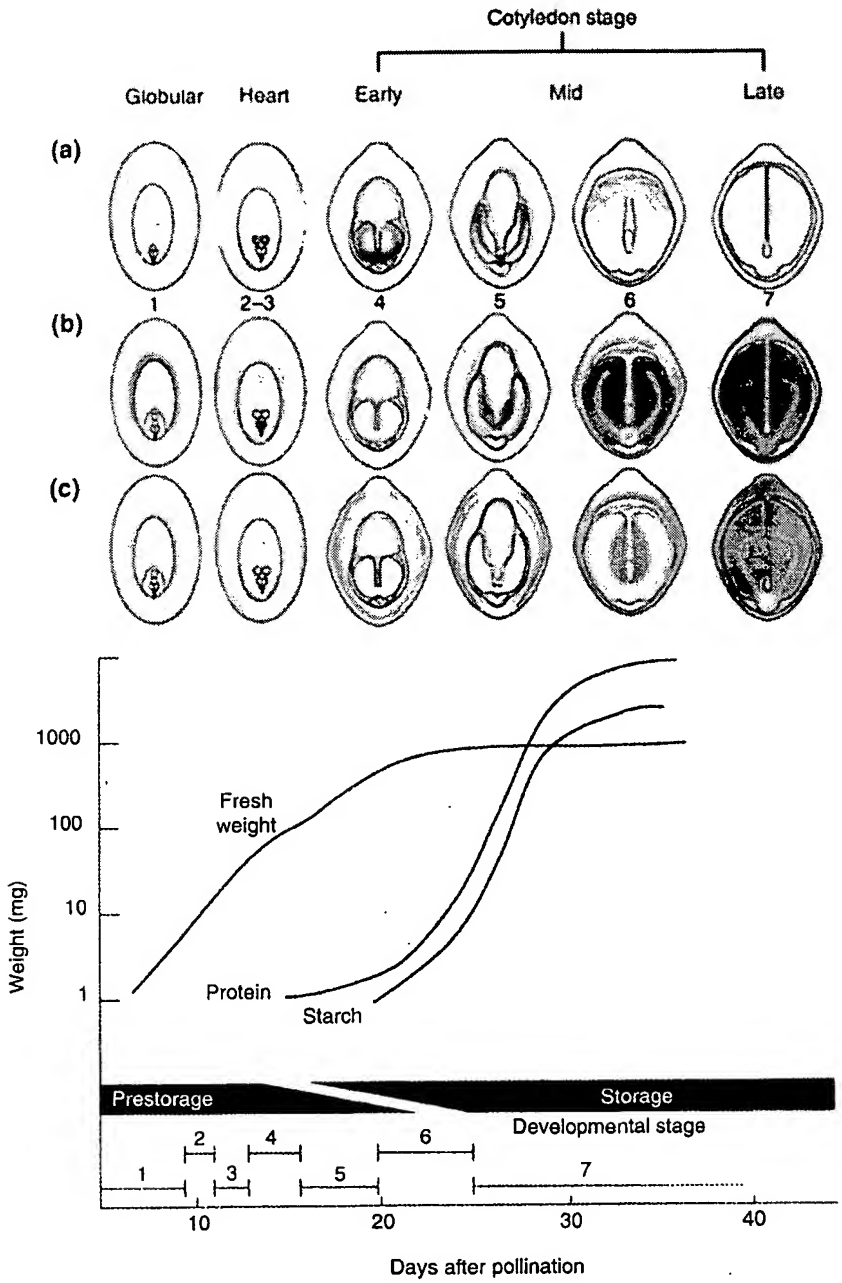

Fig. 1. Seed development of *Vicia faba* is divided into seven stages, based on morphological and histochemical characteristics: the globular stage (1); the early and late heart stage (2–3); and four stages covering early to late cotyledon development (4–7). The patterns of mitotic activity [red, shown in (a)], expression of storage protein genes [blue, shown in (b)] and starch accumulation [yellow, shown in (c)] occur in different tissues of the developing seed. Deeper colours indicate higher rates. The distribution of mitotic activity followed by differentiation leads to a developmental gradient within the seed. The accumulation of storage products – proteins and starch – is directly coupled to this developmental gradient, as shown in the graph. Storage function is inversely related to mitotic activity. *Reproduced, with permission, from Ref. 3.*

In *V. faba* seeds, the sieve elements of the phloem terminate in the seed coat and are symplastically connected with coat cells[5]. Phloem unloading and subsequent transport through the seed coat are thought to be symplastic[5], with regulated transfer occurring through the plasmodesmata[8]. Inhibitor studies and selective removal of the inner cell layers of the coat, the thin-walled parenchyma, identified this tissue as the unloading site into the apoplast[9]. The possible mechanisms of seed coat unloading are still controversial, and it is not known whether transport is controlled by the maternal or embryonic seed tissue, or whether the site of control changes during development.

In pea, it has been suggested that unloading may be a passive process, mediated by a porin-like transporter[10]. However, unloading from *V. faba* seed coats is thought to be carrier-mediated, even though the portion of passive unloading may be as high as 50% (Ref. 5). In addition, seed coat unloading is sensitive to turgor, and a turgor–homoestat model has been proposed for the regulation of efflux from the seed coat, by rates of sucrose utilization in the cotyledons[5]. A clearer picture of sugar uptake by the embryo has emerged from analysing seeds of different species[5]. In general, both saturable and nonsaturable uptake systems are present. Several different experimental approaches have provided evidence that the saturable component is an H^+–sucrose symporter that is located in the outer epidermal transfer cell complex, but that the passive uptake system is less important[5,7]. It has been stated that transport control resides at the plasma membrane of the epidermal transfer cells[5]. The necessary proton-motive force in the epidermal cells is provided by a colocalized H^+-translocating ATPase[11].

A cDNA encoding an H^+–sucrose symporter that is expressed in cotyledons during the storage phase has recently been isolated in *V. faba*. *In situ* hybridization revealed that expression is confined to the epidermal cell layer covering the outer surface of the cotyledons[12]. This pattern correlates with the differentiation of these cells into transfer cells, and is accompanied by storage activity in the underlying parenchyma [visualized by the expression of the storage protein gene vicilin (Fig. 2)]. The spatial and temporal expression pattern of the symporter in epidermal transfer cells indicates an active uptake mechanism for sucrose into cotyledonary epidermal cells during the storage phase. However, sugar uptake by the storage parenchyma cells appears to be passive[7].

Acid invertase activities and the phase of initial seed growth

Seeds import sucrose, which must be hydrolysed prior to its use in either metabolism or storage product synthesis.

Two enzymes are involved in catalysing this cleavage process – sucrose synthase and invertase – and it has been proposed that each operates in a pathway of specific significance. In general, in sink tissues, the invertase pathway is directed towards growth and cell expansion, whereas the sucrose synthase pathway is associated with storage product biosynthesis[13]. A polar distribution is often found if both enzymes are present in the same organ, signifying the different roles in sugar metabolism.

Sucrose cleavage, catalysed by cell wall-bound invertase, occurs in the placento–chalazal cells of developing maize kernels, and has been implicated as a necessary step in either carbohydrate transport out of the vascular system or into the endosperm[14]. Invertase activity seems to be important for early seed growth, because the *mn-1* ('miniature') mutant, lacking this enzyme, is inhibited in the early stages of seed development[14]. The *mn-1* locus encodes an endosperm-specific cell wall-bound invertase. Below a threshold level of about 6% of the wild-type activity, the enzyme controls the developmental stability of maternal cells in the pedicel in a rate-limiting manner[14]. Also, in *Sorghum*, invertase activity is maximal at the initial stages of seed development, and later declines[15]. Accordingly, the activity of a cell wall-bound invertase in the seed coat of legumes is confined to early development. In the pea seed coat, high levels of both soluble and cell wall-bound invertase activity are correlated with high concentrations of glucose and fructose in the apoplast bathing the early embryo[16]. In *V. faba*, seed coat-associated invertase is present during early seed development, and generates high concentrations of hexose sugars in the embryo. During the prestorage phase, a cell wall-bound invertase gene is specifically expressed in the thin-walled parenchyma of the seed coat[17] – the region of photoassimilate unloading[5]. It was concluded that sucrose hydrolysis was catalysed by extracellular invertases after unloading from the seed coat, facilitating transfer out of the seed coat parenchyma. In addition, an environment rich in hexose sugars is generated for the young embryo engaged in organ formation. During this phase of development, the final number of cells of the storage organs, cotyledons and/or endosperm is established. The invertase pathway therefore appears to be specific to the cell division phase of development and is associated with cell division and growth, rather than storage[17].

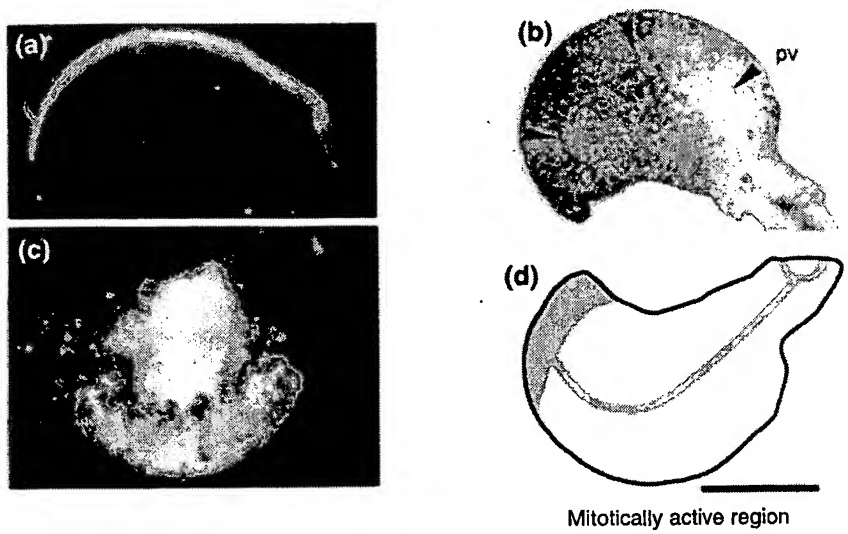

Fig. 2. A sucrose transporter is expressed exclusively in the outer epidermis of developing cotyledons of *Vicia faba* at the mid-cotyledon stage (a, white grains). The toluidine blue-stained structure is shown in (b). Storage product synthesis is visualized by the expression of the major storage protein vicilin, and occurs in the adaxial parenchyma cells of the cotyledons (c, white grains). The cotyledon cells of the provascular tissue and the most abaxial part of the cotyledons do not express vicilin, and are still mitotically active (d, shaded area). The spatial correlation between the epidermal transfer cell/sucrose transport region and the underlying parenchyma engaged in vicilin gene expression suggests a causal relationship. Abbreviation: pv, provascular tissue. Scale bar represents 1 mm.

Carbohydrate status as a control element in seed development

The invertase-mediated unloading process in legume seeds creates a high ratio of hexose sugars to sucrose at a time when mitotic activity proceeds in the cotyledons. This special sugar status is necessary for promoting growth. Studies in pea[18] and *V. faba*[19] have shown that feeding high concentrations of sucrose to young cotyledons favours storage as compared with growth. The explanted cotyledons age prematurely, as indicated by an earlier decrease in mitotic rate, together with early onset of endopolyploidization. This process is accompanied by starch accumulation and the transcription of storage protein genes[18]. Conversely, a hexose-based medium maintains cell division rates, but impairs proper storage functions, as seen by reduced levels of storage protein gene transcripts and an increased ratio of sucrose to starch[19,20]. It may therefore be that the carbohydrate status of the premature embryo, as controlled by cell wall-bound invertase, favours cell division. The link between sugar status and cell proliferation during development might be achieved by a direct effect of sugar on cell cycle gene expression[21]. Apoplastic hexoses could be sensed by a plasma membrane-spanning receptor. It will be interesting to see whether a hexose transporter can itself serve as a sensor, as shown for a glucose transporter in yeast[22].

The transition from the cell division phase to the maturation or storage phase in the embryo is accompanied by a decrease in the hexose to sucrose ratio and a dramatic increase in fresh weight. In *V. faba* seeds, this developmental switch is correlated with a gradual loss of invertase activity in the seed coat. When the enlarging embryo contacts the seed coat, the inner cell rows of the thin-walled parenchyma become degraded and cell wall-bound invertase activity declines[17]. The process occurs in a manner that is temporally and spatially related to the developmental gradient in the cotyledons, suggesting that it has a triggering function in differentiation. The loss of the invertase-mediated pathway and the gain in the embryo's ability to import sucrose directly are both associated with a switch to storage functions (Fig. 3).

Cotyledonary sucrose metabolism

Seed tissues actively engaged in storage often have a remarkably low level of acid invertase activity, but high

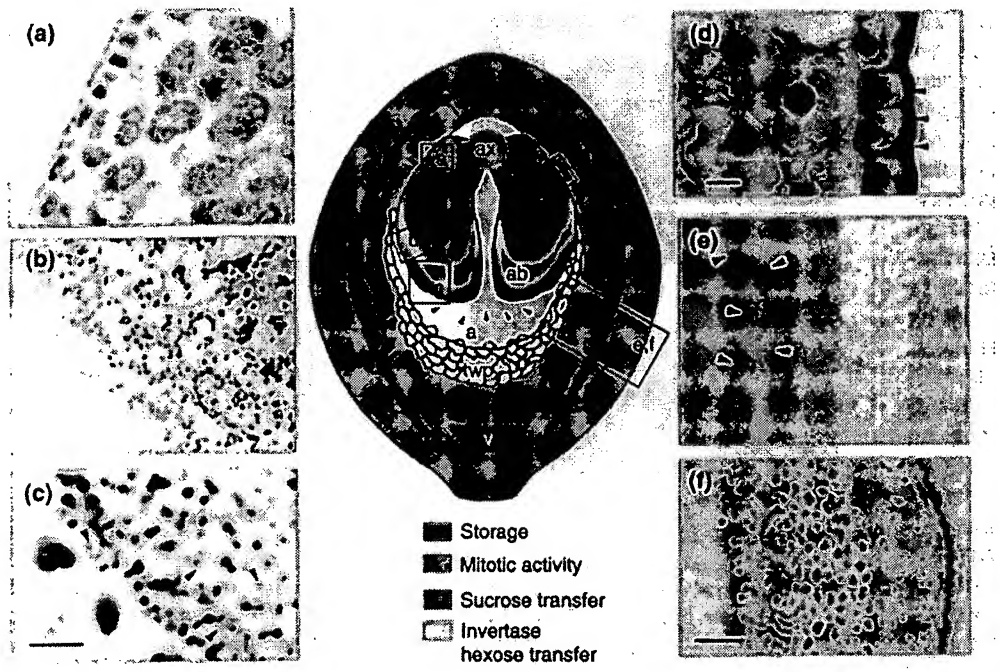

Fig. 3. Visualizing the developmental gradient during seed development in a *Vicia faba* seed at the beginning of the storage phase. (a) Immunolocalization of storage protein bodies within cotyledon cells in the adaxial region. (b) Distribution of starch grains from the boundary of the storage region to the mitotically active region of the cotyledon; grains are fewer and smaller at the periphery. (c) Staining of nuclei in the abaxial part of the cotyledon, showing a high proportion of metaphase stages (arrowheads). (d) Outer region of the storage region. The single cell-layered epidermis reveals cell wall thickening, indicating transfer cell morphology (arrowheads). (e) Seed coat at the chalazal region. Expression of a cell wall-bound invertase is visualized in the thin-walled parenchyma by *in situ* hybridization (dark grains, arrowheads). (f) As in (e), but after toluidine blue staining. The cell wall-bound invertase is active in the chalazal part of the thin-walled parenchyma of the coat (shaded yellow), and causes a high ratio of hexoses to sucrose in the abaxial region of the cotyledons. This carbohydrate state promotes mitotic activity within this region (shaded brown). Invertase activity is low where the enlarging embryo contacts the seed coat, and cells of the thin-walled parenchyma are dissolved. The outer epidermal cell layer in that region establishes a transfer cell–sucrose transport complex. Abbreviations: ab, abaxial part of the cotyledon; a, apoplast; ad, adaxial part of the cotyledon; ax, embryonic axis; twp, thin-walled parenchyma of the seed coat; v, chalazal vein. Boxed regions (a–f) in the central diagram refer to the outer panels. Scale bars represent 100 μm (a–c), 10 μm (d) and 50 μm (e, f).

levels of sucrose synthase activity[13]. Sucrose synthase has frequently been cited as a marker for sink strength, and the onset of starch synthesis is accompanied by an increase in enzyme activity[13]. The reaction of the enzyme is readily reversible[23], but it is rendered irreversible by rapid removal of the cleavage products, via high fructokinase activity and starch synthesis[13].

Sucrose-phosphate synthase activity is frequently found in nonphotosynthetic tissues, and is thought to be involved in the resynthesis of sucrose. Degradation and metabolization via a cycle of breakdown and synthesis is a general phenomenon that operates to varying degrees in both seeds[20] and vegetative sink tissues[24] to control sucrose levels. In *V. faba* cotyledons, the expression of sucrose synthase and sucrose-phosphate synthase is coordinately induced in cells differentiating into storage tissues, and both enzymes are regulated at several levels[20].

Changes in the carbohydrate status during *V. faba* seed development are likely to play a role in controlling the ratio of sucrose synthase to sucrose-phosphate synthase, and thus the flux through the cycle of breakdown and synthesis. In cotyledons, the affinity of sucrose synthase for sucrose is very low, with an estimated K_m of 169 mM (Ref. 25). The prestorage phase is characterized by a high ratio of hexose sugars to sucrose, and sucrose synthase is unlikely to make a large contribution to sucrose degradation at this point. In addition, the hexose sugars present at this stage can lead to a considerable inhibition of sucrose synthase activity in the cotyledons[25]. In maize endosperm, hexose sugars act as inhibitors of sucrose synthase, and may impede the enzyme in the basal regions of the kernel where they accumulate[26].

In contrast, during the storage phase, a low ratio of hexose sugars to sucrose occurs in the cotyledons. In maturing *V. faba*[27] and pea cotyledons[18], dry weight accumulation *in vitro* is dependent on high sucrose levels. In wheat endosperm, the rate of storage starch accumulation is a function of the concentration of sucrose[28]. Therefore, in a storage organ, a high sucrose state and low hexose levels would promote sucrose breakdown for storage product synthesis via a sucrose synthase pathway. Transcription of the gene for sucrose synthase is induced by sucrose[29,30]. The significance of a highly active sucrose-phosphate synthase during the switch from the cell division phase to the storage phase may be for the synthesis of sucrose, thereby decreasing the high hexose sugar : sucrose ratio to a level that induces the storage pathway. However, sucrose-phosphate synthase becomes partially inactivated during the storage phase[20], possibly by phosphorylation and/or indirectly by sucrose feedback regulation[31] (Fig. 4).

Some seeds contain alkaline invertase. However, its activity is far below that of sucrose synthase and increases during the last stages of development[32]. Although alkaline invertase can catalyse the breakdown of sucrose, sucrose synthase is thought to make the greater contribution.

Seeds usually accumulate large amounts of storage proteins, as well as starch or oil. This indicates that there is a need to integrate carbohydrate and nitrogen metabolism. Developing legume seeds import amides and are able to synthesize a wide range of amino acids. Therefore, a part of the imported carbon must be partitioned into amino acid biosynthesis. Carbon partitioning into amino acids is effected when

the sucrose : starch ratio is altered. The supply of hexose sugars to *V. faba* storage phase cotyledons *in vitro* has been shown to increase the sucrose : starch ratio by inducing sucrose-phosphate synthase, whereas free amino acids and storage protein legumin B mRNA levels are lowered[20]. A similar effect on legumin mRNA was reported for the pea seed mutant *rug* ('rugosus'), which partitions less carbohydrate into starch and is characterized by an increased sucrose : starch ratio[33]. Transgenic potato tubers with reduced ADP-glucose pyrophosphorylase activity[34] stored large amounts of both sugars instead of starch, and this was accompanied by increased transcription of sucrose-phosphate synthase mRNA and decreased transcript levels of storage protein genes. Similar effects on protein metabolism were observed in the *sh* ('shrunken') and *bt* ('brittle') mutants of maize seeds[35]. Thus, the synthesis of starch and storage proteins is interrelated, and a reduction or defect in starch synthesis is coupled to a reduction in the storage of proteins.

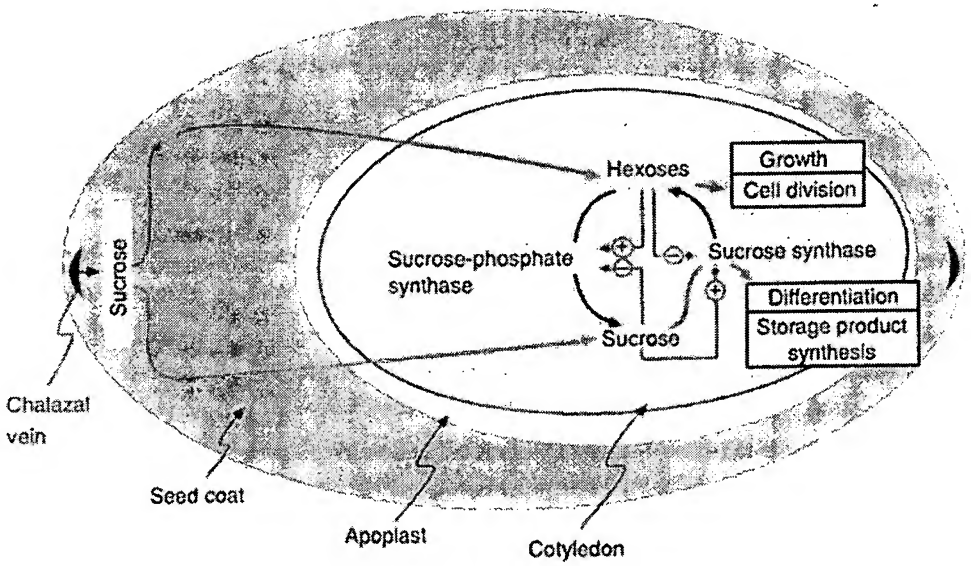

Fig. 4. The invertase control hypothesis of seed development. The import and metabolism of sucrose is shown in the diagram. Sucrose enters the seed coat via the chalazal vein (left). During the prestorage phase, sucrose is degraded via the catalytic action of seed coat-associated, cell wall-bound invertase [pathway from sucrose (on the left of the diagram) via hexoses to growth and cell division] . The invertase activity is high during the prestorage phase of development, and the resulting high ratio of hexoses to sucrose promotes growth via cell division. Invertase activity is low during the storage phase of development, when sucrose is taken up directly by the cotyledons [pathway from sucrose (on the left of the diagram) via sucrose (in the centre of the diagram) and sucrose synthase to differentiation and storage product synthesis]. A low ratio of hexoses to sucrose promotes differentiation and storage product synthesis. Sucrose metabolism in the cotyledons is catalysed by a cycle of synthesis and breakdown (black arrows) via sucrose-phosphate synthase and sucrose synthase. Net sucrose breakdown occurs by a sucrose synthase-dependent pathway.

Future perspectives

Further experimentation is needed to test the validity of the current thinking discussed in this review, and to integrate other aspects, such as the role of hormones. Several approaches are especially promising. For example, mutants are available in legumes and cereals that are either altered in early development or have defects in storage metabolism. Also, large sets of cDNAs can be used to analyze coordinated gene expression and regulation under different conditions of carbohydrate or nitrogen supply. One of the major challenges will be to identify nutrient sensing mechanisms and signal transduction pathways that link, for example, the carbohydrate status to the cell cycle. Also, because carbohydrate and nitrogen metabolism are interconnected, the identification of branch points will help clarify the changes in assimilate partitioning between starch, proteins and fatty acids. The characterization of genes for sugar and amino acid transporters should help to unravel the significance of transport processes for phloem and seed coat unloading, as well as for uptake into storage organs. Transgenic approaches are vital, and transformation and regeneration protocols for different legume species are becoming more readily available. However, there is still a need for promoters that are active in specific seed tissues or cell types at precise developmental stages. The use of sense or antisense technology will allow the alteration of specific developmental and/or metabolic processes, enabling further definition and manipulation of seed development.

Acknowledgements

Work in the authors' lab is supported by the European Union (FAIR Ct0066), the Deutsche Forschungsgemeinschaft (SPP 322 1005) and the Fonds der Chemischen Industrie (U.W.). The authors would like to thank Marc Stitt and two anonymous reviewers for valuable comments on the manuscript.

References

1 Perez-Grau, L. and Goldberg, R.B. (1989) Soybean seed protein genes are regulated spatially during embryogenesis, *Plant Cell* 1, 1095–1109
2 Hauxwell, A.J. *et al.* (1990) Storage protein gene expression is localised to regions lacking mitotic activity in developing pea embryos. An analysis of seed development in *Pisum sativum* XIV, *Development* 110, 283–289
3 Borisjuk, L. *et al.* (1995) Embryogenesis of *Vicia faba* L.: histodifferentiation in relation to starch and storage protein synthesis, *J. Plant Physiol.* 147, 203–218
4 Fisher, D.B. and Wang, N. (1995) Sucrose release into the endosperm cavity of wheat grains apparently occurs by facilitated diffusion across the nucellar membranes, *Plant Physiol.* 109, 579–585
5 Patrick, J.W. and Offler, C.E. (1995) Post-sieve element transport of sucrose in developing seeds, *Aust. J. Plant Physiol.* 22, 681–702
6 Gahrtz, M. *et al.* (1996) Expression of the PmSUC1 sucrose–H^+ carrier gene from *Plantago major* L. is induced during seed development, *Plant J.* 9, 93–100
7 McDonald, R., Fieuw, S. and Patrick, J.W. (1996) Sugar uptake by the dermal transfer cells of developing cotyledons of *Vicia faba* L.

Experimental systems and general transport properties, *Planta* 198, 54–63
8 Stitt, M. (1996) Plasmodesmata play an essential role in sucrose export from leaves: a step toward an integration of metabolic biochemistry and cell biology, *Plant Cell* 8, 565–571
9 Wang, X.D. *et al.* (1995) Cellular pathway of photosynthate transport in coats of developing seed of *Vicia faba* L. and *Phaseolus vulgaris* L. 2. Principal cellular site(s) of efflux, *J. Exp. Bot.* 46, 49–63
10 DeJong, A. *et al.* (1996) Characterization of the uptake of sucrose and glucose by isolated seed coat halves of developing pea seeds. Evidence that a sugar facilitator with diffusional kinetics is involved in seed coat unloading, *Planta* 199, 486–492
11 Bouché-Pillon, S. *et al.* (1994) Asymmetric distribution of the plasma-membrane H^+-ATPase in embryos of *Vicia faba* L. with special reference to transfer cells, *Planta* 193, 392–397
12 Borisjuk, L. *et al.* (1996) Transfer cell-specific expression of a putative sucrose–H^+ symporter in developing embryos of *Vicia faba*. *Plant Physiol. Biochem.* (Special issue), 180
13 Quick, W.P. and Schaffer, A.A. (1996) Sucrose metabolism in sources and sinks, in *Photoassimilate Distribution in Plants and Crops, Source–Sink Relationships* (Zamski, E. and Schaffer, A.A., eds), pp. 115–156, Marcel Dekker
14 Cheng, W.H., Talierico, E.W. and Chourey, P.S. (1996) The *Miniature1* seed locus encodes a cell wall invertase required for normal development of endosperm and maternal cells in the pedicel, *Plant Cell* 8, 971–983
15 Maness, N.O. and McBee, G.G. (1986) Role of placental sac in endosperm carbohydrate import in *Sorghum* caryopses, *Crop Sci.* 26, 1201–1207
16 Déjardin, A. *et al.* Purification, characterization and physiological role of sucrose synthase in the pea seed coat (*Pisum sativum* L.), *Planta* (in press)
17 Weber, H. *et al.* (1995) Seed coat-associated invertases of Fava bean control both unloading and storage functions: cloning of cDNAs and cell type-specific expression, *Plant Cell* 7, 1835–1846
18 Wang, T.L. and Hedley, C.L. (1993) Genetic and developmental analysis of the seed, in *Peas: Genetics, Molecular Biology and Biochemistry* (Casey, R. and Davies, D.R., eds), pp. 83–120, Cab International
19 Weber, H., Borisjuk, L. and Wobus, U. (1996) Controlling seed development and seed size in *Vicia faba*: a role for seed coat-associated invertases and carbohydrate state, *Plant J.* 10, 823–834
20 Weber, H. *et al.* (1996) Sucrose metabolism during cotyledon development of *Vicia faba* is controlled by the concerted action of both sucrose-phosphate synthase and sucrose synthase: expression pattern, metabolic regulation and implications for seed development, *Plant J.* 9, 841–850
21 Soni, R. *et al.* (1995) A family of cyclin D homologs from plants differentially controlled by growth regulators and containing the conserved retinoblastoma protein interaction motif, *Plant Cell* 7, 85–103
22 Özcan, S. *et al.* (1996) Two glucose transporters in *Saccharomyces cerevisiae* are glucose sensors that generate a signal for induction of gene expression, *Proc. Natl Acad. Sci. U. S. A.* 93, 12428–12432
23 Geigenberger, P. and Stitt, M. (1993) Sucrose synthase catalyses a readily reversible reaction *in vivo* in developing potato tubers and other plant tissues, *Planta* 189, 329–339
24 Wendler, R. *et al.* (1990) Sucrose storage in cell suspension cultures of *Saccharum* is regulated by a cycle of synthesis and degradation, *Planta* 183, 31–39
25 Ross, H.A. and Davies, H.V. (1992) Purification and characterization of sucrose synthase from the cotyledons of *Vicia faba* L., *Plant Physiol.* 100, 1008–1013
26 Doehlert, D.C. (1987) Substrate inhibition of maize endosperm sucrose synthase and its interaction with glucose inhibition, *Plant Sci.* 52, 153–157
27 Barratt, D.H.P. and Pullen, A. (1984) Control of seed protein accumulation in field bean, *Ann. Bot.* 54, 31–38
28 Jenner, C.F., Uglade, T.D. and Aspinall, D. (1991) The physiology of starch and protein deposition in the endosperm of wheat, *Aust. J. Plant Physiol.* 18, 211–226
29 Heim, U. *et al.* (1993) A sucrose-synthase gene of *V. faba* L.: expression pattern in developing seeds in relation to starch synthesis and metabolic regulation, *Planta* 191, 394–401
30 Koch, K.E. (1996) Carbohydrate-modulated gene expression in plants, *Annu. Rev. Plant Physiol. Plant Mol. Biol.* 47, 509–540
31 Reimholz, R., Geigenberger, P. and Stitt, M. (1994) Sucrose-phosphate synthase is regulated via metabolites and protein phosphorylation in potato tubers, in a manner analogous to the enzyme in leaves, *Planta* 192, 480–488
32 Ross, H.A., McRae, D. and Davies, H.V. (1996) Sucrolytic enzyme activities in cotyledons of the Faba Bean, *Plant Physiol.* 111, 329–338
33 Turner, R.T., Barratt, D.H.P. and Casey, R. (1990). The effect of different alleles at the *r* locus on the synthesis of seed storage proteins in *Pisum sativum*, *Plant Mol. Biol.* 14, 793–803
34 Müller-Röber, B., Sonnewald, U. and Willmitzer, L. (1992) Inhibition of the ADP-glucose pyrophosphorylase in transgenic potatos leads to sugar-storing tubers and influences tuber formation and expression of tuber storage protein genes, *EMBO J.* 11, 1229–1238
35 Giroux, M.J. *et al.* (1994) Coordinated transcriptional regulation of storage protein genes in maize endosperm, *Plant Physiol.* 106, 713–722

Hans Weber* and Ulrich Wobus are at the Institut für Pflanzengenetik und Kulturpflanzenforschung, D-06466 Gatersleben, Germany; Ljudmilla Borisjuk is at the Center for Agricultural Molecular Biology, Rutgers University, New Brunswick, NJ 08903-0231, USA.

*Author for correspondence (tel +49 394 825 208; fax +49 394 82 280; e-mail weber@IPK-gatersleben.de).

Write to *Trends in Plant Science*

Can you expand on a topic raised in a recent issue of the magazine, or is there a matter of general interest that you want to share? Have you made a new discovery, or do you have a fresh perspective on an area of current research? Is there a point about scientific policy that you feel should be made. Maybe you would like to discuss science education, plant genetic engineering, or funding issues?

Correspondence to *Trends in Plant Science* can cover a very wide range of issues. Letters should be **no more than 500 words long with up to 10 references and a single figure**. Letters should be sent, together with an electronic version on disk, to the Editor (or sent as an e-mail attachment to plants@elsevier.co.uk). The decision to publish rests with the Editor, and the author(s) of any *Trends in Plant Science* article discussed in a Letter will normally be invited to reply.

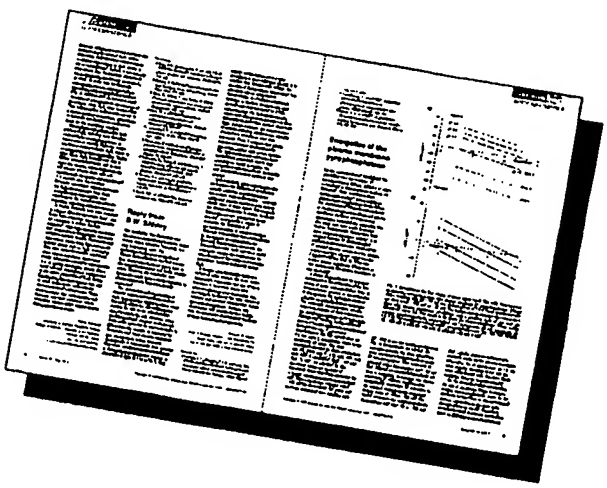

doi:10.1016/j.jmb.2003.10.066 J. Mol. Biol. (2004) 335, 987–995

JMB

Available online at www.sciencedirect.com

SCIENCE DIRECT®

ELSEVIER

The Invertase Inhibitor Nt-CIF from Tobacco: A Highly Thermostable Four-helix Bundle with an Unusual N-terminal Extension

Michael Hothorn[1], Igor D'Angelo[1], José Antonio Márquez[1] Steffen Greiner[2]* and Klaus Scheffzek[1]*

[1]*European Molecular Biology Laboratory (EMBL), Structural and Computational Biology Programme, Meyerhofstr. 1 69117 Heidelberg, Germany*

[2]*Heidelberger Institut für Pflanzenwissenschaften, Abt. Molekulare Ökophysiologie, Im Neuenheimer Feld 360, 69120 Heidelberg, Germany*

**Corresponding authors*

Plant invertases are sucrolytic enzymes essential for plant metabolism and development. Enzyme activity is regulated on a posttranslational level *via* inhibitory proteins, referred to as invertase inhibitors. Ectopic expression of invertase inhibitors in crop plants has high biotechnological potential. However, little biochemical and up to now no detailed structural information is available about this class of plant regulatory proteins. Here, we present the crystal structure of the cell wall-associated invertase inhibitor Nt-CIF from tobacco at a resolution of 1.87 Å. The structural model reveals an asymmetric four-helix bundle with an uncommon N-terminal extension that appears to be critical for the structural integrity of the protein. Structure analysis of a second crystal form grown in the presence of $CdCl_2$ reveals two metal binding sites. Nt-CIF is highly thermostable and retains full inhibitory activity after cooling to ambient temperatures. The structure of Nt-CIF provides the first three-dimensional information source for the posttranslational regulation of plant invertases. Based on the recently discovered sequence homology between inhibitors of invertases and pectin methylesterases, our structural model is likely to represent a scaffold also used for the regulation of the latter enzymes, which do not share sequence similarity with invertases. Thus, our structural model sets the 3D-stage for the investigation of posttranslational regulation of invertases as well as pectin methylesterases.

Keywords: pectin methylesterase; crystal structure; posttranslational regulation; *Nicotiana tabacum*

Introduction

Plant acid invertases catalyze the hydrolytic cleavage of the transport sugar sucrose,[1] which is the major transport form of carbohydrates in higher plants. Sucrose is exported from the source tissues (leaves) and transported *via* the phloem to the different sink tissues (roots, stem, reproductive organs and vegetative storage organs). Cells in the target tissue may take up sucrose symplastically or apoplastically, and the sucrose can be hydrolyzed by invertases subsequently. These enzymes reside in the vacuole and the extracellular space, where invertase activity facilitates long-range carbohydrate transport by creating sucrose concentration gradients.[2] Sucrose and its hydrolysis products glucose and fructose provide growing tissues with energy and can serve as signals regulating gene-expression.[3] Therefore, invertase activity at the wrong time and place can dramatically affect plant viability and development.[4] Antisense repression of invertase genes distorts seedling morphology and leaf-to-root ratios[5] and induces male sterility in tobacco.[6] Thus, invertases are tightly regulated in order to maintain normal plant development. While control of invertase activity can occur at the level of transcription,[7] the

Present address: J. A. Marquez, EMBL Outstation Grenoble, BP181, 38042 Grenoble Cedex 9, France.

Abbreviations used: Nt-CIF, *Nicotiana tabacum* cell wall inhibitor of beta fructosidase; PME, pectin methylesterase.

E-mail addresses of the corresponding authors: scheffzek@embl-heidelberg.de; sgreiner@hip.uni-heidelberg.de

posttranslational regulation appears to be of equal importance. Hereby, activity is modulated *via* interaction with highly specific inhibitory proteins, a general strategy also found for other enzymes involved in carbohydrate metabolism.[8,9] These invertase inhibitors have been shown to be heat-stable, non-glycosylated monomers, affecting invertase activity in a pH-dependent manner.[10] The inhibition process can be modulated *in vitro* by the substrate sucrose and divalent cations in the millimolar range.[10,11] Biotechnological relevance has been pointed out in the case of cold-induced sweetening of potato tubers. Transgenic expression of invertase inhibitors can interfere with this major food storage problem.[12]

Recent plant genome sequencing projects have identified a novel protein family formed by invertase inhibitors and the related inhibitors of pectin methylesterase (PME),[13] the latter being involved in the control of pectin metabolism. Common features of this plant-specific family include an N-terminal signal peptide, four conserved cysteine residues involved in the formation of two disulfide bridges[13,14] and a total size of about 18 kDa. *In vitro* assays have confirmed that particular members of the protein family either inhibit invertase or pectin methylesterase activity, but never both.[14]

The limited availability of pure protein components has been a major obstacle in the biochemical and structural investigation of invertase–inhibitor interaction. As a first step to characterize the inhibition mechanism in detail, we have recently expressed and crystallized a biologically active invertase inhibitor, termed Nt-CIF (*Nicotiana tabacum* cell wall inhibitor of beta fructosidase),[15] previously cloned from tobacco.[16] The crystal structure reported here reveals the first three-dimensional model for a member of the inhibitory protein family. In addition, we show that the recombinant protein is heat-stable and retains biological activity upon cooling to ambient temperature. Using site-directed mutagenesis along with protein deletions, we have identified major determinants of the inhibitors' structural integrity. The presented work implies relevance for the posttranslational inhibition of pectin methylesterases, since (based on sequence homology) the structures of their cognate inhibitors are likely to be similar to our Nt-CIF structure.

Results and Discussion

Nt-CIF was expressed, purified and crystallized as described.[15] Briefly, overexpression as a thioredoxin A fusion protein in *Escherichia coli* Origami cells resulted in soluble protein that was purified in a three-step procedure[15] and crystallized in four different crystal forms at pH values ranging from 4.6 to 9. The structure was determined by the multiple isomorphous replacement (MIR) method using the crystal form (native 1) grown in the presence of $CdCl_2$ (see Table 1). Using the coordinates for molecular replacement in a second crystal form (native 2) yielded a model that has been refined including data up to 1.87 Å resolution, as described in Materials and Methods (see Table 1). The description below is primarily based on this structure that comprises all 147 residues and 122 water molecules.

Overall structure: an asymmetric four-helix bundle

Nt-CIF forms an asymmetric four-helix bundle in up-down topology with a shorter C-terminal helix pair. The bundle is preceded by an N-terminal extension forming a helical hairpin along with an additional small helix (see Figure 1(a), see below). A secondary structure assignment is included in Figure 1(c). The core of the bundle is stabilized by hydrophobic interactions involving primarily non-aromatic residues and by a disulfide bridge (Cys73 and Cys114) connecting helices α5 and α6. Analysis of the surface charge distribution revealed an acidic area originating from residues in those two helices (Figure 1(b)). The significance of this is presently unclear (see below).

Four-helix bundles represent a common topological fold found in numerous proteins, either stand alone like in cytochrome *c*, or as an integral part of a larger structural entity.[17] A homology search with the program DALI[18] returned as top hit a mitochondrial protein kinase involved in α-ketoacid metabolism (Z-score 8.4),[19] aligning 116 residues of Nt-CIF with a four-helix bundle that in this case is an integral part of the enzyme.

Unusual thermal stability of Nt-CIF

Using circular dichroism (CD) spectroscopy (see Materials and Methods), we have estimated the melting temperature of Nt-CIF to be approximately 70 °C at pH 4.0 (Figure 2(b)). After heating the protein at 95 °C for several minutes and cooling to ambient temperature, the inhibitor retained its folding state as concluded from CD spectra (Figure 2(a) and (b)). In addition, no loss in activity was observed in invertase inhibition assays (see Hothorn *et al.*,[15] data not shown). These data are consistent with our structural analysis, accounting for loop regions of minimal lengths, disulfide bridge stabilization as well as tight structural integration of N and C termini. The high thermal stability of invertase inhibitors, in particular under oxidizing conditions, may be relevant for their *in vivo* function. The expression of cell wall invertase inhibitors and their target enzyme(s) is strongly regulated during plant development[7,20,21] (Manuela Link, S. G. & Thomas Rausch, unpublished data). In particular, these inhibitors, together with their target enzymes, are assumed to form a metabolic switch responsible for the regulation of photoassimilate transfer to the developing seeds. Therefore, their function must be assured at high

Table 1. Summary of crystallographic analysis

	Native 1	$Pb(NO_3)_2$	$K_2Pt(CN)_4$	Native 2
Data collection				
Space group	$P2_12_12_1$			$C222_1$
Unit cell *a*, *b*, *c* (Å)	59.2, 95.6, 126.2			60.7, 106.4, 55.8
Wavelength (Å)	0.934	0.933	0.933	0.93
Resolution (Å)	2.0	2.50	2.85	1.87
Highest shell (Å)	2.15–2.0	2.60–2.50	3.0–2.85	2.0–1.87
No. unique reflections	49,059 (9428)	47,532 (5303)	31,378 (4502)	15,167 (2455)
Multiplicity	7.3 (7.1)	3.2 (3.1)	6.6 (3.8)	8.3 (5.3)
I/σ[a]	16.09 (7.72)	14.24 (4.43)	17.44 (4.83)	23.8 (8.92)
R_{sym} (%)[a]	8.1 (25.8)	6.6 (35.6)	10.2 (34.0)	5.7 (12.7)
Completeness (%)	100 (100)	99.6 (100)	99.7 (100)	97.8 (88.2)
MIRAS analysis				
Resolution (Å)		15–3.0	15–3.0	–
Phasing power[b]		1.17	0.71	–
Anomalous phasing power[b]		0.6	0.41	–
Number of sites		4	3	–
Figure of merit[b]	0.44			
Refinement				
Resolution range (Å)	19.67–2.0			19.25–1.87
No. reflections	49,059			15,112
R_{work} (%)[b]	21.2			19.4
R_{free} (%)[b]	25.5			23.2
Number of atoms				
Protein	4388			1107
Cd^{2+}	8			–
Bis-Tris	64			–
Solvent	236			122
R.m.s. deviations				
Bond length	0.014			0.012
Angles	1.5			1.5

[a] As defined in XDS.[29]
[b] As defined in CNS.[30]

ambient temperatures. Furthermore, as the cell wall compartment represents an oxidizing environment, the structural stability of invertase inhibitors must be maintained under these conditions.

An N-terminal extension and its importance for structural stability

A helical hairpin comprising residues 3–24 followed by a short helix (residues 25–31) packs approximately perpendicular to the N (α4) and C-terminal (α7) helices of the bundle core (Figure 1(a)), respectively. The bundle–hairpin interface is stabilized primarily through hydrophobic residues (Figure 3), suggesting that pH-variations affecting activity do not induce major conformational changes of this area. In fact, crystal structures covering crystallization conditions in the pH range from 4.6 to 9 are strikingly similar with respect to the bundle–hairpin interface (M.H., unpublished results). The C terminus of Nt-CIF apparently contributes to interface stabilization, consistent with deletions in this area rendering the protein inactive (data not shown).

While four-helix bundles are common structural scaffolds in proteins, the N-terminal extension as seen in our structure appears to be unprecedented according to the results of the program DALI.[18] It is nevertheless reminiscent of a helical hairpin in Rho protein specific guanine nucleotide dissociation inhibitor (RhoGDI), where a similar hairpin is a major contributor to GDI activity.[22–24] In order to find out whether the additional helical feature is important for the inhibitory activity of Nt-CIF, we carried out mutagenesis studies. However, partial (Δ1-15) and full (Δ1-22) deletion of the helical hairpin as well as removal of the whole extension including the third small helix (Δ1-29) (Figure 1) resulted in heavy protein precipitation after cleavage of the fusion partner, possibly by exposing the hydrophobic bundle–hairpin interface at the surface of the remaining molecule. We have probed the importance of the disulfide bridge in this segment by substituting Cys8 by Ser, resulting in soluble but highly aggregated Nt-CIF using purification schemes similar to that of the wild-type protein. This suggests a structural role of the disulfide bridge, consistent with inactivation of Nt-CIF upon DTT treatment.[16] Similarly, disrupting the salt-bridge between Asp24 and Arg26 (Figure 3) by substituting the latter with Glu resulted in heavy protein precipitation during purification, supporting again a structural role of the underlying interactions. Investigating the pattern of residues conserved between PMEIs and invertase inhibitors, it appears that they are involved in intramolecular interactions suggesting a common role for structural stability.

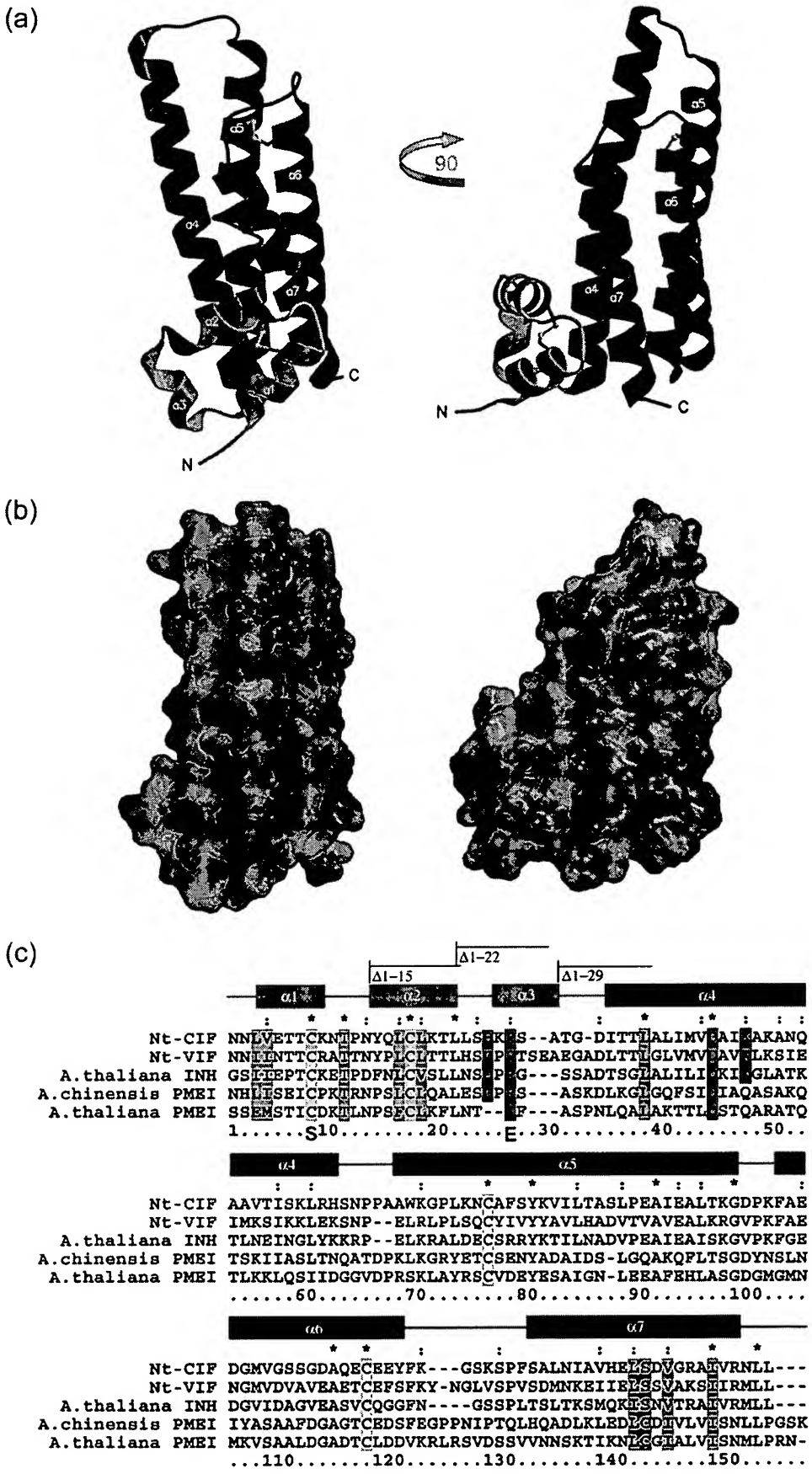

Figure 1. Structure of cell wall invertase inhibitor Nt-CIF. (a) Ribbon representation of the four-helix bundle in two orientations separated by a 90° rotation about a vertical axis, as indicated. (b) Surface view with electrostatic potential included to indicate the acidic patch discussed in the text, orientations as in (a). (c) Sequence comparison of representative invertase inhibitors with secondary structure assignment according to the program DSSP[37] included.

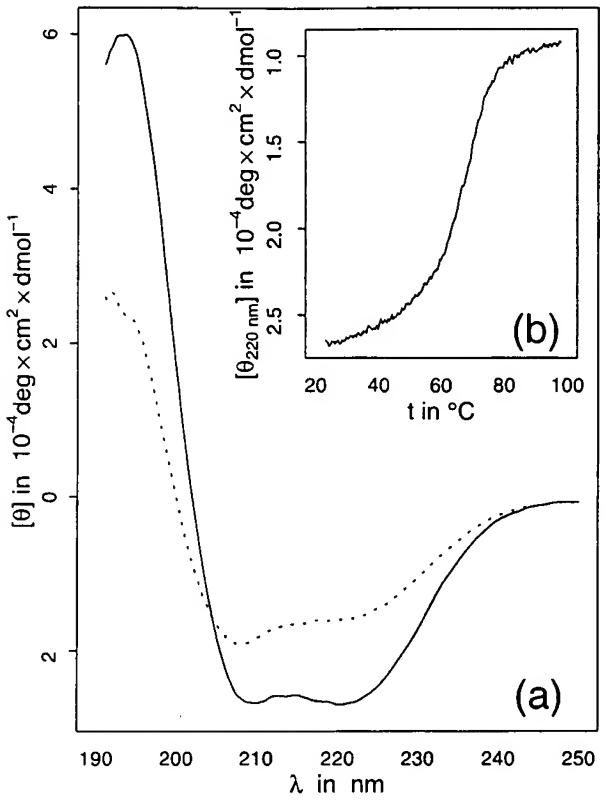

Figure 2. Circular dichroism spectra of Nt-CIF. (a) Representative far-UV spectrum at 20 °C (continuous line) and 70 °C (dash-dot line). (b) Melting spectrum of Nt-CIF at a wavelength of 220 nm and within a temperature-range of 20–98 °C. Wavelength spectra were averaged over 30 runs.

Implications for the pH dependence of inhibition

Invertase inhibition has been demonstrated to be strongly pH-dependent (Weil *et al.*,[10] and literature cited therein). The tempting hypothesis that pH-variation may affect the interface between the N-terminal extension and the bundle core, is inconsistent with experimental data and the hydrophobic nature of this interface. Alternatively, the observed pH dependence of invertase inhibition might be explained as follows. In the plant cell, invertase metabolism operates in the cell wall compartment where the pH ranges between 4 and 6. Cell wall invertase activity is strongly pH-dependent with a maximum activity at about pH 4. Thus, it may be speculated that the inhibitor gets access to the binding site only in the active enzyme conformation. As the cell wall invertase is a highly basic protein, the acidic patch at the inhibitor's surface might play a role in the initial inhibitor

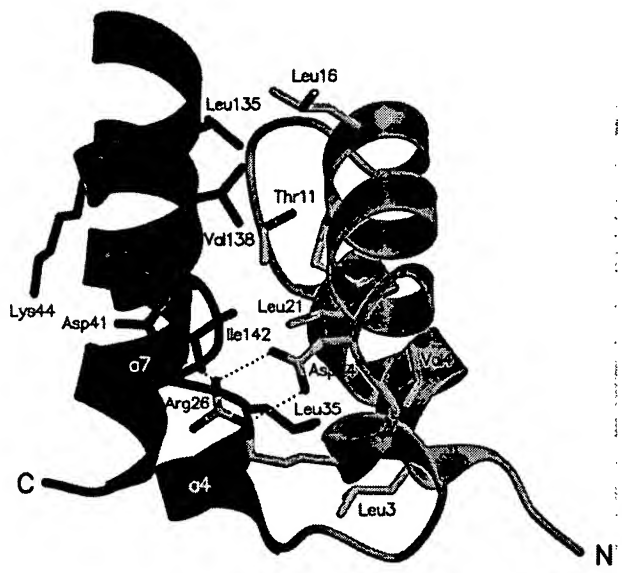

Figure 3. Close-up view of the interface buried between the N-terminal helical extension and the bundle core with selected side-chains included.

recruitment to the target enzyme, whereas other structural features such as the N-terminal hairpin might mediate the required specificity.

Does Nt-CIF bind divalent cations?

During our crystallization experiments[15] we identified a crystal form obtained in the presence of $CdCl_2$. The structural analysis revealed two spherical density maxima per molecule present at contour levels of 18 σ in the $2F_o - F_c$ and $F_o - F_c$ map and absent from crystals grown in the absence of $CdCl_2$. These peaks were interpreted as cadmium ions and subsequently included in the model. Glu113 in concert with a molecule of bis-Tris buffer coordinates the first cadmium, thereby contributing to the interface with a symmetry-related molecule. In contrast, His133, Asp137 and two water molecules establish a second site located in the C-terminal helix of the bundle (Figure 4).

Since modulation of the inhibition activity by divalent cations such as Ca^{2+}, Mg^{2+} and Zn^{2+} has been reported previously,[10] we have investigated their influence on the inactivation of cell wall invertase by Nt-CIF. However, preincubation of the inhibitor with $CdCl_2$ or $ZnCl_2$ even in millimolar concentrations did not lead to significant changes in invertase activity (data not shown). This suggests that the effect of metal ions observed earlier[10] is mediated through a more complex mechanism.

Regions and positions mutated are indicated with the corresponding mutation in red. The four cysteine residues involved in two disulfide bridges are shown in yellow, the fifth cysteine in PMEIs is highlighted in orange. Conserved residues, contributing to the bundle–hairpin interface, are indicated, dependent on their properties, in green or red.

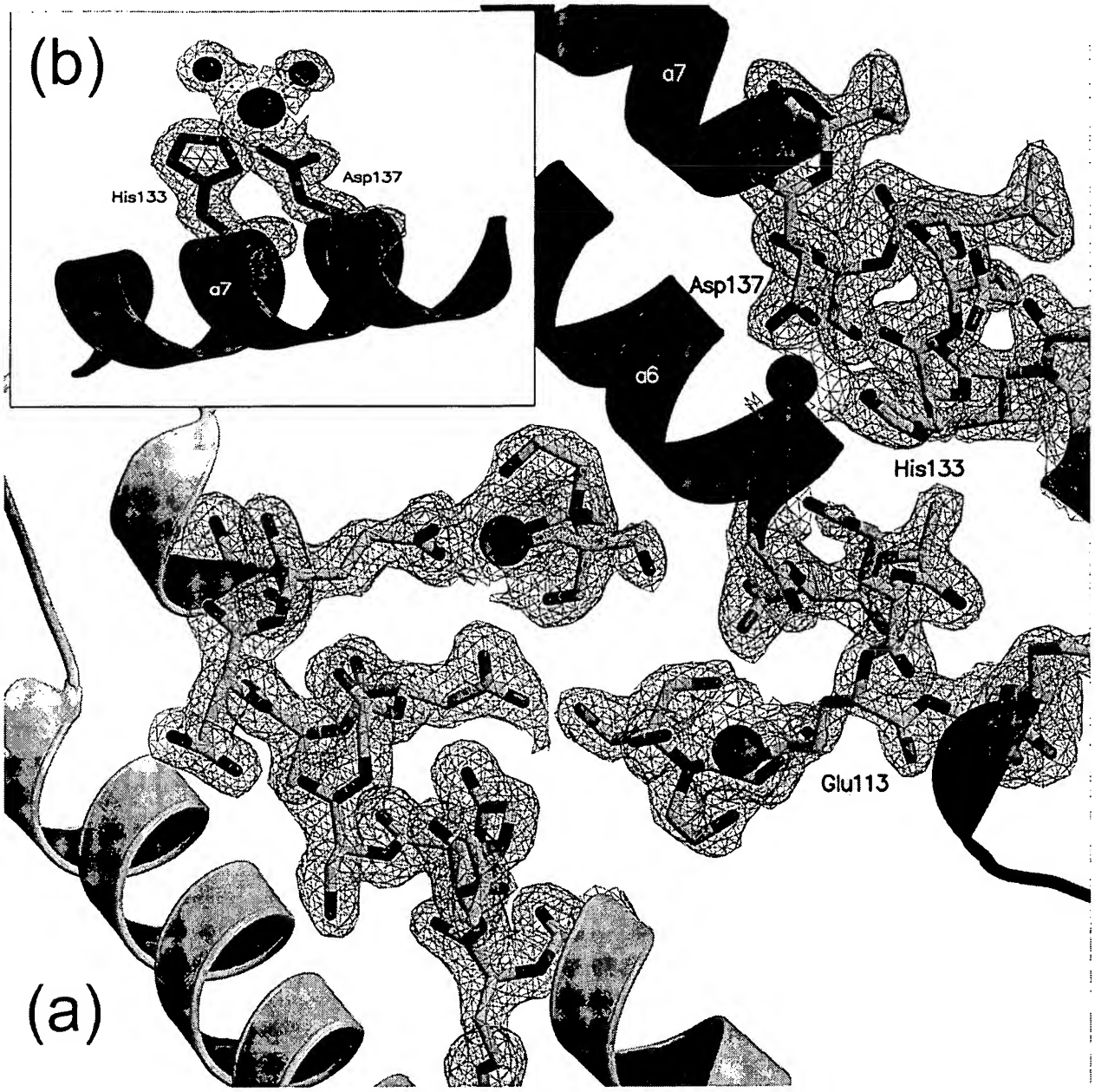

Figure 4. Metal ions in Nt-CIF. Ribbon representation of the metal binding regions with chelating residues along with bis-Tris molecules in bonds representation and including the final $2F_o - F_c$ electron density map (contoured at 1.5 σ) covering the respective areas. (a) Interface between two symmetry-related molecules of Nt-CIF involving a cadmium ion (in magenta) coordinated by Glu113 along with one molecule of bis-Tris. (b) Second cadmium coordination site involving His133, Asp137 and two water molecules (in red).

Concluding Remarks

Based on secondary structure prediction and data presented,[13,14] inhibitors of invertase and pectin methylesterase appear to be structurally very similar. The fifth conserved cysteine residue in PMEIs is replaced by serine in Nt-CIF (Figure 1(c)) pointing towards the center of the bundle. Since we have mapped other conserved residues within the protein family to be of predominant structural importance, it seems likely that specificity towards two totally unrelated enzymes is achieved by a complex pattern of surface properties, as indicated for Nt-CIF. Two recent X-ray structures of bacterial[25] and plant[26] PME did not reveal insight into regulatory aspects. Plant invertases are highly glycosylated proteins that are found in the extracellular acidic compartments (cell wall and vacuole) whereas PMEs are exclusively targeted to the cell wall. These enzymes do not share apparent similarity in the primary sequences. However, the sequence similarity of their cognate inhibitors suggests the inhibitory power to be implemented on a similar structural scaffold. Thus, our structure offers a platform for biochemical experiments to elucidate the mechanistic details of the underlying protein–protein interactions.

The expression of invertase inhibitors during plant development is tightly regulated, suggesting that, together with their target enzymes, these inhibitors serve as a metabolic switch from a $hexose_{high}/sucrose_{low}$ to a $sucrose_{high}/hexose_{low}$ state. The molecular basis of this switch and the signal triggering it are to be determined. Our structural analysis in four different crystalline environments make it unlikely that pH variations induce conformational changes in Nt-CIF directly, but rather act in a more complex scheme to modulate invertase inhibitory activity. Thus, a pH-dependent change in target enzyme conformation, allowing access of the inhibitor to the binding site exclusively near the pH optimum of cell wall invertase, could explain the observed pH effects (see above).

A recent analysis of tobacco Nt-CIF-promoter::β-glucuronidase (GUS) transformants has revealed that Nt-CIF and cell wall invertase may be co-expressed along the conducting tissues (phloem parenchyma) and in the funiculus structure, which attaches the developing seed to the mother plant (Manuela Link, S. G. & Thomas Rausch, unpublished results). In both cases, the regulation of cell wall invertase by a specific inhibitor protein may be part of a rapid posttranslational silencing of invertase activity, required for a proper orchestration of sucrose metabolism in response to endogenous and/or environmental cues. Thus, upon wounding, cell wall invertase expression is induced in the leaves along the conducting tissues, a process that may be required for the observed source–sink transition.[27] Here, the co-expression of the inhibitor may be required to fine-tune the spatial and temporal window of invertase activity. During seed filling, a switch from high to low cell wall invertase activity has been established for several plant species.[20,28] This switch has been shown to be responsible for the transition from the cell division phase to the phase of storage compound accumulation. Again, the co-expressed inhibitor may be involved in fine-tuning this transition. We conclude that although the *in vivo* regulation of inhibitor–invertase complex formation has not yet been elucidated, this post-translational mechanism of enzyme regulation appears to be involved in several important developmental processes. The resolution of the first invertase inhibitor structure is another step towards a better understanding of this control mechanism.

Materials and Methods

X-ray analysis

Bacterial protein expression, purification and crystallization of the presented inhibitor from tobacco are reported elsewhere.[15] Briefly, Nt-CIF was expressed as a thioredoxin A fusion protein in *E. coli* Origami cells (Novagen), and crystallized by using the hanging-drop method with 4 M sodium formate, in 0.1 M bis-Tris (pH 7) as precipitant. Heavy atom derivatives were prepared by soaking orthorhombic crystals grown in the presence of $CdCl_2$ in crystallization buffer supplemented with 0.5 mM $Pb(NO_3)_2$ and 1 mM $K_2Pt(CN)_4$, respectively. Diffraction data were collected at beamline ID14-2 of the European Synchrotron Radiation Facility (ESRF), Grenoble, France. An initial native dataset (not shown) has been collected at beamline BW7-A, Deutsches Elektronen Synchrotron (DESY), Hamburg. Data processing was carried out with the program XDS.[29] Subsequently, isomorphous difference patterson analysis with CNS[30] yielded four Pb sites giving rise to an initial electron density map at 3.5 Å resolution. The contribution of three additional Pt sites from another derivative along with density modification and solvent flattening resulted in an improved map at 3.0 Å resolution comprising four molecules in the asymmetric unit. The model was built using a template bundle and completed in alternating cycles of manual model correction (O,[31]) and refinement (CNS,[30]). The addition of cadmium ions, buffer and water molecules was carried out in the final stage of refinement against a dataset at 2.0 Å resolution (native 1) collected at ID14-2. A summary of the crystallographic analysis is given in Table 1.

The structure of the cadmium-free form (native 2) has been determined by molecular replacement using one refined Nt-CIF molecule as search model in calculations with the program CNS. The solution (starting R_{free} 42.8%) comprises one molecule in the asymmetric unit superimposing well with the model derived from the first crystal form and lacking strong electron density at the cadmium binding sites (Table 1).

Inspection of the refined models with PROCHECK[32] did not reveal any unfavorable ϕ,ψ combinations. Structure visualization was done with POVSCRIPT[33] and Raster3D.[34]

Activity assay for inhibitor function

Tobacco cell-wall invertase has been prepared from cell-suspension cultures as described.[10] Inhibition assays of invertase activity were performed following the protocol of Weil & Rausch.[35]

Circular dichroism (CD) spectroscopy

For CD spectroscopy, protein samples were diluted to 0.05 mg/ml and dialyzed against 5 mM sodium acetate (pH 4.0), 7.5 mM NaCl. The measurements were performed on a J-710 spectropolarimeter (Jasco) at a cell-path of 2 mm and at a sensitivity of 50 mdeg. Melting curves were recorded at a wavelength of 220 nm covering a temperature range between 15 °C and 99 °C. Spectra were analyzed using the statistical package R.[36]

Site-directed mutagenesis

Site-specific mutations were introduced with the QuickChange mutagenesis kit (Stratagene) following the manufacturer's instructions and subsequently verified by DNA-sequencing. Protein expression and purification followed the protocols established for wild-type Nt-CIF.[15] Finally, the purified inhibitor was analyzed by analytical size-exclusion chromatography using a Superdex 75 HR 10/30 column (Pharmacia).

Atomic coordinates

Coordinates and structure factors have been submitted

to the Protein Data Bank (http://www.rcsb.org) with codes 1RJ4 (native 1) and 1RJ1 (native 2).

Acknowledgements

We thank Thomas Rausch for generous support, helpful discussions and critically reading the manuscript, Manuela Lopez de la Paz for discussion, the staff at beam lines ID29 of the European Synchrotron Radiation Facility (ESRF), Grenoble, France, of beam lines BW7A of the Deutsches Elektronen Synchrotron, Hamburg, Germany, for technical support during data collection. We gratefully acknowledge financial support from the Südzucker AG Mannheim (Germany) and the KWS Saat AG, Einbeck (Germany), grants to S.G. and Thomas Rausch.

References

1. Sturm, A. (1999). Invertases. Primary structures, functions, and roles in plant development and sucrose partitioning. *Plant Physiol.* **121**, 1–8.
2. Sturm, A. & Tang, G. Q. (1999). The sucrose-cleaving enzymes of plants are crucial for development, growth and carbon partitioning. *Trends Plant Sci.* **4**, 401–407.
3. Xu, J., Avigne, W. T., McCarty, D. R. & Koch, K. E. (1996). A similar dichotomy of sugar modulation and developmental expression affects both paths of sucrose metabolism: evidence from a maize invertase gene family. *Plant Cell*, **8**, 1209–1220.
4. von Schaewen, A., Stitt, M., Schmidt, R., Sonnewald, U. & Willmitzer, L. (1990). Expression of a yeast-derived invertase in the cell wall of tobacco and Arabidopsis plants leads to accumulation of carbohydrate and inhibition of photosynthesis and strongly influences growth and phenotype of transgenic tobacco plants. *Embo J.* **9**, 3033–3044.
5. Tang, G. Q., Luscher, M. & Sturm, A. (1999). Antisense repression of vacuolar and cell wall invertase in transgenic carrot alters early plant development and sucrose partitioning. *Plant Cell*, **11**, 177–189.
6. Goetz, M., Godt, D. E., Guivarc'h, A., Kahmann, U., Chriqui, D. & Roitsch, T. (2001). Induction of male sterility in plants by metabolic engineering of the carbohydrate supply. *Proc. Natl Acad. Sci. USA*, **98**, 6522–6527.
7. Cheng, W. H., Taliercio, E. W. & Chourey, P. S. (1999). Sugars modulate an unusual mode of control of the cell-wall invertase gene (Incw1) through its 3′ untranslated region in a cell suspension culture of maize. *Proc. Natl Acad. Sci. USA*, **96**, 10512–10517.
8. Federici, L., Caprari, C., Mattei, B., Savino, C., Di Matteo, A., De Lorenzo, G. *et al.* (2001). Structural requirements of endopolygalacturonase for the interaction with PGIP (polygalacturonase-inhibiting protein). *Proc. Natl Acad. Sci. USA*, **98**, 13425–13430.
9. Payan, F., Flatman, R., Porciero, S., Williamson, G., Juge, N. & Roussel, A. (2003). Structural analysis of xylanase inhibitor protein I (XIP-I), a proteinaceous xylanase inhibitor from wheat (*Triticum aestivum*, var Soisson). *Biochem. J.* **372**, 399–405.
10. Weil, M., Krausgrill, S., Schuster, A. & Rausch, T. (1994). A 17-kDa *Nicotiana tabacum* cell-wall peptide acts as an *in vitro* inhibitor of the cell-wall isoform of acid invertase. *Planta*, **193**, 438–445.
11. Sander, A., Krausgrill, S., Greiner, S., Weil, M. & Rausch, T. (1996). Sucrose protects cell wall invertase but not vacuolar invertase against proteinaceous inhibitors. *FEBS Letters*, **385**, 171–175.
12. Greiner, S., Rausch, T., Sonnewald, U. & Herbers, K. (1999). Ectopic expression of a tobacco invertase inhibitor homolog prevents cold-induced sweetening of potato tubers. *Nature Biotechnol.* **17**, 708–711.
13. Camardella, L., Carratore, V., Ciardiello, M. A., Servillo, L., Balestrieri, C. & Giovane, A. (2000). Kiwi protein inhibitor of pectin methylesterase amino-acid sequence and structural importance of two disulfide bridges. *Eur. J. Biochem.* **267**, 4561–4565.
14. Scognamiglio, M. A., Ciardiello, M. A., Tamburrini, M., Carratore, V., Rausch, T. & Camardella, L. (2003). The plant invertase inhibitor shares structural properties and disulfide bridges arrangement with the pectin methylesterase inhibitor. *J. Protein Chem.* **22**, 363–369.
15. Hothorn, M., Bonneau, F., Stier, G., Greiner, S., Scheffzek, K. (2003). Expression, purification and crystallization of a thermostable tobacco invertase inhibitor. *Acta Crystallog. sect. D*, **59**, 2279–2282.
16. Greiner, S., Krausgrill, S. & Rausch, T. (1998). Cloning of a tobacco apoplasmic invertase inhibitor. Proof of function of the recombinant protein and expression analysis during plant development. *Plant Physiol.* **116**, 733–742.
17. Kamtekar, S. & Hecht, M. H. (1995). Protein Motifs 7. The four-helix bundle: what determines a fold? *FASEB J.* **9**, 1013–1022.
18. Holm, L. & Sander, C. (1993). Protein structure comparison by alignment of distance matrices. *J. Mol. Biol.* **233**, 123–138.
19. Machius, M., Chuang, J. L., Wynn, R. M., Tomchick, D. R. & Chuang, D. T. (2001). Structure of rat BCKD kinase: nucleotide-induced domain communication in a mitochondrial protein kinase. *Proc. Natl Acad. Sci. USA*, **98**, 11218–11223.
20. Weber, H., Borisjuk, L., Heim, U., Buchner, P. & Wobus, U. (1995). Seed coat-associated invertases of fava bean control both unloading and storage functions: cloning of cDNAs and cell type-specific expression. *Plant Cell*, **7**, 1835–1846.
21. Ehness, R., Ecker, M., Godt Dietmute, E. & Roitsch, T. (1997). Glucose and stress independently regulate source and sink metabolism and defense mechanisms *via* signal transduction pathways involving protein phosphorylation. *Plant Cell*, **9**, 1825–1841.
22. Scheffzek, K., Stephan, I., Jensen, O. N., Illenberger, D. & Gierschik, P. (2000). The Rac-RhoGDI complex and the structural basis for the regulation of Rho proteins by RhoGDI. *Nature Struct. Biol.* **7**, 122–126.
23. Hoffman, G. R., Nassar, N. & Cerione, R. A. (2000). Structure of the Rho family GTP-binding protein Cdc42 in complex with the multifunctional regulator RhoGDI. *Cell*, **100**, 345–356.
24. Grizot, S., Faure, J., Fieschi, F., Vignais, P. V., Dagher, M. C. & Pebay-Peyroula, E. (2001). Crystal structure of the Rac1-RhoGDI complex involved in nadph oxidase activation. *Biochemistry*, **40**, 10007–10013.
25. Jenkins, J., Mayans, O., Smith, D., Worboys, K. & Pickersgill, R. W. (2001). Three-dimensional structure of Erwinia chrysanthemi pectin methylesterase reveals a novel esterase active site. *J. Mol. Biol.* **305**, 951–960.

26. Johansson, K., El-Ahmad, M., Friemann, R., Jornvall, H., Markovic, O. & Eklund, H. (2002). Crystal structure of plant pectin methylesterase. *FEBS Letters*, **514**, 243–249.
27. Zhang, L., Cohn, N. S. & Mitchell, J. P. (1996). Induction of a pea cell-wall invertase gene by wounding and its localized expression in phloem. *Plant Physiol.* **112**, 1111–1117.
28. Cheng, W.-H., Taliercio Earl, W. & Chourey Prem, S. (1996). The Miniature1 seed locus of maize encodes a cell wall invertase required for normal development of endosperm and maternal cells in the pedicel. *Plant Cell*, **8**, 971–983.
29. Kabsch, W. (1993). Automatic processing of rotation diffraction data from crystals of initially unknown symmetry and cell constants. *J. Appl. Crystallog.* **26**, 795–800.
30. Brunger, A. T., Adams, P. D., Clore, G. M., DeLano, W. L., Gros, P., Grosse-Kunstleve, R. W. *et al.* (1998). Crystallography and NMR system: a new software suite for macromolecular structure determination. *Acta Crystallog. sect. D*, **54**, 905–921.
31. Jones, T. A., Zou, J.-Y., Cowan, S. W. & Kjeldgaard, M. (1991). Improved methods for building protein models in electron density maps and the location of errors in these models. *Acta Crystallog. sect. A*, **47**, 110–119.
32. Laskowski, R. A., MacArthur, M. W., Moss, D. S. & Thornton, J. M. (1993). PROCHECK: a program to check the stereochemical quality of protein structures. *J. Appl. Crystallog.* **26**, 283–291.
33. Fenn, T., a, R. D. & Petsko, G. A. (2003). POVScript-tracing. *J. Appl. Crystallog.* **36**, 944–947.
34. Merritt, E. A. & Bacon, D. J. (1997). Raster3D: Photorealistic molecular graphics. *Methods Enzymol.* **277**, 505–524.
35. Weil, M. & Rausch, T. (1994). Acid invertase in *Nicotiana tabacum* grown-gall cells: molecular properties of the cell wall isoform. *Planta*, **193**, 430–437.
36. Ihaka, R. & Gentleman, R. (1996). R: a language for data analysis and graphics. *J. Comput. Graph. Stat.* **5**, 299–314.
37. Kabsch, W. & Sander, C. (1983). Dictionary of protein secondary structure: pattern recognition of hydrogen-bonded and geometrical features. *Biopolymers*, **22**, 2577–2637.

Edited by R. Huber

(Received 1 August 2003; accepted 27 October 2003)

The Plant Cell, Vol. 16, 3437–3447, December 2004, www.plantcell.org © 2004 American Society of Plant Biologists

Structural Insights into the Target Specificity of Plant Invertase and Pectin Methylesterase Inhibitory Proteins

Michael Hothorn,[a] Sebastian Wolf,[b] Patrick Aloy,[a] Steffen Greiner,[b] and Klaus Scheffzek[a,1]

[a] European Molecular Biology Laboratory, Structural and Computational Biology Programme, 69117 Heidelberg, Germany
[b] Heidelberg Institute for Plant Sciences, Molecular Ecophysiology, 69120 Heidelberg, Germany

Pectin methylesterase (PME) and invertase are key enzymes in plant carbohydrate metabolism. Inhibitors of both enzymes constitute a sequence family of extracellular proteins. Members of this family are selectively targeted toward either PME or invertase. In a comparative structural approach we have studied how this target specificity is implemented on homologous sequences. By extending crystallographic work on the invertase inhibitor Nt-CIF to a pectin methylesterase inhibitor (PMEI) from *Arabidopsis thaliana*, we show an α-helical hairpin motif to be an independent and mobile structural entity in PMEI. Removal of this hairpin fully inactivates the inhibitor. A chimera composed of the α-hairpin of PMEI and the four-helix bundle of Nt-CIF is still active against PME. By contrast, combining the corresponding segment of Nt-CIF with the four-helix bundle of PMEI renders the protein inactive toward either PME or invertase. Our experiments provide insight in how these homologous inhibitors can make differential use of similar structural modules to achieve distinct functions. Integrating our results with previous findings, we present a model for the PME-PMEI complex with important implications.

INTRODUCTION

At the posttranslational level, the activity of enzymes is commonly regulated by various mechanisms, including residue-directed protein modifications such as phosphorylation, glycosylation, and interaction with specific inhibitors. The nature of these inhibitors may range from small molecules to entire proteins, as found with the well-studied inhibitors of proteases (Bode and Huber, 1992). In plants, inhibitory proteins are often targeted toward sugar-modifying enzymes that escape cellular control mechanisms upon secretion into the plant cell wall or the vacuole (Juge et al., 2004). We are focusing on the structure–function relationship of an inhibitor family that regulates the activity of plant acid invertase and pectin methylesterase (PME).

Invertases convert the transport sugar sucrose into its building blocks, fructose and glucose. In higher plants, invertases exist in compartment specific isoforms, with only extracytosolic species being sensitive to inhibitory proteins. Altered activity of extracellular invertase has been shown to have dramatic effects on growth and development (Cheng et al., 1996; Tang et al., 1999; Goetz et al., 2001). This is consistent with roles of invertase activity in vital cellular processes such as carbohydrate transport (Roitsch et al., 2003), sugar signaling (Koch, 1996, 2004; Smeekens, 1998; Wobus and Weber, 1999), and stress response (Ehness et al., 1997; Roitsch et al., 2003). Protein inhibitors of invertase (Greiner et al., 1998) affect enzyme activity in a strictly pH-dependent manner (Rausch and Greiner, 2004) and have been proposed as transgenic tools to engineer post-harvest sucrose metabolism in crop plants (Greiner et al., 1999).

PMEs catalyze the demethylesterification of the homogalacturonan component of pectins, highly heterogeneous polymers (Vorwerk et al., 2004) that represent a major constituent of the plant primary cell wall. As the degree of demethylesterification determines the solidity of the wall, physiological processes requiring rearrangement of the cell wall architecture are affected by PME activity (Micheli, 2001). These include root development (Wen et al., 1999), stem elongation, and fruit ripening (Frenkel et al., 1998; Pilling et al., 2000; Brummell and Harpster, 2001). PME appears to be also involved in plant–pathogen interaction by serving as a host receptor for *Tobacco mosaic virus* (Chen et al., 2000; Chen and Citovsky, 2003). A protein inhibitor of plant PME (Giovane et al., 2004) has first been purified directly from kiwi fruit (*Actinidia deliciosa*; Camardella et al., 2000). Recently, two homologous species from *Arabidopsis thaliana* were recombinantly expressed and identified as PME inhibitors (PMEI; Wolf et al., 2003; Raiola et al., 2004).

PME and invertase inhibitors form a large plant sequence family named PMEI-related proteins (PMEI-RP). Family members share moderate sequence homology, and are selectively targeted toward apparently unrelated enzymes. Nothing is known about the molecular basis for the target specificity. As a first step to investigate this issue, we have previously determined the structure of the invertase inhibitor Nt-CIF from tobacco, CIF hereafter. The structural analysis revealed a four-helix bundle, preceded by an uncommon N-terminal extension (Hothorn et al., 2004). We suspected this small helical motif to play an important role in the inhibitory mechanism but were

[1] To whom correspondence should be addressed. E-mail scheffzek@embl.de; fax 49-6221-387-519.
The author responsible for distribution of materials integral to the findings presented in this article in accordance with the policy described in the Instructions for Authors (www.plantcell.org) is: Klaus Scheffzek (scheffzek@embl.de).
Article, publication date, and citation information can be found at www.plantcell.org/cgi/doi/10.1105/tpc.104.025684.

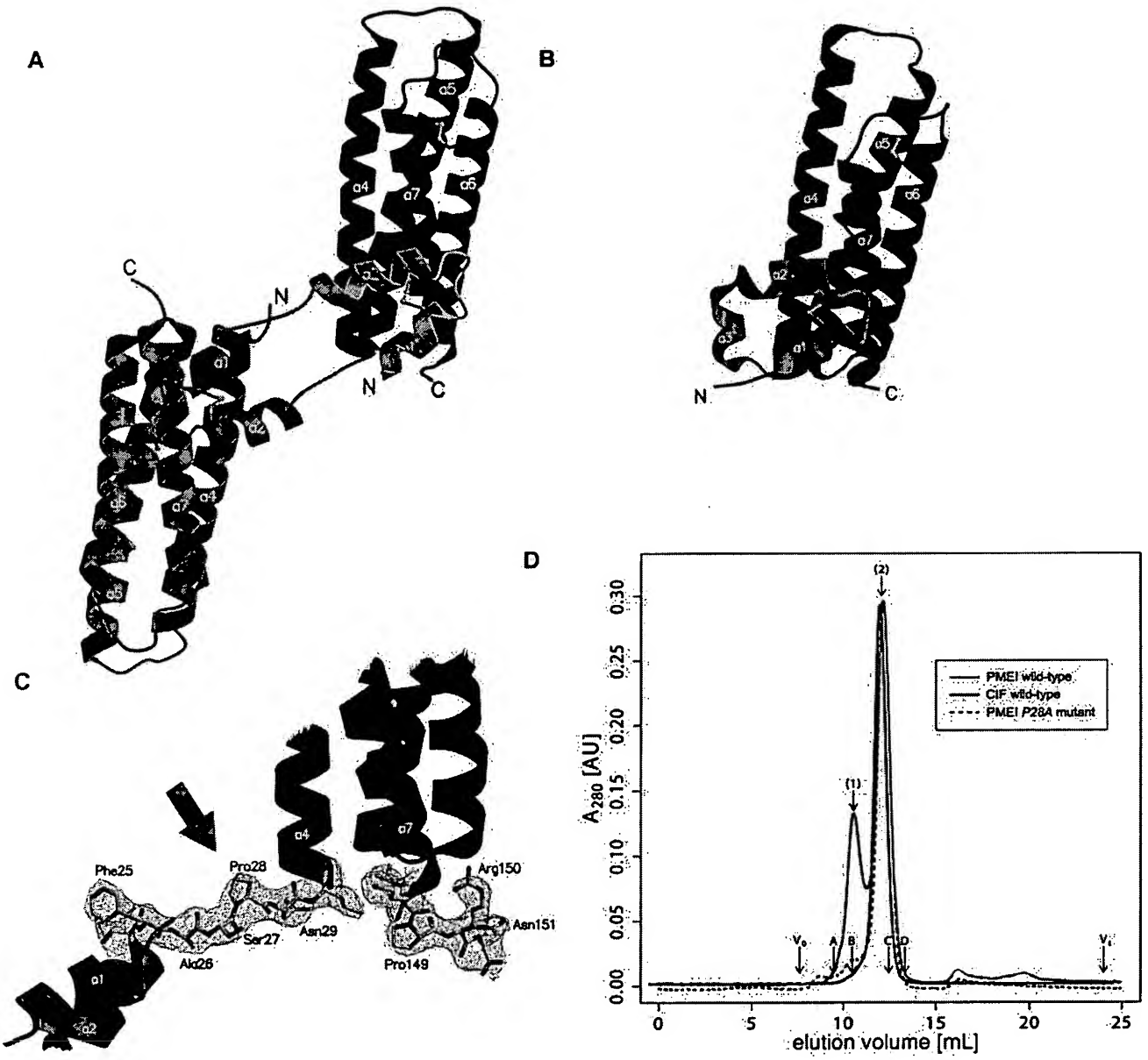

Figure 1. Structure of PMEI and Comparison with the Invertase Inhibitor CIF.

(A) Ribbon representation of the PMEI dimer with the respective molecules shown in green and yellow.

(B) CIF shown in the same orientation as the green molecule in **(A)**.

(C) The linker region (residues 25^{PMEI} to 29^{PMEI}) interconnecting the dimer as well as a C-terminal extension shown in bonds representation and including the final 2 $|F_{obs}-F_{calc}|$ electron density map (contoured at 1.2 σ).

(D) A 280-nm absorbance trace of an analytical size-exclusion chromatography reveals the presence of PMEI (shown in red) dimers (peak 1) and monomers (peak 2). The invertase inhibitor CIF (shown in blue) appears to be exclusively monomeric. PMEI mutant *P28A* (dashed red line) does not resemble the dimeric state. Void (V_0) and total (V_t) volume are shown for the column together with the elution volumes of molecular weight standards (A, BSA; B, ovalbumin; C, chymotrypsinogen A; D, ribonuclease A). The estimated molecular weight values of the At-PMEI1 monomer and dimer are 19,600 and 37,000, respectively. The calculated monomer molecular weight is 16,400.

unable to test this hypothesis because truncated forms of the inhibitor were insoluble and thus not suitable for biochemical analysis.

In this work we have extended our studies to the PMEI, the second representative of the protein family. We report the three-dimensional structure of At-PMEI1 from Arabidopsis, PMEI hereafter. Comparative structural analysis of the two inhibitors inspired us to engineer protein chimera and investigate their interaction with PME and invertase. By crystallographic analysis and functional characterization of mutants, we are now able to define major determinants of target specificity for both functional classes of inhibitors.

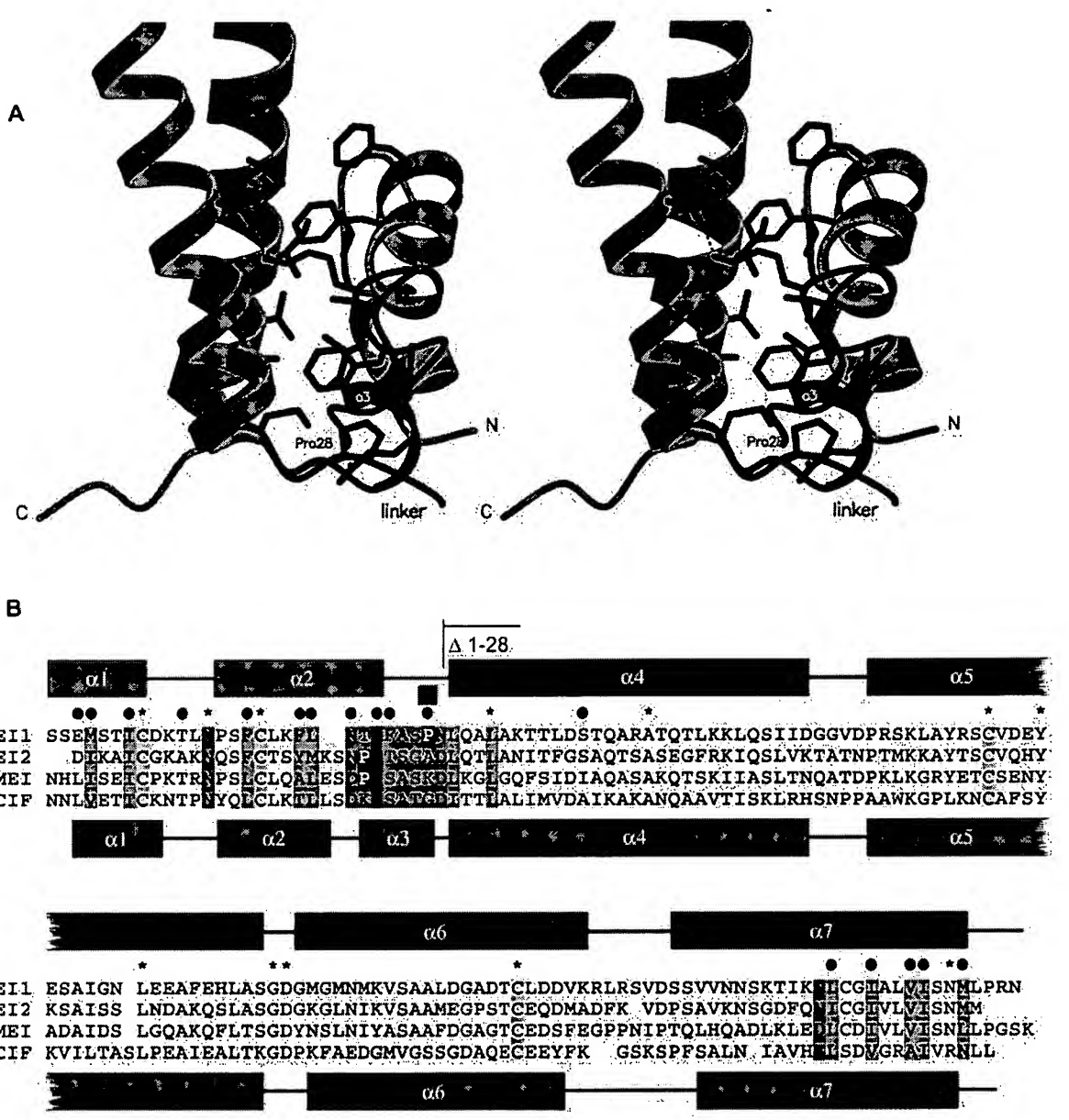

Figure 2. The α-Helical Hairpin Module in PMEI and CIF.

(A) Stereo close-up view of the bundle-hairpin interface in PMEI with invariant (blue) and conserved residues (green) contributing to interface stabilization included. The small helix-α3 connecting hairpin and bundle in CIF (blue) is unwound in PMEI (red).

(B) Sequence comparison of representative inhibitors with secondary structure assignment according to DSSP (Kabsch and Sander, 1983) and invariant Cys residues shown in yellow. Residues contributing to the bundle-hairpin interface are highlighted, dependent on their properties, in green and red. Conserved residues shown in **(A)** are denoted with a colored dot. The linker region discussed in the text is highlighted in gray; the linker Pro in PMEI is shown in blue.

RESULTS AND DISCUSSION

Overall Structure of PMEI

PMEI has been expressed, purified, and crystallized as described in the Methods section. Despite the moderate sequence identity between PMEI and CIF (~20%), we could solve the structure by molecular replacement using the coordinates of CIF as search model in calculations with the program EPMR (Kissinger et al., 1999). The final model of the asymmetric unit, refined at 2.86-Å resolution, comprises three almost-complete chains of PMEI and 22 water molecules.

PMEI is composed of a four-helix bundle (residues 29 to 153) that arranges the helical components (helices α4 to α7) in an up-down–up-down topology, thereby creating an arrangement highly similar to that seen in CIF (root-mean-square deviation [RMSD] between 114 bundle Cα atoms is lower than 1.5 Å). The structural similarity between the bundles is considerably higher than expected from the degree of sequence conservation (Chothia and Lesk, 1986), possibly attributable to the presence of a conserved disulfide bridge (Cys-71^{PMEI}/Cys-111^{PMEI}, Cys-73^{CIF}/Cys-114^{CIF}) linking helix α5 to α6 (Figures 1A and 1B). The bundle core of the inhibitor is preceded by a 28-residue extension, basically resembling the molecular architecture already observed with the invertase inhibitor CIF (Hothorn et al., 2004). The extension in PMEI can be superimposed well with the corresponding segment in CIF (RMSD between 24 corresponding Cα atoms is <0.7 Å) but is radically reoriented with respect to the bundle core. This results in extensive contacts with the bundle of a neighboring molecule (Figures 1A and 1B). The arrangement resembles a molecular handshake of the two α-hairpins, forming a dimer that may also be present in solution (see below). The third molecule in the asymmetric unit is involved in lattice contacts essentially similar to those observed in the dimer.

The helical extensions of CIF and PMEI participate in remarkably similar and mostly hydrophobic interfaces with the helix bundle that is contacted in *cis* in the former and in *trans* in the latter case (Figures 2A and 2B). In PMEI, this results in a completely unwound conformation of the linker (Figure 2B, highlighted in gray) between the helical hairpin and the bundle (Figure 1C).

Size-exclusion chromatography (see Methods) indicates a mixture of PMEI monomers and dimers in solution, compatible with the presence of a dimer in our crystals. The stability of this dimer is not affected by buffer variations in a range tested between pH 6.0 and 8.0. However, substantial reduction of ionic strength and protein concentration indicates monomer-dimer equilibrium and, as seen in the structural model, mainly hydrophobic stabilization of the dimeric state. In contrast with PMEI, CIF elutes exclusively as monomer in experiments performed under identical conditions (Figure 1D). We discuss functional aspects of this behavior below.

Truncation of the N-Terminal Extension Inactivates PMEI

We previously suspected the N-terminal α-hairpin to play a role in the inhibitory mechanism of CIF but were unable to test this hypothesis because truncated forms of the inhibitor were insoluble and thus not suitable for biochemical analysis (Hothorn et al., 2004).

Given the high overall structural similarity between CIF and PMEI, the large conformational differences in this segment prompted us to create a truncated version of the latter, deleting the entire α-hairpin (Δ1-28). The resulting construct could be purified to homogeneity using similar protocols as established for the wild-type inhibitor (Wolf et al., 2003). From size-exclusion chromatography and circular-dichroism experiments we conclude the remaining part of the inhibitor to be folded (data not shown).

Truncated PMEI is inactive in dose-dependent inhibition assays (Grsic-Rausch and Rausch, 2004), monitoring the inactivation of PME preparations from Arabidopsis flowers (Figure 3), as well as preparations from other sources. Only dramatically increased inhibitor concentrations (~5000-fold) show a mild inhibitory effect on the enzyme (data not shown). Our observations identify the N-terminal extension as a crucial determinant of PMEI activity.

Structural Determinants of the N-Terminal Flexibility

To further analyze the role of the N-terminal extension, we investigated whether alterations in the linker between hairpin and bundle can modulate structural and functional properties of PMEI. Conformational flexibility of this linker is already apparent by the different orientations of the helix hairpin in lattice dimers as observed in the wild-type inhibitor crystal (Figure 4A, shown in blue).

Considering the frequently observed role of Pro in structural rearrangements we replaced Pro-28 by Ala (Figure 1C; *P28A* mutant), hoping to induce a conformation similar to that seen in CIF. In contrast with the wild-type inhibitor, the mutant protein elutes as a monomer in size-exclusion chromatography (Figure 1D). Moreover, we observed reduced inhibitory power in activity assays against plant PME (Figure 4B).

The significant conformational alterations in solution prompted us to explore structural effects of the mutation in detail. We have determined the structure of the *P28A* mutant in two crystal forms (Table 1; see Methods). Remarkably, crystalline *P28A* mutants present the N-terminal extension in two different orientations. As anticipated from the mutant design strategy one of these conformations (form A) is strikingly similar to Nt-CIF (Hothorn et al., 2004, shown in dark blue in Figure 4C). Form A and CIF superimpose well within the bundle region (RMSD of 114 Cα

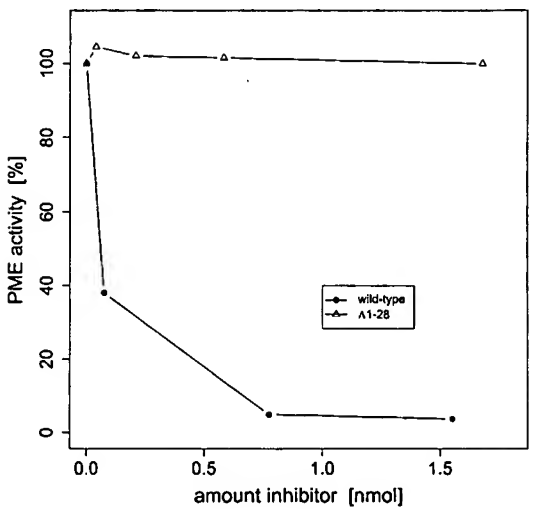

Figure 3. Removal of the N-terminal α-Helical Hairpin Inactivates PMEI.

Dose-dependent inhibition effect of the wild-type inhibitor (solid circle) and the Δ1-28 truncation on a preparation of PME from Arabidopsis flowers, prepared as described (Wolf et al., 2003).

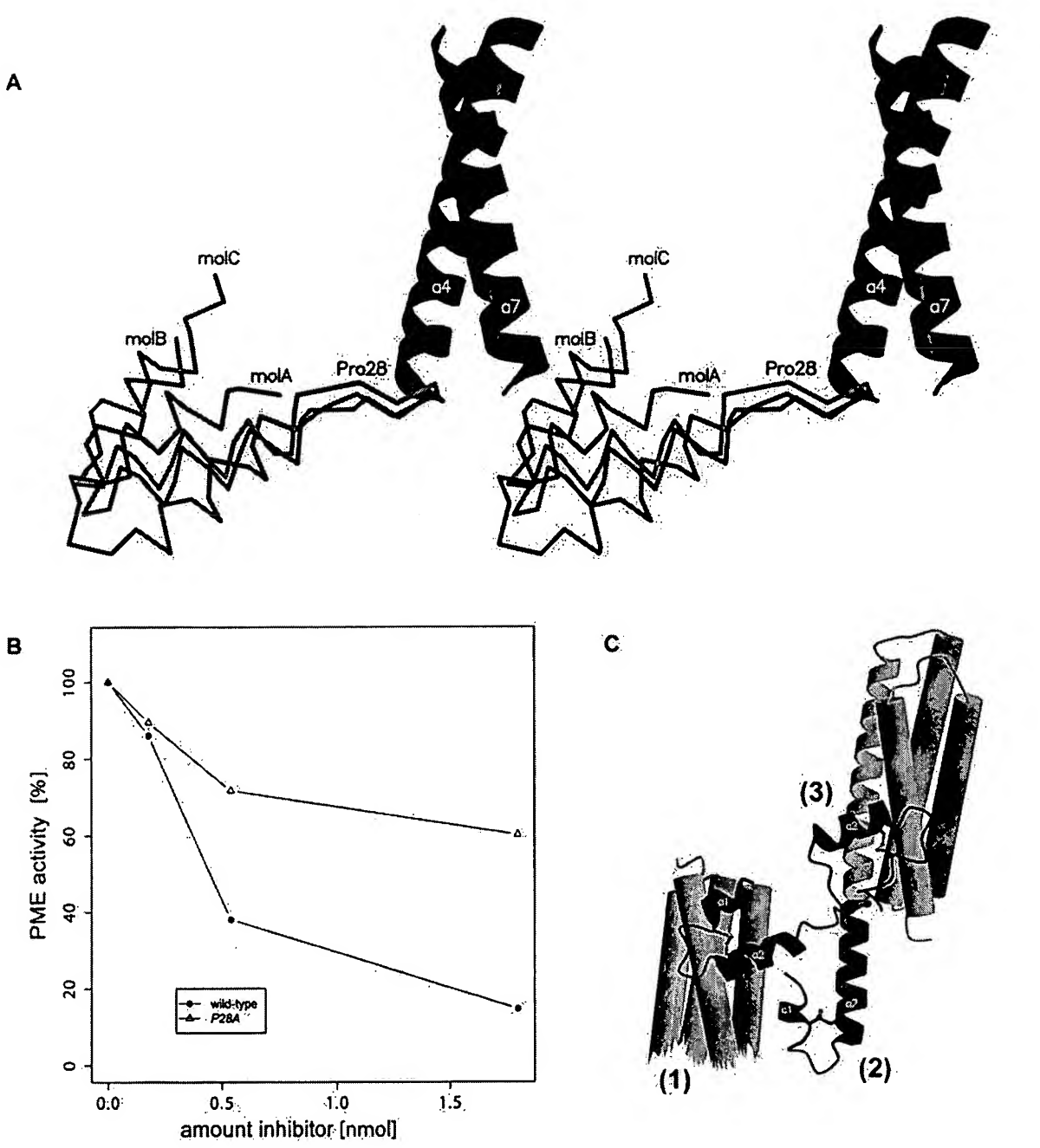

Figure 4. Structural Determinants of Flexibility within the N-terminal Hairpin Module.

(A) Stereo view of the three PMEI molecules in the asymmetric unit, superimposed with respect to the four-helix bundle. The relative displacement indicates conformational variability. Note that the difference in orientation between molA and molC is almost 90°.

(B) Decreased inhibitory power of the PMEI *P28A* mutant in comparison with the wild-type inhibitor (solid circle) in plant PME inhibition assays.

(C) Structural superposition of the wild-type PMEI dimer (green) and two *P28A* mutant structures shown in dark (form A) and light blue (form B) highlight conformational flexibility of the PMEI hairpin. The flipped-out state (2) might resemble an intermediate in transition between dimer (1) and monomer (3).

atoms <1.5 Å) whereas the α-hairpin is slightly displaced. Moreover, in the bundle-hairpin interface we find the same residues involved in structural stabilization as for the wild-type dimer (Figure 2A; see above) with the exception of Phe-25 in the linker peptide that is now flipped outwards. In the second crystal form (form B) we find the linker wound up, integrating helices α2 and α4 into a single long α-helix (Figure 4C, shown in light blue). The mutant structures demonstrate both an open and a closed conformation of PMEI. By structural analogy with CIF we hypothesize that the closed form (form A) would represent

Table 1. Summary of the Crystallographic Analysis

Data Collection	PMEI Wild Type	PMEI *P28A* Mutant (form A)	PMEI *P28A* Mutant (form B)
Space group; unit cell (Å, °)	*I222*; $a = 60.77$, $b = 106.19$, $c = 186.2$, $\alpha = \beta = \gamma = 90$	*C2*; $a = 108.40$, $b = 62.44$, $c = 22.34$, $\alpha = \gamma = 90$, $\beta = 94.05$	*H3*; $a = b = 82.41, 105.41$ $\alpha = \beta = 90$, $\gamma = 120$
Wavelength (Å)	1.0	0.933	0.8166
Resolution (Å)	2.86	1.50	2.68
Highest shell (Å)	3.04–2.86	1.50–1.54	2.85–2.68
No. of unique reflections	14,136 (2,307)	24,884 (1,833)	7,391 (1,184)
Multiplicity	3.5 (3.6)	3.6 (3.3)	5.14 (3.8)
I/σ[a]	16.9 (5.4)	15.4 (3.6)	19.8 (6.56)
R_{sym} (%)[a]	5.9 (27.4)	5.3 (35.8)	6.1 (22.1)
Completeness (%)	98.4 (98.1)	99.8 (98.7)	98.5 (93.3)
Refinement			
Resolution range (Å)	29.06–2.86	54.23–1.50	19.46–2.68
No. of reflections	14,129	24,884	7,391
R_{work} (%)[b]	21.8	18.3	21.5
R_{free} (%)[b]	28.0	20.7	25.6
No. of atoms			
Protein	3,355	1,166	2,198
Solvent	22	104	44
RMS deviations			
Bond length	0.007	0.017	0.010
Angles	1.2	1.5	1.4

[a] As defined in XDS (Kabsch, 1993).
[b] As defined in CNS (Brunger et al., 1998) or REFMAC5 (Collaborative Computational Project Number 4, 1994).

a stable monomer in solution that can also be attained by the wild-type protein (Figure 1D). The open form suggests an intermediate configuration in monomer-dimer transition (see states [1] to [3] in Figure 4C) although crystal-packing effects cannot be ruled out.

Taken together, we have used the *P28A* mutant to visualize the different conformational states of PMEI; configurations that we believe can be adopted by the wild-type inhibitor (Figure 1D) but may not be favored at protein concentrations typically used in crystallization. Our results clearly demonstrate flexibility of the N-terminal extension. Although the effect of the mutation on the inhibitory activity of PMEI is moderate, we believe that flexibility of the N-terminal module is relevant for inhibitor function.

Protein Chimera Shed Light on Target Specificity

The presence of a structurally distinct and flexible motif on an apparently rigid inhibitor core prompted us to investigate whether this module represents a determinant of target specificity. We therefore engineered chimera that combine the α-hairpin module of PMEI with the four-helix bundle of CIF ($X^{PMEI\text{-}CIF}$) and vice versa ($X^{CIF\text{-}PMEI}$; Figure 5B; see Methods). Biophysical analyses of the purified proteins indicated the engineered inhibitors were folded.

Strikingly, $X^{PMEI\text{-}CIF}$ is able to inactivate plant PME in dose-dependent inhibition assays (Figure 5A). By sharp contrast, $X^{CIF\text{-}PMEI}$ did not show inhibitory activity toward either PME or invertase under similar conditions (Figure 5A; data not shown). These results clearly indicate that the PMEI-hairpin module is necessary and sufficient to inhibit PME when attached to a four-helix bundle common to the sequence family ($X^{PMEI\text{-}CIF}$ in Figure 5A).

In this respect, it is noteworthy that PMEI and CIF share only ~17% of their residues within the bundle region (Figure 2B), most of which are located in the interior of the protein (Hothorn et al., 2004). Therefore, the surface-charge distribution is unlikely to play an important role in PME inactivation, although the inhibitory activity of $X^{PMEI\text{-}CIF}$ is decreased with respect to the wild-type inhibitor.

The inability of $X^{CIF\text{-}PMEI}$ to inactivate invertase (data not shown) suggests that the hairpin motif is not sufficient for the invertase inhibitory function. Asking whether the CIF bundle would represent the major functional module instead, we attempted to test $X^{PMEI\text{-}CIF}$ in invertase inhibition assays. Unfortunately, the protein precipitated at buffer conditions established for invertase inhibition assays (see Methods). By contrast, the $X^{CIF\text{-}PMEI}$ chimera is stable even at acidic pH and could therefore be used in invertase assays (see above).

Our observations provide compelling evidence that invertase and PMEIs have established distinct target inactivation mechanisms on virtually identical structural scaffolds. In the case of PMEI, specificity is apparently encoded in the α-hairpin, whereas the entire inhibitor and/or the four-helix bundle of CIF may contain the major determinants for specificity toward invertase.

A Model for the PME-PMEI Complex

Our analysis of PMEI has interesting implications for the interaction of the inhibitor with its target enzyme. To illustrate this, we have manually docked the inhibitor (see Methods) to the crystal structure of carrot PME (Johansson et al., 2002), an enzyme that can be inactivated by PMEI (S. Wolf, unpublished data). In the resulting model, the α-helical bundle covers the

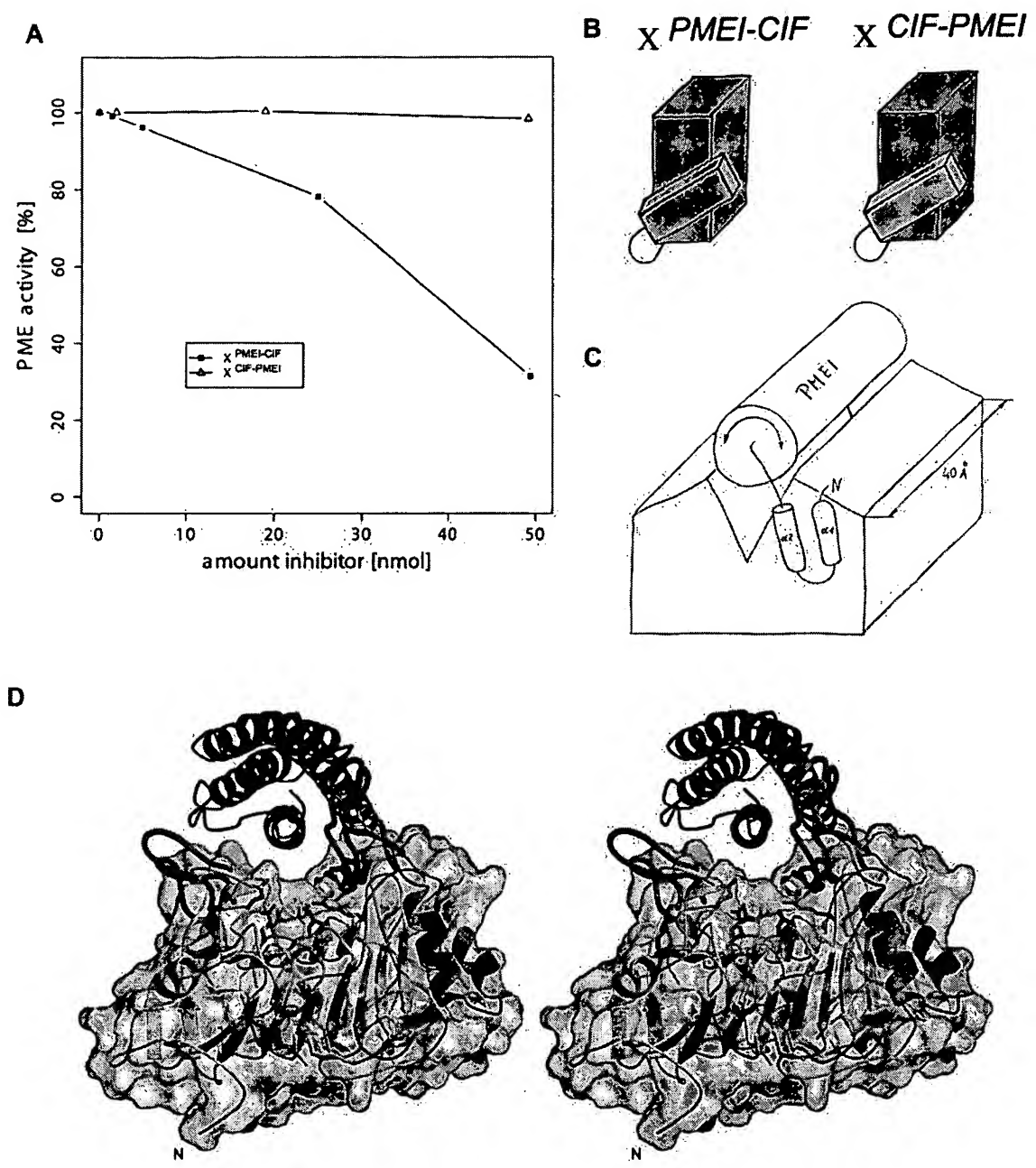

Figure 5. Determinants of Target Specificity.

(A) Dose-dependent inhibition of Arabidopsis PME by protein chimera between PMEI and the invertase inhibitor CIF.

(B) Schematic representation of protein chimera. In $X^{PMEI\text{-}CIF}$, the α-hairpin of PMEI has been connected to the bundle core of CIF. $X^{CIF\text{-}PMEI}$ combines the corresponding hairpin segment of CIF with the four-helix bundle of PMEI. The color coding follows the structural representations in Figure 1.

(C) Proposed model for the inactivation of plant PME by PMEI. Schematic view, in which the four-helix bundle covers the enzyme's pectin binding cleft, which measures ~40 Å in length. The helical hairpin anchors the inhibitor to its target enzyme and mediates specificity.

(D) Manual docking of PMEI onto the pectin binding cleft of plant PME. Carrot PME (PDB ID 1gq8) is shown in both ribbon and molecular surface representation in a view along the cleft region. The inhibitor (in green) covers the entire cleft. Active-site residues and residues W227/252 discussed in the text are highlighted in red and blue, respectively. The longer loop regions of the bacterial enzyme (PDB ID 1qjv) are indicated in magenta.

pectin binding cleft of the enzyme that harbors the substrate and active-site residues (Jenkins et al., 2001; Johansson et al., 2002; see also Figures 5C and 5D). PMEI would bind in an open conformation exposing the N-terminal α-hairpin to interact with a C-terminal helix at the surface of PME. For the following reasons we find this model, which uses large areas of the inhibitor for interaction (~1500 Å^2 buried surface), particularly attractive. (1) PMEI almost completely covers the pectin binding cleft (40 Å in length; Figure 5C) that contains the active site of the enzyme (Johansson et al., 2002). Trp residues located in this cleft become shielded upon inhibitor binding as concluded from fluorescence studies (D'Avino et al., 2003). (2) Biochemical studies indicated a 1:1 complex between PME and PMEI (D'Avino et al., 2003), consistent with our model. (3) Our docking model nicely explains why the homologous bacterial PME is not sensitive to PMEI (Wolf et al., 2003): several loop regions protruding from areas flanking the cleft (Jenkins et al., 2001; Wolf et al., 2003) would interfere with the binding of the PMEI bundle, a selection mechanism proposed earlier (D'Avino et al., 2003). (4) Our model is consistent with a fully automated docking approach employing the program FTDOCK (Gabb et al., 1997). Using surface complementarity as quality criterion, FTDOCK presents a docking solution close to our model based on biochemical data among the top 10 out of 10,000 trials (see Methods). In addition, most of the 100 top-ranked solutions cluster around the pectin binding cleft.

It is also noteworthy that our complex model brings the C terminus of PMEI in close proximity to the N terminus of PME. Such a scenario would allow convenient binding of PMEI homologous Pro-regions in type-I PMEs (Micheli, 2001) in a similar mode, although the functional role of these portions is yet unclear.

In the suggested complex model, the α-hairpin would serve as an anchor, which is essential for the positioning of the four-helix bundle that then mediates the inhibitory activity. This view is consistent with our observations that the bundle alone has no activity and that replacement of the bundle by its CIF counterpart is still functional.

Taken together, our docking model of the interaction between PME and PMEI represents a valuable hypothesis that can now be tested in biochemical studies using site-directed mutagenesis and, finally, by structure determination of the PME-PMEI complex.

Concluding Remarks

Our work reveals plant invertase inhibitors and PMEIs to represent a protein family that has implemented inhibitory activity toward different target enzymes on similar structural scaffolds. By structural comparison of PMEI with its counterpart CIF (Hothorn et al., 2004) and protein-engineering approaches we have identified determinants of target specificity within this class of proteins. It is known that sequence comparison alone does not allow predicting whether family members inhibit one or the other target. Our analysis has narrowed the major determinants of specificity to a set of ~28 residues that can now be analyzed in detail for their role in the inhibition process.

The presented protein chimeras suggest different mechanisms of enzyme inhibition by PMEI and CIF. Understanding these mechanisms in detail will require the structure of the cognate inhibitor-enzyme complexes. Invertase/PMEIs have been used to silence post-translationally their target enzymes in transgenic plants (Greiner et al., 1999; Balibrea Lara et al., 2004). From the presented protein chimera we conclude that protein engineering may represent a useful tool to gain further insights into specificity toward PME and invertase isoenzymes. These studies will allow a more specific interference with key enzymes in plant carbohydrate metabolisms and may inspire novel biotechnological applications.

METHODS

Expression, Crystallization, and Data Collection

Wild-type PMEI and mutant forms have been expressed and purified as described (Wolf et al., 2003) following protocols established for the related invertase inhibitor Nt-CIF (Hothorn et al., 2003). Before crystallization, samples were concentrated to ~5 mg/mL using a Vivapore 10/20 mL concentrator (7.5 kD MWCO; Vivascience, Hannover, Germany) and dialyzed against 100 mM NaCl, 10 mM Hepes, pH 7.0. In the case of the wild-type protein, orthorhombic crystals were grown at room temperature by vapor diffusion from hanging drops composed of equal volumes (2 + 2 μL) of protein solution and crystallization buffer (10% [v/v] PEG 8000, 0.3 M NaCl, 0.1 M Na^+/K^+ P_i, pH 6.2) suspended over 1.0 mL of the latter as reservoir solution. Thin plates of ~200 × 80 × 20 μm were transferred into reservoir solution containing 10% (v/v) glycerol and flash-frozen in liquid nitrogen. A data set at 2.86-Å resolution has been collected at beam line PX06 (Swiss Light Source, Villigen, Switzerland). Monoclinic crystals (form A; see Table 1) of the *P28A* mutant grew in 0.2 M $(NH_4)_2SO_4$, 0.3 M Na^+/K^+ tartrate, 0.1 M sodium citrate, pH 5.6, and were cryoprotected by addition of 10% (v/v) glycerol. A data set at 1.5-Å resolution has been recorded at beam line ID14-2 (European Synchrotron Radiation Facility, Grenoble, France). Rhombohedral crystals (form B in Table 1) of the *P28A* mutant developed in 2.5 M $(NH_4)_2SO_4$ and 4% (v/v) isopropanol and were cryoprotected by addition of 20% (v/v) glycerol. Data collection at beam line X11 (EMBL/DESY, Hamburg) yielded a data set at 2.68-Å resolution. Data processing and scaling was performed with XDS (Kabsch, 1993; December 2003 version).

Structure Determination and Refinement

The structure of PMEI has been determined by molecular replacement in six-dimensional searches with the program EPMR (Kissinger et al., 1999) using a polyalanine model of the previously determined invertase inhibitor Nt-CIF (PDB accession code 1RJ1; Hothorn et al., 2004). The solution comprises a trimer in the asymmetric unit, accounting for a solvent content of ~60%. The small helix-α3 connecting hairpin motif and bundle in Nt-CIF produced clashes in the crystal packing. Removal of this helix, rigid-body refinement, and the use of strict noncrystallographic symmetry allowed the calculation of an initial electron density map at 3.4 Å, in which a disulfide bridge and two Tyr residues could be located. During refinement, strong maxima in the $|F_{obs}-F_{calc}|$ and 2 $|F_{obs}-F_{calc}|$ electron density maps indicated the unfolding of helix α3 into a linker region connecting the N-terminal α-hairpin motif with the bundle of a neighboring molecule. The structure was completed in alternating cycles of model correction using the program O (Jones et al., 1991) and restrained refinement as implemented in CNS (Brunger et al., 1998). The structure of the rhombohedral *P28A* crystal form has been solved by molecular replacement using CNS. The solution comprises a dimer in the asymmetric unit (starting R_{free} 0.41). Finally, the monoclinic crystal form of the mutant protein, comprising a monomer in the asymmetric unit, has been built using Arp/Warp 6.0 (Lamzin and Wilson, 1993) starting from

a molecular replacement solution calculated with CNS. In this case, Refmac5 (Collaborative Computational Project Number, 1994) has been used for the final rounds of refinement. A summary of the crystallographic analysis is shown in Table 1.

Inspection of the refined models with PROCHECK (Laskowski et al., 1993) revealed a good stereochemistry except for some residues in poorly defined loop regions. Structure visualization was done with POVSCRIPT (Fenn et al., 2003) and RASTER3D (Merritt and Bacon, 1997).

Size-exclusion chromatography was performed using an analytical grade Superdex 75 HR 10/30 column (Amersham Biosciences, Piscataway, NJ) preequilibrated in 0.3 M NaCl, 0.1 M Na^+/K^+ P_i, pH 6.2. Fifty microliters of the sample (10.0 mg/mL) were loaded onto the column and elution at 0.8 mL/min was monitored by ultraviolet absorbance at 280 nm.

Site-Directed Mutagenesis

Site-specific mutations were introduced with the QuickChange mutagenesis kit (Stratagene, La Jolla, CA) following the manufacturer's instructions and verified by DNA sequencing.

A truncated version of PMEI lacking 28 N-terminal residues was PCR amplified using sense primer 5′-ATAGCTAAATCCATGGACTCGCCTAATCTTCAAGCCTTG-3′, antisense primer 3′-AAATTGTCAAGGTACCTTAATTACGTGGTAACATGTTAG-5′, and a pQE30 vector (Qiagen USA, Valencia, CA) containing At-PMEI1 (at1g48020) as the template. The *NcoI/KpnI*-restricted fragment was cloned into pETM20, a modified pET21d vector (Novagen, Madison, WI) providing thioredoxin A (trxA) followed by a 6×His tag (amplified from pET32a [Novagen]) and a tobacco etch virus (Tev) protease cleavage site as an N-terminal fusion partner (Hothorn et al., 2003).

Protein Chimera

$X^{PMEI\text{-}CIF}$ has been constructed by *Bam*HI/*Eco*RV digestion of wild-type Nt-CIF in pQE30 (Greiner et al., 1998) producing a fragment that encodes the CIF bundle starting at residue Ile-32. The PMEI hairpin was PCR amplified with sense primer 5′-ATAGCTAAATCCATGGACAGTTCAGAAATGAGCACAATC-3′ and antisense primer 5′-AAATTGTCAAGATATCAGGCGATGCGAATTTCGTATTG-3′ containing Asp-29 and an *Eco*RV site. After ligation, $X^{PMEI\text{-}CIF}$ was amplified and ligated into expression vector pETM20. $X^{CIF\text{-}PMEI}$ has been constructed by simultaneously ligating PCR fragments encoding the CIF hairpin and PMEI bundle into a pETM-20 expression vector. The CIF bundle was amplified using sense primer 5′-ATCGGACTGCAGCCATGGCAAATAATCTAGTAGAAACTAC-3′, antisense primer 5′-CGATACGGCATCGCTAGCGCTTGAAGATTCCCTGTTGCACTTCGTTTGTC-3′, and Nt-CIF in pQE30 as the template. The PMEI bundle was amplified with sense primer 5′-ATCGGACTGCAGGCTAGCAAAAACCACACTTGATTCTAC-3′, antisense primer 5′-AAATTGTCAAGGTACCTTAATTACGTGGTAACATGTTAG-3′, and At-PMEI1 in pQE30 as the template. Subsequently, the CIF hairpin fragment was restricted with *Nco*I and *Nhe*I, whereas the PMEI bundle was restricted with *Nhe*I and *Kpn*I. Both fragments were ligated into the *NcoI/KpnI*-restricted pETM-20 vector. Constructs were verified by DNA sequencing.

Activity Assay for Inhibitor Function

PME preparations from a mixture of Arabidopsis flowers and siliques were obtained by homogenizing the tissue in 2 mL/g extraction buffer (25 mM maleic acid, 75 mM Tris base, pH 7.0, 1 M NaCl, complemented with a complete mini EDTA-free protease inhibitor tablet (Roche, Mannheim, Germany). After incubation on ice for 30 min with gentle agitation, the homogenate was centrifuged twice at 11,000*g* for 10 min and the supernatant kept to perform inhibition assays. PME activity was determined by a coupled enzymatic assay as described (Grsic-Rausch and Rausch, 2004). In brief, the assay was performed in 50 mM phosphate buffer, pH 7.5, in the presence of 0.4 mM NAD. PME activity using commercially available pectin (Sigma, St. Louis, MO) as substrate was measured by the amount of the produced methanol, which was first oxidized to formaldehyde by alcohol oxidase (1 unit; Sigma), followed by oxidation to formate via formaldehyde dehydrogenase (0.35 unit; Sigma). The produced NADH was measured at OD_{340nm} in a spectrophotometer.

Acid invertase activity (assay buffer: 30 mM sucrose, 20 mM triethanol amine, 7 mM citric acid, 1 mM phenyl methyl sulfonyl fluoride, pH 4.6) was measured by enzymatic determination of released glucose in a coupled assay with hexokinase and glucose-6-phosphate dehydrogenase as described (Weil and Rausch, 1994).

Rigid-Body Protein Docking

A molecular surface of carrot PME (PDB ID 1gq8) calculated with VOIDOO (Kleywegt and Jones, 1994) has been used to manually navigate the inhibitor onto the PME pectin binding cleft using the program O (Jones et al., 1991). Furthermore, we used the program FTDock (Gabb et al., 1997) to perform a rigid-body docking of the PME to its inhibitor. The algorithm discretizes the surfaces of the two interacting molecules and performs a global scan of the translational and rotational space. FTDock evaluates millions of possible relative orientations between the two molecules and keeps the 10,000 solutions that show the best surface complementarity. To speed up the calculations, the PME (larger molecule) was kept static and its inhibitor was translated and rotated to explore the six degrees of associational freedom. Finally, we rescored the list of 10,000 solutions and ranked them according to electrostatics complementarity between the two interacting interfaces and empirical pair potentials (Moont et al., 1999).

Atomic coordinates and structure factors have been submitted to the Protein Data Bank (http://www.rcsb.org) with codes 1X8Z (wild type), 1X91 (*P28A* mutant form A), and 1X90 (*P28A* mutant form B).

ACKNOWLEDGMENTS

We are grateful to Thomas Rausch for continuous support and discussions on PMEI-RP physiology during the preparation of the manuscript. We thank the staff at the European Synchrotron Radiation Facility, Grenoble, France, the Deutsches Elektronensynchrotron, Hamburg, Germany, and the Swiss Light Source, Villigen, Switzerland for technical support during data collection. We acknowledge financial support from the Suedzucker AG, Mannheim, Germany and the KWS Saat AG, Einbeck, Germany (grants to S.G.). M.H. gratefully acknowledges financial support from the Peter and Traudl Engelhorn Stiftung Penzberg, Germany.

Received June 30, 2004; accepted September 7, 2004.

REFERENCES

Balibrea Lara, M.E., Gonzalez Garcia, M.C., Fatima, T., Ehness, R., Lee, T.K., Proels, R., Tanner, W., and Roitsch, T. (2004). Extracellular invertase is an essential component of cytokinin-mediated delay of senescence. Plant Cell **16,** 1276–1287.

Bode, W., and Huber, R. (1992). Natural protein proteinase inhibitors and their interaction with proteinases. Eur. J. Biochem. **204,** 433–451.

Brummell, D.A., and Harpster, M.H. (2001). Cell wall metabolism in fruit softening and quality and its manipulation in transgenic plants. Plant Mol. Biol. **47,** 311–340.

Brunger, A.T., et al. (1998). Crystallography & NMR system: A new software suite for macromolecular structure determination. Acta Crystallogr. D Biol. Crystallogr. **54,** 905–921.

Camardella, L., Carratore, V., Ciardiello, M.A., Servillo, L., Balestrieri, C., and Giovane, A. (2000). Kiwi protein inhibitor of pectin methylesterase amino-acid sequence and structural importance of two disulfide bridges. Eur. J. Biochem. **267,** 4561–4565.

Chen, M.H., and Citovsky, V. (2003). Systemic movement of a tobamovirus requires host cell pectin methylesterase. Plant J. **35,** 386–392.

Chen, M.H., Sheng, J., Hind, G., Handa, A.K., and Citovsky, V. (2000). Interaction between the tobacco mosaic virus movement protein and host cell pectin methylesterases is required for viral cell-to-cell movement. EMBO J. **19,** 913–920.

Cheng, W.-H., Taliercio Earl, W., and Chourey Prem, S. (1996). The Miniature1 seed locus of maize encodes a cell wall invertase required for normal development of endosperm and maternal cells in the pedicel. Plant Cell **8,** 971–983.

Chothia, C., and Lesk, A.M. (1986). The relation between the divergence of sequence and structure in proteins. EMBO J. **5,** 823–826.

Collaborative Computational Project Number 4. (1994). The CCP4 suite: Programs for protein crystallography. Acta Crystallogr. D Biol. Crystallogr. **50,** 760–763.

D'Avino, R., Camardella, L., Christensen, T.M., Giovane, A., and Servillo, L. (2003). Tomato pectin methylesterase: Modeling, fluorescence, and inhibitor interaction studies-comparison with the bacterial (Erwinia chrysanthemi) enzyme. Proteins **53,** 830–839.

Ehness, R., Ecker, M., Godt Dietmute, E., and Roitsch, T. (1997). Glucose and stress independently regulate source and sink metabolism and defense mechanisms via signal transduction pathways involving protein phosphorylation. Plant Cell **9,** 1825–1841.

Fenn, T.D., Ringe, D., and Petsko, G.A. (2003). POVScript+: A program for model and data visualization using persistence of vision raytracing. J. Appl. Crystallogr. **36,** 944–947.

Frenkel, C., Peters, J.S., Tieman, D.M., Tiznado, M.E., and Handa, A.K. (1998). Pectin methylesterase regulates methanol and ethanol accumulation in ripening tomato (*Lycopersicon esculentum*) fruit. J. Biol. Chem. **273,** 4293–4295.

Gabb, H.A., Jackson, R.M., and Sternberg, M.J. (1997). Modelling protein docking using shape complementarity, electrostatics and biochemical information. J. Mol. Biol. **272,** 106–120.

Giovane, A., Servillo, L., Balestrieri, C., Raiola, A., D'Avino, R., Tamburrini, M., Ciardiello, M.A., and Camardella, L. (2004). Pectin methylesterase inhibitor. Biochim. Biophys. Acta **1696,** 245–252.

Goetz, M., Godt, D.E., Guivarc'h, A., Kahmann, U., Chriqui, D., and Roitsch, T. (2001). Induction of male sterility in plants by metabolic engineering of the carbohydrate supply. Proc. Natl. Acad. Sci. USA **98,** 6522–6527.

Greiner, S., Krausgrill, S., and Rausch, T. (1998). Cloning of a tobacco apoplasmic invertase inhibitor. Proof of function of the recombinant protein and expression analysis during plant development. Plant Physiol. **116,** 733–742.

Greiner, S., Rausch, T., Sonnewald, U., and Herbers, K. (1999). Ectopic expression of a tobacco invertase inhibitor homolog prevents cold-induced sweetening of potato tubers. Nat. Biotechnol. **17,** 708–711.

Grsic-Rausch, S., and Rausch, T. (2004). A coupled spectrophotometric enzyme assay for the determination of pectin methylesterase activity and its inhibition by proteinaceous inhibitors. Anal. Biochem. **133,** 14–18.

Hothorn, M., Bonneau, F., Stier, G., Greiner, S., and Scheffzek, K. (2003). Bacterial expression, purification and preliminary X-ray crystallographic characterization of the invertase inhibitor Nt-CIF from tobacco. Acta Crystallogr. D Biol. Crystallogr. **59,** 2279–2282.

Hothorn, M., D'Angelo, I., Marquez, J.A., Greiner, S., and Scheffzek, K. (2004). The invertase inhibitor Nt-CIF from tobacco: A highly thermostable four-helix bundle with an unusual N-terminal extension. J. Mol. Biol. **335,** 987–995.

Jenkins, J., Mayans, O., Smith, D., Worboys, K., and Pickersgill, R.W. (2001). Three-dimensional structure of *Erwinia chrysanthemi* pectin methylesterase reveals a novel esterase active site. J. Mol. Biol. **305,** 951–960.

Johansson, K., El-Ahmad, M., Friemann, R., Jornvall, H., Markovic, O., and Eklund, H. (2002). Crystal structure of plant pectin methylesterase. FEBS Lett. **514,** 243–249.

Jones, T.A., Zou, J.-Y., Cowan, S.W., and Kjeldgaard, M. (1991). Improved methods for building protein models in electron density maps and the location of errors in these models. Acta Crystallogr. A **47,** 110–119.

Juge, N., Svensson, B., Henrissat, B., and Williamson, G. (2004). Plant proteinaceous inhibitors of carbohydrate-active enzymes. Biochim. Biophys. Acta **1696,** 141.

Kabsch, W. (1993). Automatic processing of rotation diffraction data from crystals of initially unknown symmetry and cell constants. J. Appl. Crystallogr. **26,** 795–800.

Kabsch, W., and Sander, C. (1983). Dictionary of protein secondary structure: Pattern recognition of hydrogen-bonded and geometrical features. Biopolymers **22,** 2577–2637.

Kissinger, C.R., Gehlhaar, D.K., and Fogel, D.B. (1999). Rapid automated molecular replacement by evolutionary search. Acta Crystallogr. D Biol. Crystallogr. **55,** 484–491.

Kleywegt, G.J., and Jones, T.A. (1994). Detection, delineation, measurement and display of cavities in macromolecular structures. Acta Crystallogr. D Biol. Crystallogr. **50,** 178–185.

Koch, K. (2004). Sucrose metabolism: Regulatory mechanisms and pivotal roles in sugar sensing and plant development. Curr. Opin. Plant Biol. **7,** 235–246.

Koch, K.E. (1996). Carbohydrate-modulated gene expression in plants. Annu. Rev. Plant Physiol. Plant Mol. Biol. **47,** 509–540.

Lamzin, V.S., and Wilson, K.S. (1993). Automated refinement of protein models. Acta Crystallogr. D Biol. Crystallogr. **49,** 129–147.

Laskowski, R.A., MacArthur, M.W., Moss, D.S., and Thornton, J.M. (1993). PROCHECK: A program to check the stereochemical quality of protein structures. J. Appl. Crystallogr. **26,** 283–291.

Merritt, E.A., and Bacon, D.J. (1997). Raster3D: Photorealistic molecular graphics. Methods Enzymol. **277,** 505–524.

Micheli, F. (2001). Pectin methylesterases: Cell wall enzymes with important roles in plant physiology. Trends Plant Sci. **6,** 414–419.

Moont, G., Gabb, H.A., and Sternberg, M.J. (1999). Use of pair potentials across protein interfaces in screening predicted docked complexes. Proteins **35,** 364–373.

Pilling, J., Willmitzer, L., and Fisahn, J. (2000). Expression of a Petunia inflata pectin methyl esterase in *Solanum tuberosum* L. enhances stem elongation and modifies cation distribution. Planta **210,** 391–399.

Raiola, A., Camardella, L., Giovane, A., Mattei, B., De Lorenzo, G., Cervone, F., and Bellincampi, D. (2004). Two *Arabidopsis thaliana* genes encode functional pectin methylesterase inhibitors. FEBS Lett. **557,** 199–203.

Rausch, T., and Greiner, S. (2004). Plant protein inhibitors of invertases. Biochim. Biophys. Acta **1696,** 253–261.

Roitsch, T., Balibrea, M.E., Hofmann, M., Proels, R., and Sinha, A.K. (2003). Extracellular invertase: Key metabolic enzyme and PR protein. J. Exp. Bot. **54,** 513–524.

Smeekens, S. (1998). Sugar regulation of gene expression in plants. Curr. Opin. Plant Biol. **1,** 230–234.

Tang, G.Q., Luscher, M., and Sturm, A. (1999). Antisense repression of vacuolar and cell wall invertase in transgenic carrot alters early plant development and sucrose partitioning. Plant Cell **11,** 177–189.

Vorwerk, S., Somerville, S., and Somerville, C. (2004). The role of plant cell wall polysaccharide composition in disease resistance. Trends Plant Sci. **9,** 203–209.

Weil, M., and Rausch, T. (1994). Acid invertase in *Nicotiana tabacum* crown-gall cells: Molecular properties of the cell-wall isoform. Planta **193,** 430–437.

Wen, F., Zhu, Y., and Hawes, M.C. (1999). Effect of pectin methylesterase gene expression on pea root development. Plant Cell **11,** 1129–1140.

Wobus, U., and Weber, H. (1999). Sugars as signal molecules in plant seed development. Biol. Chem. **380,** 937–944.

Wolf, S., Grsic-Rausch, S., Rausch, T., and Greiner, S. (2003). Identification of pollen-expressed pectin methylesterase inhibitors in Arabidopsis. FEBS Lett. **555,** 551–555.

P/2107-162

IN THE UNITED STATES PATENT AND TRADEMARK OFFICE

In re Patent Application of

Thomas Rausch

Serial No.: 09/762,782
Filed: March 30, 2001

Group Art Unit: 1638
Examiner: R.Kallis

For: TRANSGENIC PLANTS AND CELLS COMPRISING A REDUCED EXPRESSION OF PLANT INVERTASE INHIBITORS

Assistant Commissioner for Patents
Washington D.C. 20231

DECLARATION OF THOMAS RAUSCH UNDER 37 C.F.R.§1.132

Sir:

I, Thomas Rausch, having residence at Im Neuenheimer Feld 360, D-69120-Heidelberg, Germany, hereby declare that

1. I am inventor of the above-identified application and am familiar with the subject application.

2. Total RNA was isolated from *B. napus* siliques (6 days-after-pollination), and mRNA was purified by oligo-dT cellulose chromatography. A cDNA library was prepared in ZAP-Express EcoRI/XhoI (Stratagene). The library was screened with a biotinylated probe corresponding to the *A. thaliana Bn-inhh1* homolog with the accession number AA712621 (this EST clone showing significant homology to the tobacco *Nt-inh1* cDNA; Greiner *et al.*, 1998). The obtained *Bn-inhh1*-full length clone was sequenced in both directions (for cDNA sequence see below). The *Bn-inhh1* cDNA was cloned in *antisense* orientation behind the 35S promoter into the pBinar vector for *A. tumefaciens*-mediated transformation of *B. napus* (Drakkar). Following this procedure, a transgenic rape plant was generated, which showed an increased seed weight and seed storage oil content.

a) Reserve material content of seeds of a transgenic rape plant transformed with a rape invertase inhibitor sequence (Bn-Inhh1) in comparion to wild-type plants:

Parameter	Rape (type Drakkar, WT)	*Antisense*-transformants (type Drakkar)		
		Line 11	Line 13	Line 24
Average weight of seed	3.8 ± 0.3 mg	4.1 ± 0.4 mg	4.2 ± 0.3 mg	4 4 ± 0.4 mg
% w/w oil content	43 ± 3 %	55 ± 7%	56 ± 5%	53 ± 4%

b) Protein sequence of the rape invertase inhibitor isoform (Bn-inhh1) in comparison to the protein sequence of the tobacco invertase inhibitor (Nt-Inh1; Greiner et al., 1998):

```
                  *        20         *        40         *
Ntinh1  : -------MKNLIFLTMFLTILLQTNANNLVETTCKNTFNYQLCLKTLLSD :  43
Bninhh1 : -------MKKMVVVKMDMMVTVMVSEASMIEQTCKETPDFNLCVSLLDSD :  43

                 60         *        80         *        100
Ntinh1  : KRSATGDITTLALIMVDAIKAKANQAAVTISKLRHSNPP--AAWKGPLKN :  91
Bninhh1 : PRGSSADTSGLALILVDKIKGLATKTLKEINSLYKKRP----ELKQALDE :  89

                  *       120         *       140         *
Ntinh1  : CAFSYKVILTASLPEAIEALTKGDFKFAEDGMVGSSGDAQECEEYFKGSK : 141
Bninhh1 : CSRRYKTILKADVPEAIEATSKGVPKFGEDGVIDAGVEAAVCEGEFKG-K : 138

                160         *       180
Ntinh1  : -----SPFSALNIAVHELSDVGRAIVRNIL- : 166
Bninhh1 : -----SPLTSLTKSMQKVSNVTRAIVRMLL- : 163
```

c) Nucleic acid sequence coding for Bn-inhh1

ATGAAGAAGATGGTGGTGGTGAAGATGATCATGATGGTAACAGTGATGGTGAGTGAAGCGAGTATGAT
AGAGCAGACATGCAAAGAGACACCAGATTTCAATCTCTGCGTCTCTCTCCTCGACTCCGACCCACGTG
GCTCCTCTGCCGACACCTCTGGCCTCGCTCTTATCCTCGTCGATAAAATCAAGGGGTTGGCGACGAAG
ACCTTGAAAGAAATCAACAGTCTATATAAAAAGAGACCGGAACTGAAACAGGCTTTAGACGAATGTAG
TCGAAGATACAAAACGATCTTAAAGGCTGATGTTCCCGAAGCCATTGAAGCTATATCTAAAGGCGTTC
CGAAGTTCGGTGAAGACGGTGTGATCGATGCTGGTGTGGAAGCTGCTGTATGTGAAGGAGAATTTAAA
GGGAAATCTCCGTTGACTAGTTTGACCAAATCAATGCAAAAAGTCTCTAATGTGACTAGAGCCATTGT
GAGAATGTTGCTTTGATTTTATCTTTTATGTTCGTTCATACAAGCATGTGGTATGGGTGTTTGATGGG
AT

3. I further declare that all statements made herein are made of my own knowledge and are true except for those statements made on information and belief, which are believed to be true, and further that these statements are made with the knowledge that willful false statements and the like so made are punishable by fine or imprisonment, or both, under Section 1001 of Title 18 of the United States Code and that such willfull false statements may jeopardize the validity of this declaration of this application and any United States patent issuing therefrom.

Feb 9th 2003
Date

Thomas Rausch

Ectopic expression of a tobacco invertase inhibitor homolog prevents cold-induced sweetening of potato tubers

Steffen Greiner[1], Thomas Rausch[1]*, Uwe Sonnewald[2], and Karin Herbers[2]

*[1]Botanisches Institut, INF 360, D-69120-Heidelberg, Germany. [2]IPK Gatersleben, Corrensstraße 3, D-06466-Gatersleben, Germany. *Corresponding author (e-mail: trausch@botanik1.bot.uni-heidelberg.de).*

Received 17 November 1998; accepted 15 April 1999

We have transformed potato with *Nt-inhh* cDNA, encoding a putative vacuolar homolog of a tobacco cell wall invertase inhibitor, under the control of the CaMV 35S promoter. In transgenic tubers, cold-induced hexose accumulation was reduced by up to 75%, without any effect on potato tuber yield. Processing quality of tubers was greatly improved without changing starch quantity or quality, an important prerequisite for the biotechnological use of Nt-inhh for potato transformation.

Key words: potato, cold sweetening, vacuolar invertase, invertase inhibitor

To prevent sprouting during storage, potato tubers are either treated with dormancy-prolonging chemicals or are stored at low temperature. In the cold, starch is converted into soluble sugars, a phenomenon recognized as cold-induced sweetening[1]. The hexoses react with free amino acids, thereby negatively affecting the processing quality of potato tubers[2]. Hexose accumulation is thought to be caused by an imbalance between the rate of starch degradation and the rate of glycolysis[3] leading to accumulation of sucrose[4], which subsequently is split into glucose and fructose via invertase(s). Despite general agreement on the enzymes thought to be involved in the cold-induced starch–hexose conversion, little is known about their relative contribution and their in vivo regulation. To overcome hexose accumulation, two general strategies have been envisaged: (1) inhibition of starch degradation and (2) reduction in the activity of invertase(s). Overexpression of a mutated ADP-glucose pyrophosphorylase gene (*glgC16*) from *Escherichia coli* led to an increased rate of starch synthesis in tubers of transgenic potato plants[5]. Cold storage of these tubers revealed that hexose accumulation was largely inhibited[6]. The reason for the observed decrease in hexose accumulation has been speculated to be the higher starch biosynthetic capacity of the transgenic tubers. Studying the role of starch granule-bound proteins of unknown function, Lorberth et al.[7] created transgenic plants with decreased levels of the so-called R1 protein. Antisense inhibition of R1 led to a reduced phosphate content of potato starch, resulting in a less digestable starch. As a further consequence, cold-induced sweetening was inhibited[7]. Although successful in reducing cold-induced hexose accumulation, both approaches are of limited value because either starch quantity or quality was altered.

To inhibit the formation of sucrose-derived hexoses, Zrenner et al.[8] adopted a more direct approach, transforming potato with a particular cold-inducible vacuolar invertase (VI) isoform in antisense orientation. In transgenic tubers analyzed immediately after harvest, no effect was found on hexose concentrations and hexose:sucrose ratios in different transformants; however, hexose:sucrose ratios were significantly reduced in transgenic tubers after storage at 4°C, the effect showing a good correlation with the residual VI activities in different transgenic lines. Interestingly, an absolute reduction in cold-induced hexose accumulation (-34%) was observed only in the strongest antisense line, where residual VI activity was <10% as compared with wild-type plants. Based on these results, the authors concluded that other invertase isoforms may contribute to cold-induced hexose accumulation. Alternatively, the results could indicate that the cold-inducible VI isoform is expressed well in excess over cellular demand, thus requiring a >90% reduction in activity before a significant effect is observed on cold-induced hexose formation.

With the aims of strongly inhibiting the activity of the cold-induced VI in potato tubers and circumventing the possible limitations of isoform-specific antisense repression of VI, we have now investigated the possibility of repressing the action of cold-induced VI by expression of a putative vacuolar invertase inhibitor from tobacco, called Nt-inhh (ref. 9), in potato plants under the control of the CaMV 35S promoter.

Results and discussion

Cloning. The physiological role of the cell wall invertase inhibitor Nt-inh1, the first cloned plant invertase inhibitor[10], has been investigated in tobacco suspension-cultured cells[11], and proof of function for the recombinant protein expressed in *E. coli* has been reported[10]. Subsequently, a cDNA clone for a structurally related homolog, *Nt-inhh*, has been isolated from the same cDNA library (obtained from suspension-cultured cells) by screening with an *Nt-inh1* probe at low stringency. The open reading frame of the *Nt-inhh* cDNA predicts a protein of 172 amino acids and an M_r of 19,000 (M_r 17,000 after potential signal peptide removal). Four cysteine residues are present at positions conserved in Nt-inh1 and an invertase inhibitor homolog from *Arabidopsis thaliana*[10]. At the protein level, Nt-inhh (Fig.1A) is 46% homologous to Nt-inh1 (ref. 10). Analysis of the *Nt-inhh* cDNA sequence with the SignalSeq program predicts a signal peptide for amino acid residues 3–17 (ref. 12), albeit with a weak score. Thus, similar to Nt-inh1, Nt-inhh most likely enters the secretory pathway; however, sequence analysis alone did not allow prediction of its final target, which could be a VI or a cell wall invertase (CWI).

Transformation. To address the question of which invertase isoform is affected by Nt-inhh, potato and tobacco plants were transformed with *Nt-inhh* in sense-orientation (Fig. 1B and C). A com-

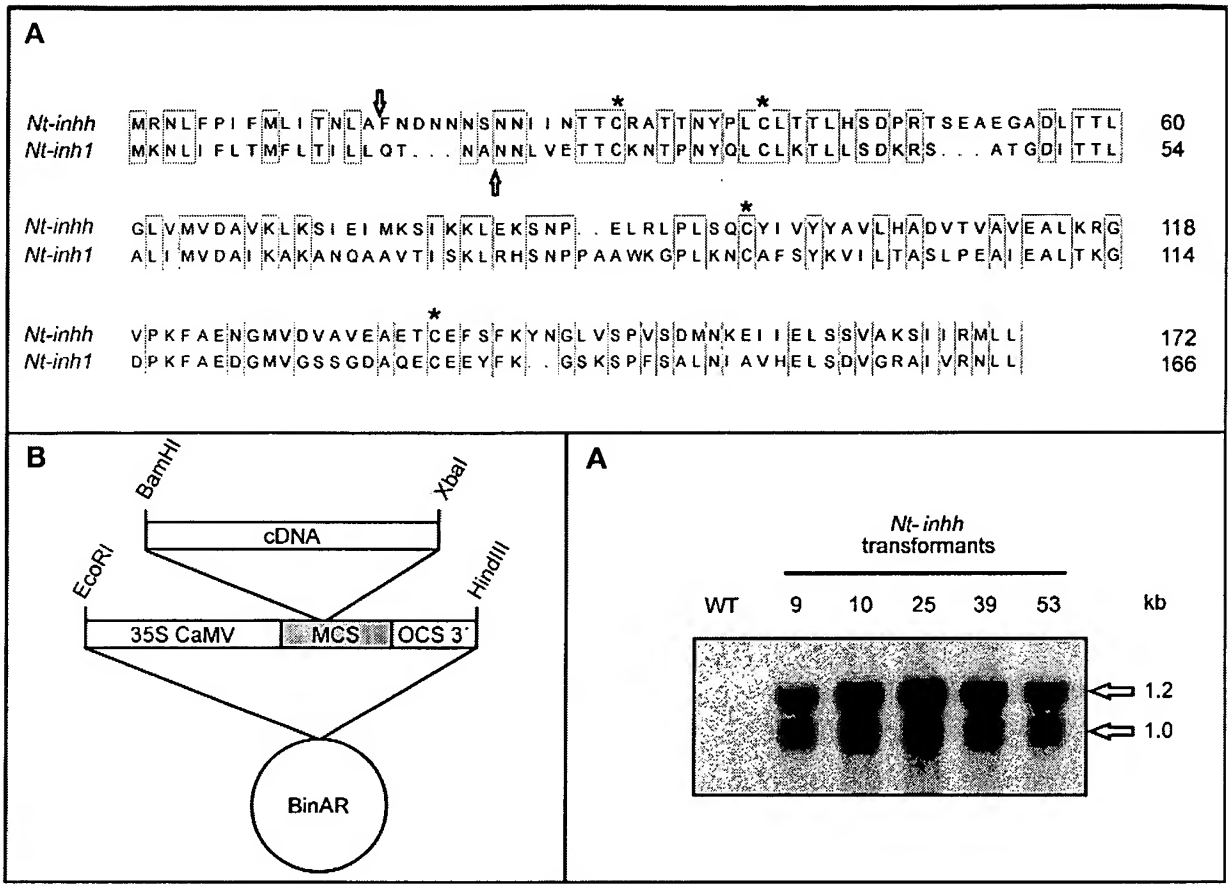

Figure 1. (A) Alignment of the predicted Nt-inhh and Nt-inh1 protein sequences. The first amino acids of the mature Nt-inh1 and Nt-inhh proteins are indicated by arrows. Note that for Nt-inh1 the N-terminal amino acid has been confirmed by protein sequencing[10], whereas for Nt-inhh the N terminus is predicted from the SignalSeq program[12] which detects a weak score signal peptide for amino acids 3–17. Conserved cysteine residues are marked by asterisks. (B) Illustration of gene construct used to transform potato and tobacco with *Nt-inhh* in sense orientation. MCS, multiple cloning site; BinAR, binary plant transformation vector. (C) Northern blot analysis of leaf samples from potato transformants expressing *Nt-inhh* under the regulation of the CaMV 35S promoter. The two hybridization signals result from transcription termination at either the cDNA poly-adenylation site or at the octopine synthase terminator signal (OCS). WT, untransformed control plant.

parison of acid invertase activities in cell wall protein and soluble protein fractions from leaves of potato *Nt-inhh*-transformants revealed that VI, but not CWI, was affected by *Nt-inhh* expression (Table 1). The activity of VI was reduced by about 80%, whereas CWI activity remained unchanged. Whether the observed decrease of VI activity in vitro reflects the full potential for in vivo inhibition by Nt-inhh remains to be investigated; however, it is conceivable that some dissociation of Nt-inhh from its target VI may occur during preparation of enzyme extracts (see below). The inhibitory effect of *Nt-inhh* expression on VI activity in leaf extracts was observed in several independent potato *Nt-inhh*-transformants (Fig. 2), and a similar decrease of VI activity was observed in tobacco. In four independent *Nt-inhh*-transformant lines of tobacco, VI activities in concanavalin A (ConA)-bound fractions obtained from leaf extracts were reduced by 61%, 76%, 66%, and 79%, respectively. As ConA-bound fractions are not contaminated with nonglycosylated neutral or alkaline invertases, the observed effect is certainly due to selective reduction of VI activity.

The selective inhibition of leaf VI by Nt-inhh indicated the possibility that the process of cold-induced sweetening in potato tubers was also affected by ectopic *Nt-inhh* expression[8]. When *Nt-inhh* was constitutively expressed under the control of the CaMV 35S promoter in potato (or tobacco), transformed plants did not show any visible difference in phenotype from wild-type plants (data not shown). In particular, potato tuber number and weight was not adversely affected.

Effect of *Nt-inhh* expression on cold-induced hexose accumulation. Tubers were stored at 4°C for six weeks and thereafter analyzed for their hexose, sucrose, and starch contents (Table 2). Compared with wild-type plants, tubers from several *Nt-inhh* transformants showed a conspicuous reduction of cold-induced hexose accumulation, ranging for glucose from –52% to –83% and for fructose from –51% to –73%. Interestingly, sucrose concentrations ranged from 64% to 323% in different transformants compared with wild-type plants. Obviously, the production of Nt-inhh did not only change the hexose:sucrose ratio as had been previously observed in tubers

Table 1. Effect of ectopic expression of *Nt-inhh* on invertase activity in source leaves of potato plants.

	VI activity (μmol/min/m²)	CWI activity (μmol/min/m²)
Untransformed control	117.13 ± 32.13	13.04 ± 2.48
Nt-inhh transformant	23.59 ± 7.19	14.70 ± 8.11

Data are means of three independent extracts, with standard errors (*Nt-inhh*-transformant line 10; see also Fig. 2).

Table 2. Effect of ectopic *Nt-inhh* expression on cold-induced hexose accumulation in potato tubers.

Potato line	Glucose	Fructose	Sucrose	Hexose:sucrose ratio	Starch	Tuber fresh weight per plant
Wild type						
Solara	47.5 ± 2.1	44.2 ± 6.4	14.9 ± 2.0	6.15	613.2 ± 61.9	110.5 ± 15.7
Nt-inhh transformants						
9	22.6 ± 3.3	21.5 ± 4.0	38.3 ± 4.3	1.15	617.3 ± 39.8	108.0 ± 10.3
10	16.3 ± 3.7	16.2 ± 2.2	22.8 ± 6.3	1.43	604.8 ± 89.7	116.1 ± 12.7
25	18.1 ± 3.9	11.8 ± 1.9	9.6 ± 1.0	3.11	565.6 ± 76.4	132.0 ± 8.2
39	8.1 ± 1.7	14.4 ± 1.2	16.0 ± 0.8	1.4	577.9 ± 59.5	106.8 ± 12.7
53	20.9 ± 2.3	18.4 ± 2.4	48.0 ± 4.0	0.82	799.8 ± 63.0	114.6 ± 10.8

Concentrations of glucose, fructose, sucrose, and starch, and yield of tubers from nontransformed potato (var. Solara; WT) and five independent *Nt-inhh* transformants after cold storage (4°C) for six weeks are presented. Sugar and starch contents are expressed as μmol hexose equivalents per gram fresh weight; tuber weight is expressed in grams (see Experimental protocol). Data are means of five independent extractions, with standard errors.

with antisense-mediated repression of VI, but also led to a much stronger overall reduction of reducing sugars compared with the strongest VI antisense line[8]. This effect was specific for *Nt-inhh* transformants. Potato plants transformed with the cell wall invertase inhibitor isoform *Nt-inh1* in sense orientation showed a cold-induced hexose accumulation similar to wild-type plants (data not shown).

Effect on starch accumulation. In contrast to the profound effects on soluble sugar concentrations, *Nt-inhh* expression did not affect starch content of tubers and tuber fresh weight per plant when compared with wild-type plants (Table 2). Interestingly, in tubers from transformants showing the strongest reduction in cold-induced hexose accumulation (lines 39 and 25), the concentration of total soluble sugars was significantly lower than in wild-type tubers. As this unexpected result could be due to a secondary effect, we have also analyzed tubers that were exposed to a shorter cold treatment. At the transcript level, maximum induction of the cold-inducible VI isoform had been observed after one week[8]. We determined the hexose and sucrose concentrations in tubers stored for only 11 days at 4°C. At this early stage of cold adaptation, sucrose content was almost identical in wild type and all transformants, whereas a significant reduction in the hexose:sucrose ratio was already observed for all transformants except line 9 (wild type, 0.16; line 53, 0.03; line 10, 0.05; line 25, 0.02; line 39, 0.04; line 9, 0.27). These results support the assumption that the primary effect of Nt-inhh is on the activity of cold-induced VI, whereas after an extended storage period additional secondary effects of *Nt-inhh* expression on sugar metabolism may occur.

Interaction with VI isoform. To confirm the assumed interaction of Nt-inhh with the cold-induced VI isoform expressed in potato tubers[8], we have determined VI activities in extracts from cold-stored wild-type and transgenic tubers. In marked contrast to our results with leaf extracts (see above), we did not observe a reduced soluble acid invertase activity in extracts from *Nt-inhh* transformants. Conversely, a moderate increase of in vitro VI activity was found (data not shown). To investigate whether this unexpected result was due to weaker expression of *Nt-inhh* in tuber tissue than in leaf tissue, we determined *Nt-inhh* transcript amounts by RNA blot analysis (Fig. 3). The results revealed that *Nt-inhh* mRNA levels in tubers were similar to those found in leaf tissue, and cold-storage of tubers did not significantly alter *Nt-inhh* transcript levels (data not shown).

The discrepancy of the observed reduction of VI activity in leaf extracts of *Nt-inhh*-transformants with the results obtained with tuber extracts indicates that the stability of complexes between invertase inhibitors and their target enzymes during preparation of enzyme extracts may depend on tissue-specific factors. Several different procedures for VI extraction from tuber tissue, including the protocol for VI determination already described[8], as well as partial purification of VI by ConA chromatography, yielded essentially the same result. It is noteworthy that the VI isoform constitutively expressed in leaves is identical to the VI isoform induced in cold-treated tubers[13]. Therefore, we have good reason to believe that, in vivo, the cold-inducible VI isoform is also inhibited by Nt-inhh in cold-stored tubers. Based on this assumption, the above-mentioned moderate increase of in vitro VI activity in extracts from cold-treated tubers of *Nt-inhh* transformants may indicate that VI expression is upregulated in response to its in vivo deficiency.

Effect on processing quality. To demonstrate the impact of Nt-inhh-mediated reduction of cold-sweetening on the processing qual-

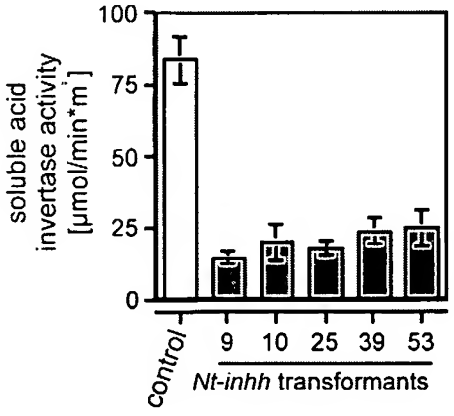

Figure 2. Reduction of soluble acid invertase activities in leaf extracts from potato *Nt-inhh*-transformants compared with nontransformed control plants. Error bars indicate standard deviation of four independent samples each.

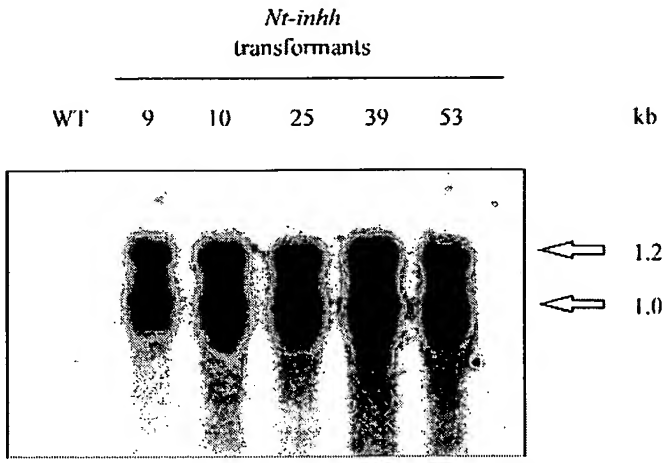

Figure 3. RNA blot analysis confirms *Nt-inhh* expression in mature potato tubers from independent transgenic lines. Storage of tubers at 4°C for 11 days did not affect transcript amounts (not shown).

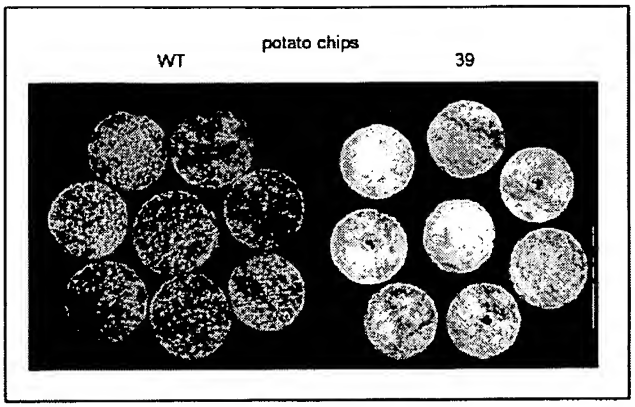

Figure 4. *Nt-inhh* expression improves processing quality for potato chip production by reducing cold-induced hexose formation in potato tubers without affecting potato tuber yield and starch concentrations (see Table 1). Tuber slices (1.5 mm thick) were fried for 2 min at 210°C.

ity of potato tubers, chips were prepared from wild-type and *Nt-inhh* plants (Fig. 4). The comparison demonstrates that *Nt-inhh* expression strongly reduces browning of tissue during the frying process. This dramatic result—and the absence of any adverse effects on tuber growth, yield, and starch content—strongly suggest that the introduction of *Nt-inhh* into commercial potato varieties may greatly improve their processing quality.

Experimental protocol

Molecular cloning and plant transformation. The *Nt-inhh* cDNA[9] was obtained by screening a cDNA library from transformed tobacco cells[14] with the cDNA of a tobacco invertase inhibitor (*Nt-inh1*)[10] at low stringency. The complete cDNA (accession no.: Y12806; 811 bp) was released by *Bam*HI/*Xba*I restriction from the pBK-CMV-Vector (Stratagene, La Jolla, CA) and then introduced into the *Bam*HI/*Xba*I site of the binary plant expression vector (BinAR)[15,16] in sense orientation (see Fig. 1B). Plant transformation was performed as described[17]. The resulting transgenic plants were screened for expression of *Nt-inhh* by northern blot analysis according to Herbers *et al.*[18]. Transformants with the highest level of expression were used for further analysis.

Cold storage, tissue sampling, and assay for sugars and starch. For cold-storage experiments, tubers were harvested from plants grown in the greenhouse after they had developed full senescence (approximately three months) and stored for six weeks either at 4°C or at 20°C (control). Samples were taken by cutting slices (0.65 cm diameter, 1.5 mm thick) from stored tubers (five independent tubers per transgenic line, two samples each), which were immediately frozen in liquid nitrogen. Determination of soluble sugars and starch was performed as described[19].

Determination of vacuolar and cell wall invertase activities. For determination of VI activity in leaves, tissue was extracted in 30 mM MOPS (3-(*N*-morpholino)propanesulfonic acid), pH 6, 250 mM sorbitol, 10 mM $MgCl_2$, 10 mM KCl, and 1 mM phenylmethylsulfonyl fluoride (PMSF). After centrifugation for 10 min (6,500 *g*, 4°C) aliquots from the supernatants were incubated in 30 mM NaAc, pH 4.7, 30 mM sucrose at 37°C for 1 h. After incubation, aliquots were assayed for liberated D-glucose with hexokinase/glucose-6-phosphate dehydrogenase as described[20].

To obtain a cell wall-enriched fraction, the pellet collected after the 6,500 *g* centrifugation step was resuspended in extraction buffer including 1% (vol/vol) Triton X-100. The suspension was shaken vigorously for 10 min at 4°C. After another centrifugation, the pellet was washed in extraction buffer without Triton X-100, and finally resuspended in assay buffer. For determination of CWI activity, sucrose was added to a final concentration of 30 mM, and liberated D-glucose was assayed as described already.

To separate VI from cytosolic (neutral and/or alkaline) invertases, the soluble protein fraction (see above) was mixed with four volumes of ConA-binding buffer (50 mM NaAc, 1 mM $CaCl_2$, 1 mM $MgCl_2$, 1 mM $MnCl_2$, 1 mM PMSF, pH 6.3), and incubated with ConA-Sepharose 4B (Sigma, Deisenhofen, Germany) 1 ml matrix per 3 g fresh weight equivalent) for 1 h at 4°C under shaking. After washing twice with ConA-binding buffer, bound glycoproteins including VI were released with 15% (wt/vol) methyl-α-D-glucopyranoside (Sigma) in Con-A buffer. For determination of VI activity, aliquots of the eluate were incubated in 30 mM NaAc, pH 4.7, 30 mM sucrose as described already.

Acknowledgments

This work was supported by a grant from the Deutsche Forschungsgemeinschaft to T.R. (SFB 199, TP C3). The authors are grateful to Anita Winger for excellent technical assistance. We would also like to thank Andrea Knospe and Sibylle Freist for the tissue culture work, and Katja Lauer for the determination of VI activities in ConA-fractions from tobacco Nt-inhh transformants.

1. Müller-Thurgau, H. Über Zuckeranhäufung in Pflanzentheilen in Folge niederer Temperatur. *Landwirtschaftliches Jahrbuch* **11**, 751–828 (1882).
2. Burton, W.G. in *The potato*. 3rd edn (Longman Scientific & Technical, Harlow, Essex, England, 1989).
3. Pollock, C.J. & ap Rees, T. Activities of enzymes of sugar metabolism in cold stored tubers of *Solanum tuberosum*. *Phytochemistry* **14**, 613–617 (1975).
4. Isherwood, F.A. Starch-sugar interconversion in *Solanum tuberosum*. *Phytochemistry* **12**, 2579–2591 (1973).
5. Stark, D.M., Timmerman K.P., Barry, G.F., Preiss J. & Kishore G.M. Regulation of the amount of starch in plant tissues by ADP glucose pyrophosphorylase. *Science* **258**, 287–292 (1992).
6. Stark, D.M., Barry, G.F. & Kishore G.M. Engineering plants for commercial products and applications. *Ann. NY Acad. Sci.* **792**, 26–37 (1996).
7. Lorberth, R., Ritte, G., Willmitzer, L. & Kossmann, J. Inhibition of a starch-granule-bound protein leads to modified starch and repression of cold sweetening. *Nat. Biotechnol.* **16**, 473–477 (1998).
8. Zrenner, R., Schüler, K. & Sonnewald, U. Soluble acid invertase determines the hexose-to-sucrose ratio in cold-stored potato tubers. *Planta* **198**, 246–252 (1996).
9. Greiner, S., Krausgrill, S. & Rausch, T. *N. tabacum* mRNA for invertase inhibitor homolog. EMBL Nucleotide Sequence Database, acc .Y12806.
10. Greiner, S., Krausgrill, S. & Rausch, T. Cloning of a tobacco apoplasmic invertase inhibitor: Proof of function of the recombinant protein and expression analysis during plant development. *Plant Physiol.* **116**, 733–742 (1998).
11. Krausgrill, S., Greiner, S., Köster, U., Vogel, R. & Rausch, T. In transformed tobacco cells the apoplasmic invertase inhibitor operates as a regulatory switch of cell wall invertase. *Plant J.* **13**, 275–280 (1998).
12. von Heijne G. A new method for predicting signal sequence cleavage sites *Nucleic Acids Res.* **14**, 4683 (1986).
13. Zrenner, R. Klonierung und funktionelle analyse von genen kodierend für am saccharosestoffwechsel der kartoffel beteiligte proteine (PhD Thesis, Freie Universität Berlin, Germany; 1993).
14. Greiner, S., Weil, M., Krausgrill, S. & Rausch, T. A tobacco cDNA coding for cell-wall invertase. *Plant Physiol.* **108**, 825–826 (1995).
15. Höfgen, R. & Willmitzer, L. Biochemical and genetic analysis of different patatin isoforms expressed in various organs of potato (*Solanum tuberosum* L.). *Plant Sci.* **66**, 221–230 (1990).
16. Bevan, M. Binary *Agrobacterium* vectors for plant transformation. *Nucleic Acids Res* **12**, 8711–8721 (1984).
17. Rocha-Sosa, M. *et al.* Both development and metabolic signals activate the promoter of a class I patatin gene. *EMBO J.* **8**, 23–29 (1989).
18. Herbers, K., Prat, S. & Willmitzer, L. Functional analysis of a leucine aminopeptidase from Solanum tuberosum L. *Planta* **194**, 230–240 (1994).
19. Stitt, M., Lilley, R.M.C., Gerhard, R. & Heldt, H.W. Metabolic levels in specific cells and subcellular compartment of plant leaves. *Methods Enzymol.* **174**, 518–552 (1989).
20. Weil, M. & Rausch, T. Cell wall invertase in tobacco crown gall cells. *Plant Physiol.* **94**, 1575–1581 (1990).

FEBS 28715 FEBS Letters 573 (2004) 105–109

In *Arabidopsis thaliana*, the invertase inhibitors AtC/VIF1 and 2 exhibit distinct target enzyme specificities and expression profiles

Manuela Link, Thomas Rausch, Steffen Greiner*

Heidelberg Institute of Plant Sciences (HIP), Im Neuenheimer Feld 360, D-69120 Heidelberg, Germany

Received 18 June 2004; revised 26 July 2004; accepted 27 July 2004

Available online 3 August 2004

Edited by Barry Halliwell

Abstract Plant cell wall (CWI) and vacuolar invertases (VI) play important roles in carbohydrate metabolism, stress responses and sugar signaling. Addressing the regulation of invertase activities by inhibitor proteins (C/VIF, cell wall/vacuolar inhibitor of fructosidase), we have identified two C/VIFs from *Arabidopsis thaliana*. AtC/VIF1 showed specific inhibition of VI activity, whereas AtC/VIF2 inhibited both, CWI and VI. Expression analysis revealed that expression of AtC/VIF1 was restricted to specific organs, AtC/VIF2, however, was weakly expressed throughout plant development. Promoter::GUS transformants confirmed pronounced differences of tissue/cell type-specific expression between both isoforms. Growth of an AtC/VIF1 T-DNA KO mutant was unaffected, but VI activity and hexose content were slightly increased.

Keywords: Invertase inhibitor; Posttranslational regulation; Functional genomics; *Arabidopsis thaliana*

1. Introduction

Plants translocate carbohydrates from assimilating organs to sites of consumption such as storage organs and rapidly growing tissues. Most higher plants use sucrose as transport form. Within certain plant tissues like transport phloem or storage cells sucrose can be accumulated up to 20%, which is more than 500 mM. Plants possess two different classes of enzymes to break down sucrose for entry into metabolism: sucrose synthase (SuSy) and invertase. The first enzyme yields UDP-glucose and fructose in a reversible reaction in the cytosol, whereas invertases in the cytosol, the vacuole or the cell wall release glucose and fructose in an irreversible reaction. Both types of enzymes have been shown to be essential for plants, especially during growth, storage compound accumulation, and stress responses [1,2].

According to their pH optima, plant invertases can be divided into two categories: neutral and acid invertases. Acid invertases are of exceptional importance as they are the only enzymes able to cleave sucrose in extracellular compartments such as the vacuole (vacuolar invertase; VI) or the apoplastic space (cell wall invertase; CWI). Acid invertases are responsible for sucrose unloading from the conducting tissues and for the adjustment of the hexose/sucrose ratio, which affects plant development including programmed cell death [3]. Thus, the hexose/sucrose ratio acts as an important metabolic signal, which dramatically affects gene expression profiles [4–8]. Consequently, the expression patterns of CWI and VI have to be tightly controlled, both temporally and spatially. CWI and VI exist in small gene families, *Arabidopsis thaliana* having 6 putative CWI isoforms and 2 VI isoforms [9,10]. Induction of CWI or VI activities is mediated via increased transcription of the corresponding genes in response to a wide range of stress-related and developmental cues [11–13]. In contrast, rapid downregulation of invertase activity is not yet fully understood but appears to require mechanisms additional to transcriptional repression.

Given that CWI and VI show glycan decoration [14] and are therefore intrinsically very stable enzymes, silencing of CWI and VI activities depends on post-translational mechanisms. In particular, a well orchestrated downregulation of CWI and/or VI activities appears to be important during developmental transitions from high meristematic activity to differentiation and accumulation of storage compounds as observed during seed development and in the formation of vegetative storage organs. In these developmental processes, the hexose/sucrose ratio declines rapidly which correlates with an efficient silencing of CWI and/or VI activities [15,16]. The molecular mechanisms of this downregulation of CWI and VI activities are not yet fully understood but one specific mechanism operates via complex formation of CWI and VI with proteinaceous invertase inhibitors [17–19]. A recent study proposed a crucial role to an apoplastic invertase inhibitor in the control of leaf senescence [3].

Invertase inhibitors have been known for a long time [20,21], but have only recently been cloned [17] and characterized [22,23]. Functional genomics approaches revealed that invertase inhibitors and inhibitors of pectin methylesterase (PMEI) [24] belong to the same diverse protein family. Within this protein family, PMEIs are more abundant than invertase inhibitors. Moreover, invertase inhibitors and PMEIs show a significant homology with the pro-domains of type I pectin methylesterase. Therefore, the entire protein family is referred to as PMEI-related proteins (PMEI-RP). Here, we report that two PMEI-RP genes from *Arabidopsis thaliana* indeed encode invertase inhibitors with different target enzyme specificities. Furthermore, a detailed expression analysis is presented and implications for invertase regulation are discussed.

* Corresponding author. Fax: +49-6221-545859.
E-mail address: sgreiner@hip.uni-hd.de (S. Greiner).

0014-5793/$22.00
doi:10.1016/j.febslet.2004.07.062

2. Materials and methods

2.1. Plant material

Arabidopsis thaliana cv Wassilewskija plants were grown in a growth chamber in standard potting soil (9 cm pots) under short-day conditions (8 h light at 24 °C, 16 h dark at 18 °C, and approx. 50% humidity).

2.2. Construction of expression plasmids

The coding regions of AtC/VIF1 (at1g47960) and AtC/VIF2 (at5g64620) without the signal peptide (predicted by psort: http://psort.nibb.ac.jp/form.html) were amplified by polymerase chain reaction (PCR) from flower cDNA using the following primers (RE sites underlined): AtC/VIF1, sense 5′-GATAGCCATGGAAGGAAGTATAATAGAGCCAA-3′, antisense 5′-TATAAGCGGCCGCTAAAGCAACATTCTCACAAT-3′; AtC/VIF2, sense 5′-ATCGTAACCATGGGAGCATCAACCCTAATCT-3′, antisense 5′-TATATGCGGCCGCTATTCAACAAGGCGATCAA-3′. The amplification products were digested with *NcoI*/*NotI* and after gel purification (Kit from Qiagen, Hilden, Germany) ligated into the *NcoI*/*NotI* restricted pETM-20 vector (http://www.emblheidelberg.de/ExternalInfo/geerlof/draft_frames/flowchart/clo_vector/pETM/pETM-20.pdf). Expression from this vector produces 6 × His-tagged thioredoxinA-AtC/VIF fusion proteins with a TEV protease cleavage site to separate the fusion partners after purification.

2.3. Expression and purification of recombinant AtC/VIF1 and 2 proteins

The expression and purification of recombinant AtC/VIF1 and 2 proteins was performed following the protocol earlier reported for the invertase inhibitor NtCIF [22].

2.4. Acid invertase and PME enzyme assays

Partially purified acid invertase preparations were isolated from *A. thaliana* source leaves. The tissue was ground in liquid nitrogen and homogenized in 2 ml/g extraction buffer (30 mM MOPS, 250 mM sorbitol, 10 mM $MgCl_2$, 10 mM KCl, and 1 mM PMSF, pH 6). After centrifugation (10 min, 3500 × *g*), the pellet was washed once (10 min) with extraction buffer containing 1% Triton X-100, twice with extraction buffer, finally resuspended in 1 ml/g assay buffer (20 mM triethanol amine, 7 mM citric acid, and 1 mM PMSF, pH 4.6), and used for the determination of cell wall invertase activity. The supernatant was mixed with 1/9 volume ConA buffer (500 mM sodium acetate, 10 mM $CaCl_2$, 10 mM $MgCl_2$, 10 mM $MnCl_2$, and 1 mM PMSF, pH 6.3), 2 ml/100 g fresh weight concanavalin A (ConA)-sepharose (Sigma, Steinheim, Germany), and incubated for 1 h on ice under constant agitation. After centrifugation (5 min, 3000 × *g*) and washing with 10-fold diluted ConA buffer, the bound protein fraction was eluted with 5 volumes (of initially used ConA-sepharose) of elution buffer (10-fold diluted ConA buffer containing 10% (w/v) methyl α-D-glucopyranoside), and used for the determination of vacuolar invertase activity.

The acid invertase assay was performed by mixing 50 μl invertase preparation, 100 μl substrate (100 mM sucrose, in assay buffer), and assay buffer up to a volume of 300 μl. After a 1 h incubation at 37 °C, acid invertase activity was measured by enzymatic determination of released glucose in a coupled assay with hexokinase and glucose-6-phosphate dehydrogenase according to [25]. The PME assay was performed with commercially available PME from orange peel (Sigma) as previously described [24,26].

For inhibition studies, enzyme preparations were mixed with recombinant AtC/VIF proteins and coincubated in assay buffer without substrate for 30 min at 37 °C (invertase assay) or 25 °C (PME assay). Thereafter, substrate was added and enzyme activity determined. As a control, invertase or PME preparations were pre-incubated without inhibitory proteins for the same period of time before activity measurement.

2.5. Transcript estimation by real-time PCR

Total RNA was extracted from various tissues of *A. thaliana* WT plants using the RNeasy Plant Mini Kit (Qiagen) following the manufacturer's instructions. To eliminate residual genomic DNA present in the preparations, the samples were treated with RNase-free DNaseI (Promega, Mannheim, Germany) and subsequently the RNA was bound to RNeasy Spin columns (Qiagen) for purification. After elution with RNase-free water, 2 μg of RNA was transcribed into first strand cDNA using the Omniscript RT Kit (Qiagen) with an oligo dT primer.

Real-time PCR was performed using the Platinum Taq-DNA polymerase (Invitrogen, Karlsruhe, Germany) and SYBR-Green as fluorescent reporter in Biorad iCycler. Primers were designed against the coding region of AtC/VIF1 (sense 5′-TGGCCTCGCTCTCATCCTCATTG-3′; antisense 5′-GCTTCTATGGCTTCGGGAACATC-3′) and AtC/VIF2 (sense 5′-GTTGGTATGACAAACGCCACCTC-3′; antisense 5′-ATGGAGGCATAGTCATAAGCTTCAT-3′). Primers against actin were described previously [27]. A serial dilution of source leaf cDNA was used as standard curve to optimize amplification efficiency for AtC/VIF and actin primers. Each reaction was performed in triplicates, and specificity of amplification products was confirmed by melting curve and gel electrophoresis analysis. Relative expression levels of AtC/VIF1 and AtC/VIF2 were calculated and normalized with respect to Act2/8 mRNA according to the method in [28].

2.6. Generation of promoter::GUS plants

The promoter regions of AtC/VIF1 and AtC/VIF2 were amplified from genomic DNA with the following primers (RE sites underlined): AtC/VIF1, sense 5′-GGCGGCAAGCTTATTGAAAGTTTACTCGAA-3′, antisense 5′-AGTTCTCCCGGGCTTCTTTGATGATTATCT-3′; AtC/VIF2, sense 5′-AGCCTAAAGCTTTCTTCGAAGCATCCGATT-3′, antisense 5′-ATTATTCCCGGGTTCAGGAAGAAGGTTTTG-3′. The amplification products were digested with *Hind*III/*Sma*I and after gel purification ligated into the *Hind*III/*Sma*I restricted pGPTV-bar vector [29]. The resulting constructs consisted of the promoter in front of a beta-glucuronidase (uidA) gene. After mobilizing the constructs in *Agrobacterium tumefaciens*, *A. thaliana* cv Wassilewskija plants were transformed using the floral dip method [30]. Transformants were screened for resistance to the herbicide Basta™.

For analysis of GUS activity, tissue samples of T2 transformants were treated with GUS staining buffer (100 mM Na_2HPO_4/NaH_2PO_4), pH 7.0, 10 mM Na_2EDTA, 0.5 mM $K_3[Fe(CN)6]$, 0.5 mM $K_4[Fe(CN)_6]$, and 0.08% X-GlcA (Duchefa, Haarlem, The Netherlands) for 20 h at 37 °C. Green tissues were bleached with ethanol before examination.

2.7. Isolation of a T-DNA-tagged AtC/VIF1 KO mutant

Access to T-DNA-tagged *Arabidopsis* knockout lines was available through the Arabidopsis Knockout Facility at the University of Wisconsin [31]. The screening for mutants was performed as described at http://www.biotech.wisc.edu/Arabidopsis/.

3. Results and discussion

In a functional genomics approach to PMEI-RPs, we currently analyse the entire protein family in *Arabidopsis*. Recently, we have identified two of these genes as coding for inhibitors of PME [24]. Here, we identify two other genes from the same family as invertase inhibitors.

3.1. Heterologous expression of recombinant AtC/VIF1 and 2 proteins and in vitro proof of function

To express AtC/VIF1 and 2 as recombinant proteins, the open reading frames without the predicted N-terminal signal sequences were cloned into the pETM-20 vector. Expression in the *E. coli* strain Origami(DE3) yielded recombinant AtC/VIF1 and 2 as N-terminal thioredoxinA-AtC/VIF fusion proteins. From the fusion proteins, AtC/VIF1 and 2 were released by cleavage with TEV protease [32]. ThioredoxinA and TEV protease are both provided with his-tags, therefore pure AtC/VIF1 and 2 proteins were recovered in the flow-through of a Ni-affinity chromatography column (data not shown). The

E. coli strain Origami(DE3) was chosen because of its deficiencies in thioredoxin reductase and glutathione reductase activities, thus providing an oxidizing environment to facilitate disulfide bridge formation.

Purified AtC/VIF1 and 2 proteins were analyzed by SDS–PAGE using sample buffer with and without reductant. Under non-reducing conditions their mobility increased, indicating the presence of intramolecular disulfide bridges in the recombinant proteins (data not shown). The presence of disulfide bridges was previously observed for the recombinant tobacco invertase inhibitor NtCIF and for the pectin methylesterase inhibitors AtPMEI1 and 2 [24]. The recent crystallographic analysis of NtCIF has highlighted the importance of these disulfide bridges for structural stabilization of both the four-helix-bundle core of the inhibitor as well as an N-terminal α-hairpin module [23]. Thus, it was assumed that the AtC/VIF1 and 2 proteins were correctly folded, and their in vitro activities were determined with CWI and VI enzyme preparations (Figs. 1 and 2).

The analysis of in vitro activities of recombinant AtC/VIF1 and 2 clearly defined both proteins as inhibitors of invertases. Conversely, both proteins showed no activities against PME preparations which were completely inhibited by AtPME1 and 2 proteins, respectively (data not shown). Interestingly, AtC/VIF1 and 2 were clearly distinct in their target specificities. AtC/VIF1 appeared to be rather selective for VI with little activity against CWI (Fig. 1). However, AtC/VIF2 inhibited both enzymes (Fig. 2), but the affinity for VI was about 10-fold higher than for CWI. Based on these results, AtC/VIF1 is likely to operate as an inhibitor of VI also in vivo, whereas the situation is less clear for AtC/VIF2. Previous studies suggested that individual members of the PMEI-RP family show either PMEI activity or C/VIF activity, but never both (S. Wolf, S. Grsic-Rausch, S. Greiner and T. Rausch, unpublished results; [33]). This notion has now been extended to two C/VIF proteins from *Arabidopsis thaliana*. However, within the subgroup of C/VIF proteins, different inhibitor isoforms may in vitro exhibit either narrow or broad specificities. Thus, NtCIF, an experimentally confirmed cell wall isoform, inhibits in vitro

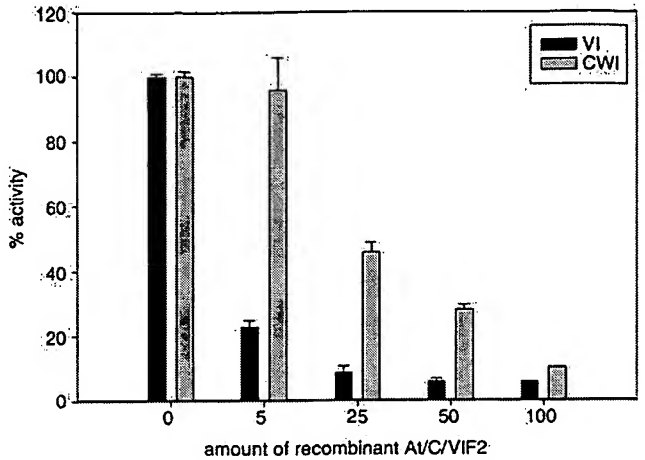

Fig. 2. Inhibitory effect of recombinant AtC/VIF2 protein on different invertase preparations. Dose-dependent effects of AtC/VIF2 protein on VI and CWI activities isolated from *Arabidopsis* leaves are shown. Target enzyme preparations were preincubated with inhibitor proteins for 30 min prior to enzyme assay.

CWI and VI, whereas recombinant NtVIF appears to be selective for VI. Conversely, an invertase inhibitor from sugar beet, for which the vacuolar targeting has been demonstrated, inhibited in vitro VI and CWI (Jan Eufinger, unpublished data). The structural basis for the target enzyme specificities of PMEI-RPs, i.e., PMEI versus C/VIF activity, is currently being investigated.

3.2. *Expression analysis by real time PCR and promoter::GUS fusions*

To compare the expression of *AtC/VIF1* and *2* mRNAs in different tissues, transcripts were quantitatively estimated by real time PCR, using *Actin2/8* for normalization (Fig. 3). The results revealed a low but consistent expression of *AtC/VIF2* in different plant organs, whereas *AtC/VIF1* showed an overall higher expression, with highest transcript levels in roots, senescent leaves and flowers. To explore the expression of *AtC/*

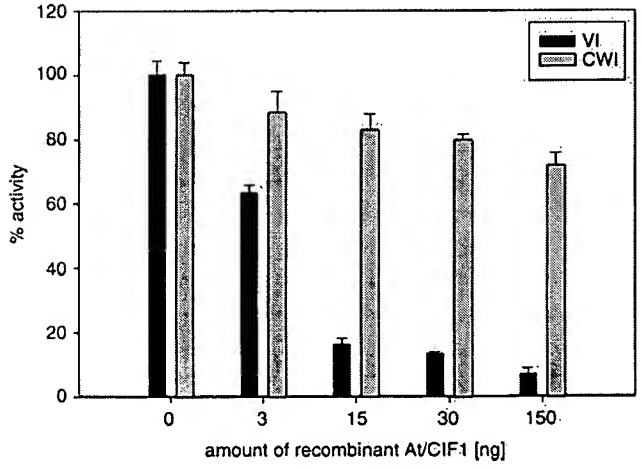

Fig. 1. Inhibitory effect of recombinant AtC/VIF1 protein on different invertase preparations. Dose-dependent effects of AtC/VIF1 protein on VI and CWI activities isolated from *Arabidopsis* leaves are shown. Target enzyme preparations were preincubated with inhibitor proteins for 30 min prior to enzyme assay.

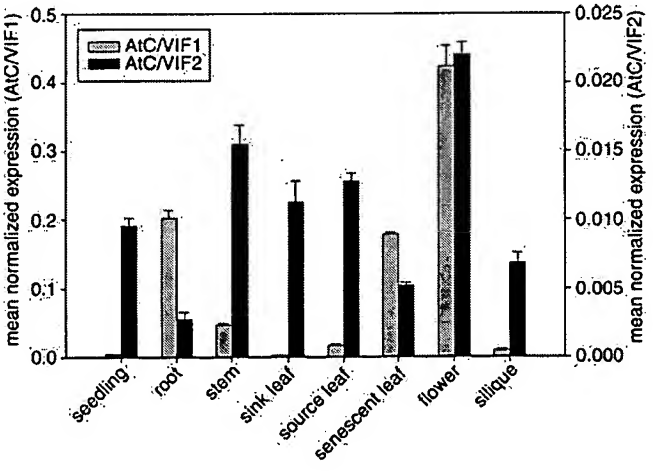

Fig. 3. Quantitative determination of AtC/VIF1 and 2 transcripts in different organs of *Arabidopsis thaliana* by real time PCR. Data for AtC/VIF1 and AtC/VIF2 are presented as relative expression normalized with respect to Actin2/8 mRNA (= 1). Tissue samples were collected from 8-week-old flowering plants.

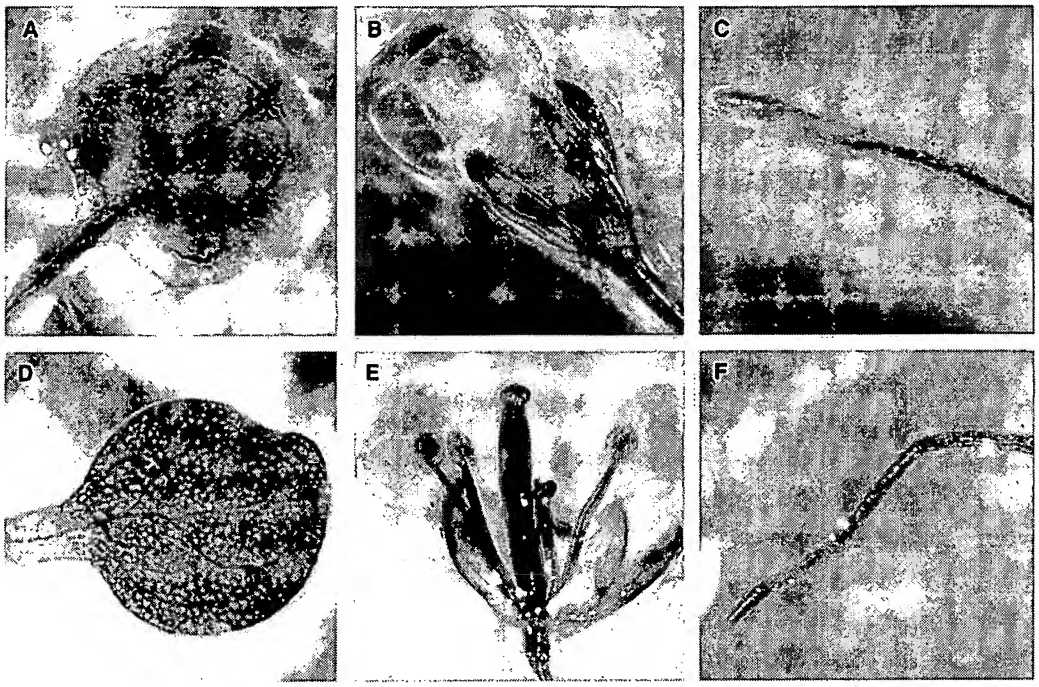

Fig. 4. Expression analysis of AtC/VIF1 and 2, using promoter::GUS fusions. Panels A, B, and C represent AtC/VIF1 promoter::GUS fusions, panels D, E, and F AtC/VIF2 promoter::GUS fusions. Cotyledons and roots (A/D, and C/F) were taken from 3 week old *Arabidopsis* plants, whereas flowers (B/E) were taken from 8 week old plants. The strong expression of *AtC/VIF1* was localized to the vascular tissue. Conversely, *AtC/VIF 2* expression was more evenly distributed.

VIF1 and *2* at higher spatial resolution, we generated *promoter::GUS* lines for both isoforms, containing 1486 and 1525 bp of 5′-upstream sequence for *AtC/VIF1* and *2*, respectively. The analysis of *promoter::GUS* transformants revealed pronounced differences between the inhibitor isoforms (Fig. 4). In cotyledons and roots (Fig. 4 A/D, and C/F), the strong expression of *AtC/VIF1* was localized to the vascular tissue, and the same was true for all leaf stages (data not shown). Cross sections revealed that the GUS-staining was confined to the phloem (data not shown). Conversely, *AtC/VIF 2* expression was more evenly distributed. Likewise, conspicuous qualitative differences of GUS-staining patterns were observed in flowers (Fig. 4B/E). While strong *GUS* expression in *AtC/VIF1* lines was concentrated in the vascular tissue of the sepals only, all floral organs were stained in *AtC/VIF2* plants.

3.3. Acid invertase activities and sugar levels in a T-DNA-tagged AtC/VIF KO mutant

To address the in vivo functions of the strongly expressed AtC/VIF1 isoform, we have analyzed a T-DNA tagged AtC/VIF1 KO mutant obtained from the Arabidopsis Knockout Facility at the University of Wisconsin [31]. The T-DNA insert was localized in the only intron, 96 bases downstream of the exon-intron border (base 295 relative to the translational start site). Real time PCR analysis confirmed the absence of *AtC/VIF1* transcripts (data not shown). A comparison of extractable total VI activities in leaf extracts from wild type and KO plants revealed a 43% increase in the latter (Table 1), whereas CWI activities were not affected. This effect is most likely underestimated, since expression of *AtC/VIF1* is confined to the vascular (phloem) tissues (see above), whereas at least one of the two VI isoforms in *Arabidopsis thaliana* appears to be expressed in the entire leaf blade (Christina Hofmann, unpublished results). Therefore, the effect within the vascular tissue may be more pronounced. When comparing the tissue concentrations of sucrose, fructose and glucose, only minor changes were observed in the KO mutant (Table 1), the hexose/sucrose ratio being 4.42 in the mutant and 3.72 in the WT plants. Again, this effect could be underestimated for the reasons given above. When plants were cultivated under optimum growth conditions (green house, growth chamber), a preliminary analysis of KO mutant plants showed no visible changes in phenotype compared to wild type plants during vegetative growth, flowering and seed production. However, as the expression of the target enzymes, VI (and possibly CWI), is strongly regulated in response to various biotic and abiotic stress factors, a comprehensive search for possible mutant phenotypes under stress exposure has been initiated.

Table 1
VI activities, hexose and sucrose contents in source leaves of 6 week old WT and AtC/VIF1 T-DNA KO mutant plants grown in the green house under non-stressed conditions

		WT	KO
Invertase activities (nkat)	VI	54.26 ± 13.31	77.77 ± 14.48
	CWI	3.36 ± 1.24	3.40 ± 0.89
Sugar contents (μmol/g)	glucose	4.00 ± 1.51	5.02 ± 1.61
	fructose	1.44 ± 0.58	2.02 ± 0.71
	sucrose	1.46 ± 0.50	1.59 ± 0.62

Acknowledgements: The authors thank Klaus Scheffzek (EMBL Heidelberg) for generous support, helpful discussions and the opportunity to perform some of the cloning and expression work in his laboratory. The authors also thank Christina Hofmann, Sebastian Wolf and Michael Hothorn for critical reading of the manuscript. Financial support of the KWS Saat AG and the Südzucker AG to TR and SG is gratefully acknowledged.

References

[1] Tang, G.Q., Luscher, M. and Sturm, A. (1999) Plant Cell 11, 177–189.
[2] Tang, G.Q. and Sturm, A. (1999) Plant Mol. Biol. 41, 465–479.
[3] Balibrea Lara, M.E., Gonzalez Garcia, M.C., Fatima, T., Ehness, R., Lee, T.K., Proels, R., Tanner, W. and Roitsch, T. (2004) Plant Cell 16, 1276–1287.
[4] Smeekens, S. (2000) Annu. Rev. Plant Physiol. Plant. Mol. Biol. 51, 49–81.
[5] Smeekens, S. and Rook, F. (1997) Plant Physiol. 115, 7–13.
[6] Jang, J.C. and Sheen, J. (1994) Plant Cell 6, 1665–1679.
[7] Rolland, F., Moore, B. and Sheen, J. (2002) Plant Cell 14, 185–205.
[8] Koch, K.E. (1996) Annu. Rev. Plant Physiol. Plant Molecular Biol. 47, 509–540.
[9] Tymowska-Lalanne, Z. and Kreis, M. (1998) Planta 207, 259–265.
[10] The Arabidopsis Genome Initiative (2000) Nature 408, 796–815.
[11] Sturm, A. (1999) Plant Physiol. 121, 1–8.
[12] Sturm, A. and Chrispeels, M.J. (1990) Plant Cell 2, 1107–1119.
[13] Roitsch, T. (1999) Curr. Opin. Plant Biol. 2, 198–206.
[14] Yamaguchi, H. (2002) Trends Glycosci. Glycotechnol. 14, 139–151.
[15] Wobus, U. and Weber, H. (1999) Biol. Chem. 380, 937–944.
[16] Hill, L.M., Morley-Smith, E.R. and Rawsthorne, S. (2003) Plant Physiol. 131, 228–236.
[17] Greiner, S., Krausgrill, S. and Rausch, T. (1998) Plant Physiol. 116, 733–742.
[18] Greiner, S., Rausch, T., Sonnewald, U. and Herbers, K. (1999) Nat. Biotechnol. 17, 708–711.
[19] Rausch, T. and Greiner, S. (2004) Biochim. Biophys. Acta 1696, 253–261.
[20] Schwimmer, S., Makower, R.U. and Rorem, E.S. (1961) Plant Physiol. 36, 313–316.
[21] Pressey, R. (1967) Plant Physiol. 42, 1780–1786.
[22] Hothorn, M., Bonneau, F., Stier, G., Greiner, S. and Scheffzek, K. (2003) Acta Crystallogr. D 59, 2279–2282.
[23] Hothorn, M., D'Angelo, I., Marquez, J.A., Greiner, S. and Scheffzek, K. (2004) J. Mol. Biol. 335, 987–995.
[24] Wolf, S., Grsic-Rausch, S., Rausch, T. and Greiner, S. (2003) FEBS Lett. 555, 551–555.
[25] Weil, M. and Rausch, T. (1990) Plant Physiol. 94, 1575–1581.
[26] Grsic-Rausch, S., Rausch, T., 2004. Anal. Biochem., in press, doi:10.1016/j.ab.2004.04.042.
[27] Ha, S.B., Smith, A.P., Howden, R., Dietrich, W.M., Bugg, S., O'Connell, M.J., Goldsbrough, P.B. and Cobbett, C.S. (1999) Plant Cell 11, 1153–1163.
[28] Muller, P.Y., Janovjak, H., Miserez, A.R. and Dobbie, Z. (2002) BioTechniques 32, 1372–1379.
[29] Becker, D., Kemper, E., Schell, J. and Masterson, R. (1992) Plant Mol. Biol. 20, 1195–1197.
[30] Clough, S.J. and Bent, A.F. (1998) Plant J. 16, 735–743.
[31] Krysan, P.J., Young, J.C. and Sussman, M.R. (1999) Plant Cell 11, 2283–2290.
[32] Parks, T., Leuther, K., Howard, E., Johnston, S. and Dougherty, W. (1994) Anal. Biochem. 216, 413–417.
[33] Scognamiglio, M.A., Ciardiello, M.A., Tamburrini, M., Carratore, V., Rausch, T. and Camardella, L. (2003) J. Protein Chem. 22, 363–369.